UCL Université catholique de Louvain

École polytechnique de Louvain (EPL)

Modelling marine connectivity in the Great Barrier Reef

Dissertation presented by
Aurélien SOUPART

for obtaining the Master's degree in
Mechanical Engineering

Supervisor(s)
Emmanuel HANERT, Eric DELEERSNIJDER

Reader(s)
Jonathan LAMBRECHTS, Sandra SOARES-FRAZÃO

Academic year 2017-2018

Abstract

Modelling marine connectivity in the Great Barrier Reef

Presented by Aurélien Soupart

The aim of this thesis is to study the variability of the connectivity in the GBR between 2008, 2010 and 2012. In order to do that, the study presents an effort to model the dispersal of coral larvae, of the species *Acropora millepora*, for the whole Great Barrier Reef (GBR) in each of the three years considered. Firstly, a high resolution ocean model is devised to build such a model. The hydrodynamic model used is a 2D version of SLIM, an unstructured mesh ocean model. This allows to increase the model's resolution close to reefs where small scale flow features are important and decrease the resolution in deeper areas where flow features are thought to be more uniform. Validation of the model shows a good agreement with real observations in the south of the GBR while the currents in the north of the GBR would still need improvements to replicate the real hydrodynamics of the region. Secondly, a Lagrangian particle tracker is used to simulate the transport of particles over the currents generated by the ocean model. It generates a connectivity matrix giving for each reef the number of larvae settled onto it and their origin. To interpret all data encapsulated in the connectivity matrix, some connectivity measures are described. Moreover, some protection and restoration measures are defined based on previous connectivity measures and two clustering methods are used. This gives a picture of the connectivity patterns linking the different reefs in the GBR. This information is useful from a management and conservation perspective because this determines which reefs play a major role in the conservation of the GBR. The analysis is made for the three spawning seasons. Finally, in order to have a broader overview of the connectivity in the GBR and to get more relevant and reliable results, data of the three years considered are gathered by using statistics such as the mean and the coefficient of variation. The conclusions drawn from this statistical study show that the reefs that would need more protection are located in the southern part of the center of the GBR and in the northern part of the south of the GBR. The reefs that would be more suitable for restoration pratices are located downstream of reefs that would need protection. They are thus located in the south of the GBR. The level of connectivity in the north of the GBR is lower but this region is characterised by a high local retention. These final results could be useful to inform marine management strategies for achieving restoration and protection of the GBR. These marine management strategies could consist of the placement of Marine Protected Areas (MPAs).

Acknowledgements

I would like first to thank my supervisors Emmanuel Hanert and Eric Deleersnijder for giving me the opportunity to be part of the SLIM project and to work on this topic which was not part of the initial list of topics. I am very grateful for the continual scientific guidance and support I received during this year. I'm also very grateful to you for always taking the time to discuss my work.

I would also like to thank Antoine Saint-Amand for the wonderful help he gives me all along the modelling process. He was always available to provide advice and useful information. He has been an invaluable and much appreciated help.

Similarly I would like to thank all remaining members of the SLIM team, especially Jonathan Lambrechts, Valentin Vallaeys and David Vincent. They spent several hours every Friday afternoon to help me understand SLIM first, and then they were very helpful when I needed some help to fix and improve my code.

Finally, I would like to acknowledge the Louvain School of Engineering which allows me to study one semester at the University of Melbourne. This exchange program in Australia allows me to snorkel and scuba dive at several places in the Great Barrier Reef. This amazing experience made me realise how critical the current situation of the Great Barrier Reef is and so the importance of bringing scientific knowledge in order to inform marine management strategies for achieving restoration and protection of the Great Barrier Reef.

Contents

Abstract **4**

Acknowledgements **6**

1 Introduction **10**
1.1 Water circulation in the Great Barrier Reef 12
1.2 Connectivity 13
1.3 Objectives 14

2 Simulating currents with an unstructured mesh ocean model **16**
2.1 Hydrodynamic model 16
2.2 Data and parameters 17
2.3 Unstructured mesh 18
2.4 Model forcings 19
2.5 Validation of the hydrodynamics 21

3 Simulating larval dispersal with a Lagrangian particle tracker **31**
3.1 Physical parameters 31
3.2 Biological parameters 32
3.3 Biophysical particle transport 34
3.4 Connectivity matrix 37

4 Studying connectivity with graph theory tools **39**
4.1 Connectivity measures 39
4.1.1 Local retention 39
4.1.2 Self-recruitment 40
4.1.3 Degree centrality 41
4.1.3.1 Incoming degree centrality 41
4.1.3.2 Outgoing degree centrality 42
4.1.4 PageRank 42
4.1.4.1 Incoming PageRank 43
4.1.4.2 Outgoing PageRank 43
4.2 Protection and restoration measures 44
4.2.1 Protection measures 44
4.2.1.1 Degree centrality protection 44
4.2.1.2 PageRank protection 45
4.2.2 Restoration measures 45
4.2.2.1 Degree centrality restoration 45
4.2.2.2 PageRank restoration 46
4.3 Identification of reef clusters 47
4.3.1 Strongly connected components 47
4.3.2 Community detection 49

5 Results and pratical implications **51**
5.1 Variability of the connectivity . . . 51
5.1.1 Connectivity measures . . . 52
5.1.2 Protection and restoration measures . . . 56
5.1.3 Identification of reef clusters . . . 57
5.1.3.1 Strongly connected components . . . 57
5.1.3.2 Community detection . . . 59
5.2 Pratical implications . . . 62
5.3 Limitations . . . 64

6 Conclusion **65**

A Appendices **71**
A.1 Validation of the hydrodynamics . . . 71
A.2 Connectivity measures . . . 83
A.2.1 Local retention . . . 83
A.2.2 Self-recruitment . . . 84
A.2.3 Degree centrality . . . 85
A.2.4 PageRank . . . 87
A.3 Protection and restoration measures . . . 89
A.3.1 Protection measures . . . 89
A.3.2 Restoration measures . . . 91
A.4 Identification of reef clusters . . . 93
A.4.1 Strongly connected components . . . 93
A.4.2 Community detection . . . 96
A.5 Variability of the connectivity . . . 97

1 Introduction

The Great Barrier Reef (GBR) is the world's best known, largest and most complex coral reef ecosystem. In 1982, the GBR was inscribed on the World Heritage List in recognition of its outstanding and universal natural values. The barrier covers an area that is about 2600 km in length and 200 km in width [1]. The GBR is located on the continental shelf off Australia's north-eastern coast (see figure 1.1).

As the largest living structure on the planet, the GBR is incredibly rich, diverse but also under threat. Corals reefs are indeed among the most threatened ecosystems on Earth. They face a number of anthropogenic pressures ranging from overfishing and coastal development to the increase in water temperature and acidity due to global warming [2]. Therefore, because of these factors, the GBR suffers from repeated impacts of cyclones, coral bleaching and outbreaks of the coral-eating crown-of-thorns starfish, losing much of its coral cover in the process [3]. The GBR is then up against a tight and unforgiving deadline. To understand what kind of policy and management actions are required in response, the main values of the GBR must first be understood because it is more than a coral reef [4].

First of all, the GBR is considered as one of the most beautiful places in Australia and it is one on the seven natural wonders of the world. The GBR is of great natural value in enabling the existence of over 600 species of coral. The GBR comprises over 3000 coral reefs which provide continuously a source of food and shelter for about 1700 species of fish and other aquatic animals. This biodiversity is nationally and internationally important for the continued survival of many species. Indeed, the GBR is home to many species of conservation concern and by continuing to damage the GBR those species could gradually disappear [4].

Secondly, the GBR has an important economic value. The economic contribution of the GBR mainly comes from the economic activities that occurs as part of tourism, commercial fishing and aquaculture production, recreational activity and scientific research and management. All these activities support the employment in these sectors and add a significant value to the Australian economy [4].

Finally, the last main value of the GBR is the cultural, social and icon value. Indeed, the value of the GBR extends far beyond what can be measured. Aboriginal and Torres Strait Islander have a strong connection to the GBR as Traditional Owners of the GBR Region. The GBR contributes clearly to Australia's cultural and national identity. Furthermore, many non-material benefits must be considered such as reflection, social relations and recreation and aesthetic experience [4].

Considering all the current threats and understanding the total value of the GBR, efficient reactions and actions have become increasingly crucial. With this in mind, the aim of this master thesis is to simulate the dispersal of coral larvae through the Great Barrier Reef to identify the reefs most likely to support regional recovery processes due to their high connectivity.

Figure 1.1: Overview of the Great Barrier Reef

1.1 Water circulation in the Great Barrier Reef

The water currents flowing through the GBR can act to transport marine organisms from one place to another, resulting in the exchange of individuals between populations in different habitats. Therefore, in order to model the larval dispersal in the GBR, it is vital to have a knowledge and understanding of the water circulation on the GBR continental shelf.

The water circulation on the GBR's continental shelf is strongly influenced by the complex topography and by three main factors whose the relative importance can vary significantly in time and space [5]:

- **Tides**: Tides are an important driver of circulation on the shelf [6]. Tidal currents tend to dominate flow in the North and South of the GBR but not in the centre. Indeed, the magnitude of the tidal currents varies significantly with latitude, and depends mainly on the width of the shelf. Tidal currents are then strongest in the southern GBR, where the shelf is at its widest, weakest in the central GBR, where the shelf is narrowest, and stronger in the northern GBR where the shelf widens again [7].
- **Wind**: The wind around the GBR (both on and off the shelf) is a very significant driver of currents through the GBR shelf [5]. The wind over the GBR is mainly driven by an area of high mean Sea Level Pressure (SLP) at around 30°S, and a low pressure area over the equatorial region (see figure 1.2). This results in a strong SLP gradient over the intervening area, which includes the entire GBR (-10°S, -26°S, 142°E, 155°E), and leads to strong south-easterly trade winds blowing towards the north-west over the GBR (see figure 1.3) [8]. These south-easterly trade winds have a significant seasonal variation. During the austral summer (during which most corals spawn) the low pressure area moves south, resulting in slightly weaker south-easterly trade winds over the GBR, most notably in the north, which becomes dominated by north-westerly monsoonal winds from November to April [7].

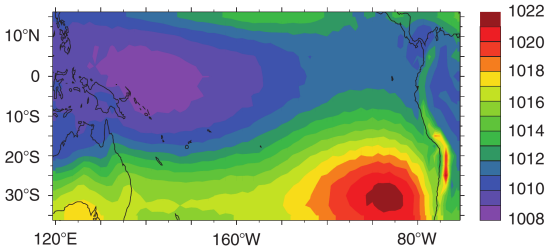

Figure 1.2: Mean Sea Level Pressure (SLP) in mb, time average from 1948 to 2009. Australia is located in the bottom left-hand corner of the map. Credit: [8]

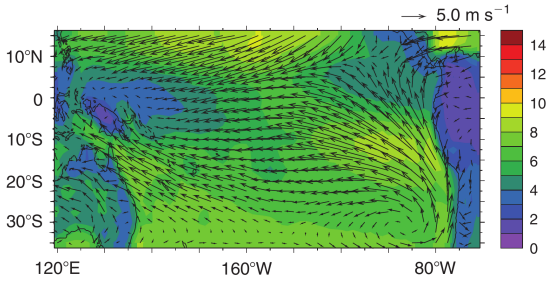

Figure 1.3: Mean wind speed in m/s, time average from 1948 to 2009. Australia is located in the bottom left-hand corner of the map. Credit: [8]

- **Water exchanges with the neighbouring Coral Sea**: In the Coral Sea, a westward flow bifurcates as it approaches the continental slope of the GBR [9]. This results in two currents along the edge of the shelf ; namely the Coral Sea Coastal Current that flows northward from the bifurcation point, and the East Australian Current that flows southward of the bifurcation point (see figure 1.4) [5]. The Coral Sea circulation is thus expected to generate both cross-shelf and a longshore regional sea level gradient on the GBR shelf [10]. To the south of the bifurcation point the longshore surface slope induces a southward net flow on the GBR shelf, which displays strong annual and seasonal fluctuations due to variability in the circulation in the Coral Sea [5]. Similarly, north of the bifurcation point a net northward longshore flow exists on the GBR shelf [11].

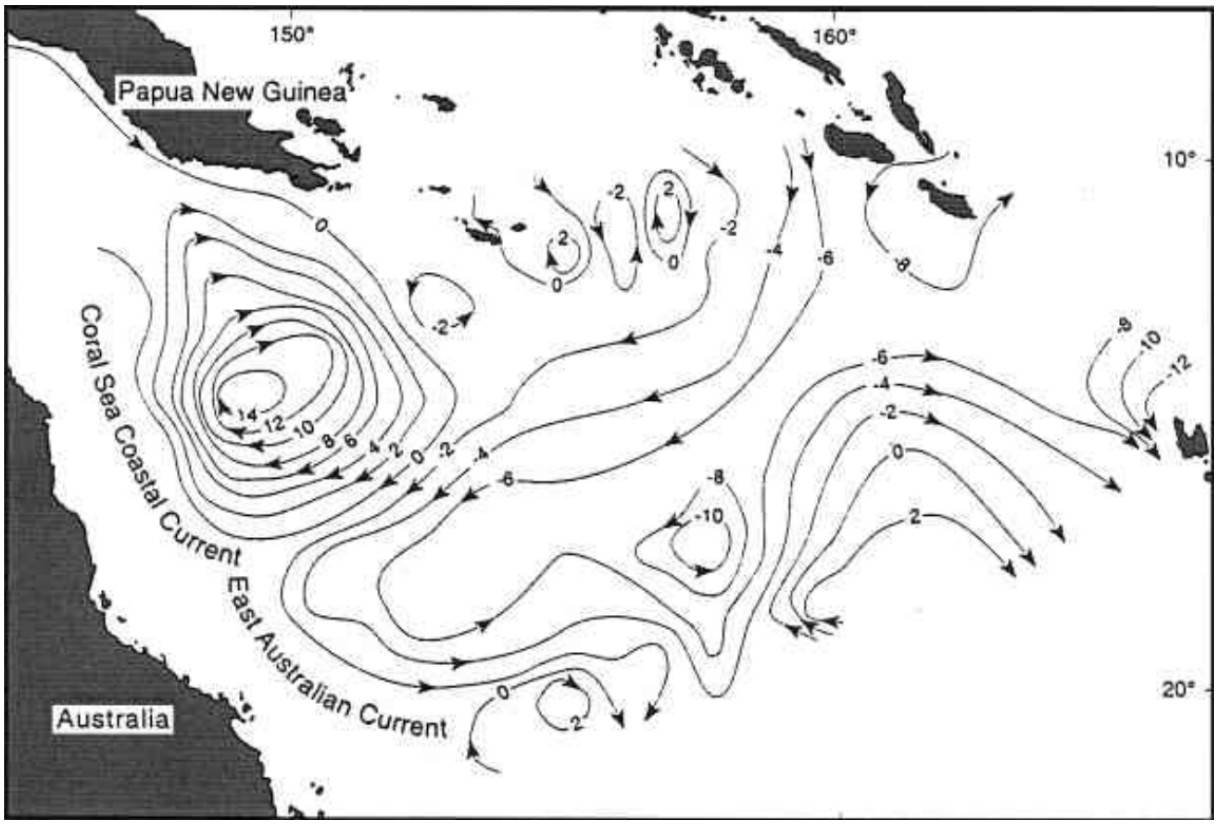

Figure 1.4: Contours of volume transport (in Sv ; 1 Sv = 1000000 m^3/s) in the Western Coral Sea. Credit: [9]

1.2 Connectivity

As said before, the water currents flowing through the GBR can act to transport marine organisms from one place to another, resulting in the exchange of individuals between populations in different habitats. This is known as connectivity, and it is a fundamental process for the dynamics of many marine ecosystems [12]. Connectivity between habitats allow species to spread to new habitats patches [13] [14], repopulate habitats which have been damaged by disturbances [15] [16] and also allows genetic mixing to occur between physically separate populations [14] [17]. The net effect is to increase the persistence and resilience of these populations. Connectivity in the GBR mainly occurs through dispersal of larvae (see figure 1.5).

Modelling larval dispersal requires the use of a hydrodynamic model in order to simulate the currents in the GBR as they are responsible for spreading larvae. Once currents are simulated and validated, larval dispersal can be achieved and then the connectivity between all reefs in the GBR can be studied.

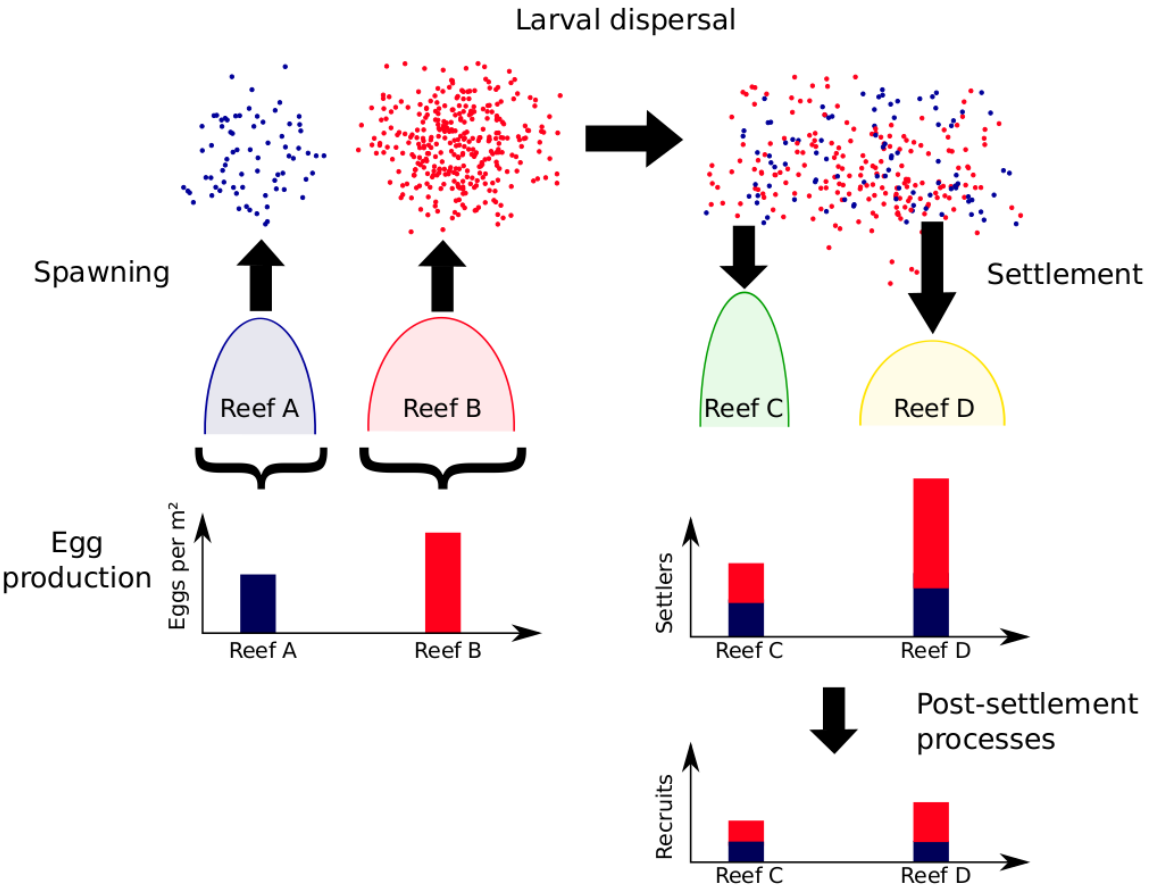

Figure 1.5: Illustration of the process of connectivity. The first step consists in the egg production. These eggs fertilise each other and become larvae. During the second step corals spawn and their larvae are released and transported by currents. This process corresponds to larval dispersal. Larvae are then transported by currents and will potentially settle onto other reefs (reefs C and D). Actual recruits are less than settlers because of post-settlement mortality. Reefs A and B are assumed connected to reefs C and D. Credit: [7]

1.3 Objectives

Several works have already been made in order to model larval dispersal in the Great Barrier Reef (PhD thesis by Christopher Thomas, [7]) or in the Florida Coral Reef Tract (master thesis by Charles Frys, [18]). This thesis is inspired by these works and follows the same structure with the objective of identifying some connectivity patterns.

However, these connectivity patterns might change over the years due to annual changes such as meteorological fluctuations or variations in oceanographic circulation. Therefore, some reefs well connected to each other in a particular year might be isolated in another year. It is thus essential to have a broader overview of the connectivity in the GBR over the years to get more reliable data.

With this in mind, the aim of this thesis is to study the variability of marine connectivity in the Great Barrier Reef between 2008, 2010 and 2012. In order to do that, here are the steps and goals that must be achieved:

- Simulation of currents in the GBR with a hydrodynamic model (SLIM)
- Simulation of larval dispersal in the GBR with a Lagrangian particle tracker
- Extraction of useful information from the connectivity matrix generated by the Lagrangian particle tracker in order to define some connectivity patterns in the GBR
- Analysis of the variability of these connectivity patterns between 2008, 2010 and 2012

The final results could be used to inform marine management strategies for achieving restoration and protection of the GBR. Knowing isolated areas and reef clusters that are well connected to each other could allow more effective placement of Marine Protected Areas (MPAs). MPAs are marine reserves within which damaging anthropogenic influences as fishing and tourism are limited [19]. With an appropriate knowledge of larval dispersal patterns, marine managers could use MPAs to protect habitats with high potential to export larvae to surrounding habitats [20] [21] [22], as well as ensuring that separate MPAs are also well connected to each other, thus increasing the resilience of the MPA network itself [23] [24].

2 Simulating currents with an unstructured mesh ocean model

To study the connectivity in the GBR, we first need to simulate the ocean currents in the GBR. This simulation is made by using a hydrodynamic model able to simulate realistic large-scale circulation in the region and able to resolve small-scale flow features down to the scale of reefs.

2.1 Hydrodynamic model

The hydrodynamic model used is SLIM (Second-generation Louvain-la-Neuve Ice-ocean Model) which is a model based on the finite element method allowing the use of unstructured grids. The resolution can thus vary in space. A higher resolution can be used where small-scale flow features are important (i.e. in coastal regions and around the reefs) while a coarser resolution can be used in regions far away from regions of interest or in more uniform areas. This model has already been successfully applied to several coastal oceans and estuaries around the world including the GBR.

SLIM is a discontinuous Galerkin finite element method which resolves the water elevation η and depth-integrated velocity $\mathbf{u}$ by solving the shallow water equations:

$$\frac{\partial \eta}{\partial t} + \nabla \cdot (H\mathbf{u}) = 0 \tag{2.1}$$

$$\frac{\partial \mathbf{u}}{\partial t} + \mathbf{u} \cdot \nabla \mathbf{u} = -f\mathbf{e}_z \times \mathbf{u} - g\nabla\eta - C_{BD}|\mathbf{u}|\mathbf{u} + \frac{\boldsymbol{\tau}}{\rho H} + \frac{1}{H}\nabla \cdot [H\nu(\nabla \mathbf{u})] \tag{2.2}$$

where H is the water column depth in m (defined as $H = h + \eta$ where h is a reference depth level and η is the variation from this depth, see figure 2.1), $\mathbf{u}$ is the depth-integrated water velocity, f is the Coriolis factor, $\mathbf{e}_z$ is a unit vector pointing vertically upwards, C_{BD} is the bottom stress coefficient, $\boldsymbol{\tau}$ is the surface wind stress, g is the gravitational acceleration, ρ is the water density and ν is the horizontal eddy viscosity.

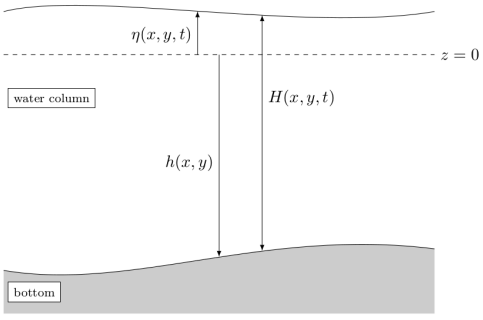

Figure 2.1: Vertical cut illustrating $\eta(x, y, t)$ the elevation above the reference level ($z = 0$), the bathymetry $h(x, y)$ and the water depth $H = \eta + h$. Credit: [25]

2.2 Data and parameters

The shallow water equations contain several parameters which depend on the region of interest. These parameters must be determined in order to solve these equations.

- The bathymetry h of the GBR is illustrated on figure 2.2. A minimum depth is set at h = 5m in order to be sure that the entire domain is under water at all time.

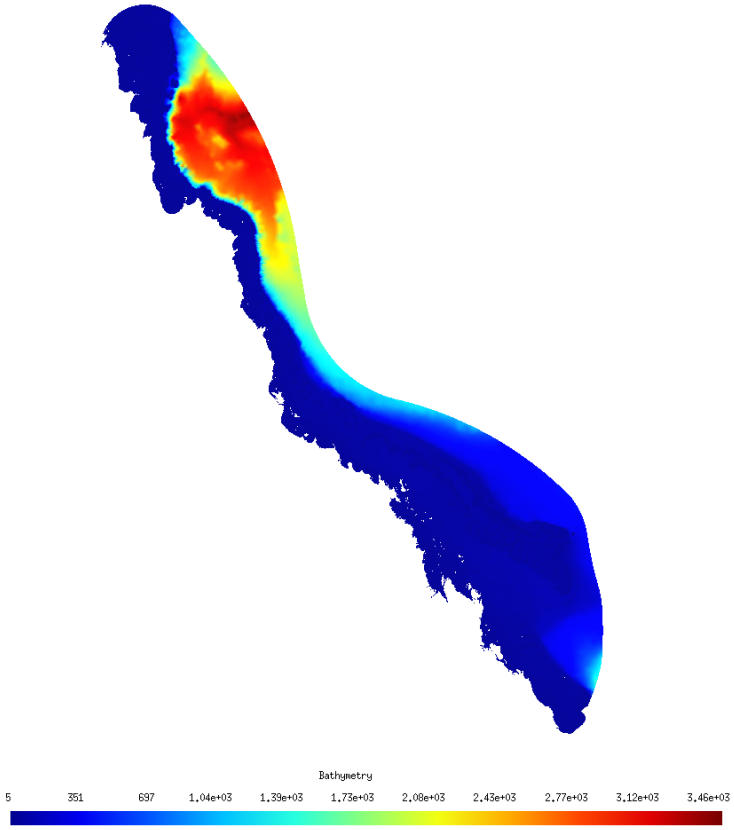

Figure 2.2: Bathymetry of the GBR with a minimum depth set at h = 5m.

- The Coriolis factor f is calculated as follows:

$$f = 2\Omega_T \sin\phi \tag{2.3}$$

where Ω_T is the angular rotation speed of the Earth which is equal to $7.2921 \cdot 10^{-5}[rad/s]$ and ϕ corresponds to latitudes.

- The bottom stress coefficient is defined as $C_{BD} = \frac{g}{C^2 H}$ where g is the gravitational acceleration, C is the Chezy coefficient and H is the water column depth.
The Chezy coefficient is defined as $C = \frac{H^{1/6}}{n}$ where n is the Manning coefficient. The Manning coefficient was set at n = 0.25 $[m^{1/3}/s]$ on reefs and n = 0.025 $[m^{1/3}/s]$ elsewhere. The second value is a typical value for sandy or muddy sea beds [26] while the first value is ten times higher as reefs are known to have particularly rough surface [27].

- The surface wind stress $\boldsymbol{\tau}$ exerted by the atmosphere on the sea is calculated as follows:

$$\boldsymbol{\tau} = \rho_{air} C_D |\mathbf{u_{10}}| \mathbf{u}_{10} \tag{2.4}$$

  where ρ_{air} is the air density, C_D is the drag coefficient and $\mathbf{u}_{10}$ is the wind speed at 10 meters above the sea surface in [m/s] [28].
  The drag coefficient C_D is parameterised by using a formula which includes the wind speed term [29]:

$$C_D = 0.001 \left(\alpha + \beta |\mathbf{u}_{10}|\right) \tag{2.5}$$

  where $\alpha = 0.63$ and $\beta = 0.066$ [s/m]. This parametrisation is applicable for wind speeds in the range of 3-21 [m/s] [30] which is commonly found over the GBR.

- The horizontal eddy viscosity ν is used in order to account for the effect of unresolved turbulent features. In Smagorinsky's parametrisation ν is dependent on the local mesh element size Δ and the flow structure [31]:

$$\nu = (C_S \Delta)^2 \sqrt{2\left(\frac{\partial u}{\partial x}\right)^2 + 2\left(\frac{\partial v}{\partial y}\right)^2 + \left(\frac{\partial u}{\partial y} + \frac{\partial v}{\partial x}\right)^2} \tag{2.6}$$

  where (x, y) are cartesian horizontal coordinates, (u, v) are the depth-integrated water velocities and C_S is a constant, equal to 0.1 [32].

The time stepping method used to resolve shallow water equations is an implicit Runge-Kutta scheme using Newton-Raphson iteration. Regarding to the spatial discretisation, the Discontinuous Galerkin finite element method is used for both the free surface elevation and the velocity field [33].

2.3 Unstructured mesh

As already mentioned above, SLIM is a hydrodynamical model based on finite element method. The main advantage of this method is that it allows the use of unstructured grids. The computational grid can therefore be refined arbitrarily in the areas of interest thus focusing the computational power where it is needed, without the need of nested grids. Therefore, it allows multi-scale modelling as the spatial resolution may vary greatly within the same grid and a single model is able to resolve both the large-scale features, such as in the open sea, but also small-scale phenomena in shallow areas, such as near the coasts [33].

The mesh used spanned the entire shelf, despite the fact that the regions under study were generally limited to areas covering only one third to half of the GBR. This is because the forcings applied at the boundaries (see section 2.4) are less accurate on the shelf than at the shelf break [7].

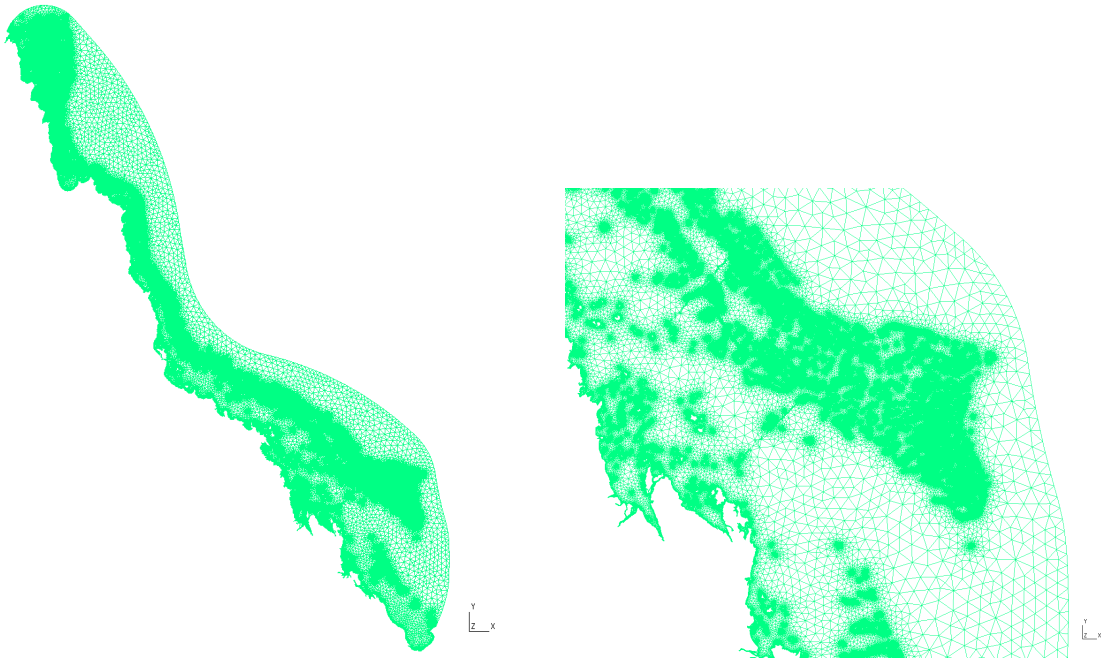

Figure 2.3: Illustration of the mesh of the GBR and a zoom on the south of the GBR where the variation of the resolution can be seen. Higher resolution is used for coastal areas and reefs while a coarser resolution is used for more uniform areas. The mesh has about $2.5 \cdot 10^6$ elements. The mesh was generated using the open source meshing software Gmsh [34].

2.4 Model forcings

The aim of the hydrodynamic model was to simulate realistic circulation conditions on the GBR shelf. In order to do that, three separate external forcings were applied to account for effects of tides, wind and water exchanges with the Coral Sea, corresponding to the three main drivers of circulation in the GBR (see section 1.1) [7].

- **Tidal forcing**: This forcing was imposed by using OSU TOPEX/Poseidon Global Inverse Solution dataset [25] which gives the amplitude and phase of the main tidal components on a 1/4° resolution grid. These were used to reconstruct tidal elevation and velocity. The tidal forcing was imposed at the model open boundary (see figure 2.4).
- **Wind forcing**: The wind data come from NOAA (National Oceanic and Atmospheric Administration) and correspond to time-series data of the wind speed at 10 meters above sea surface. This forcing was imposed through the surface wind stress $\boldsymbol{\tau}$ (see equations 2.4 and 2.5) on the entire GBR.
- **Water exchanges with the Coral Sea**: This forcing was imposed by using currents data from HYCOM (HYbrid Coordinate Ocean Model). The data provide 3D currents on a 1/25° grid. As the version of SLIM used is a 2D model, it is necessary to compute a depth-averaged velocity on each point of the mesh. This forcing was imposed at the model open boundary (see figure 2.4).

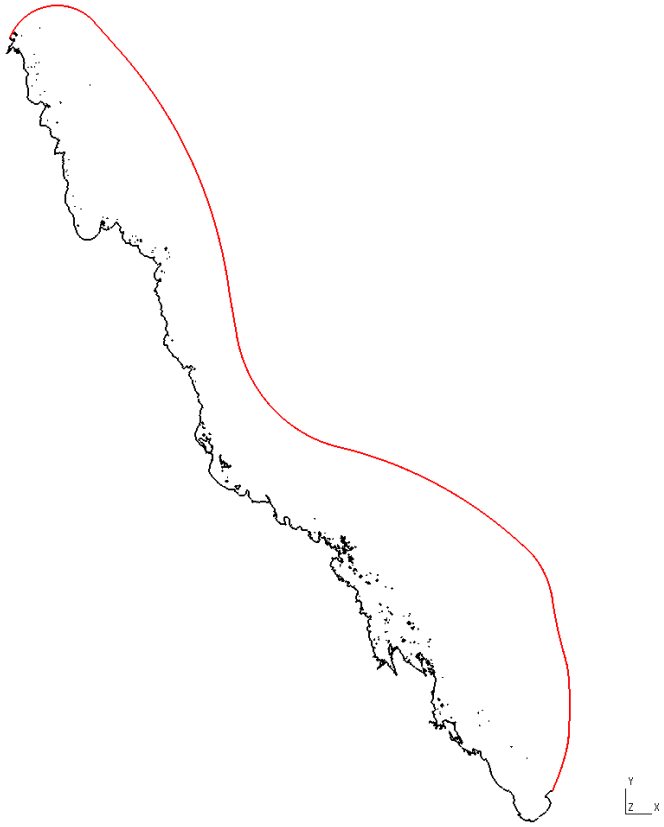

Figure 2.4: Illustration of the GBR with the coasts in black and the open sea boudary in red.

To improve the results inside the domain and get currents from SLIM close enough to currents from HYCOM, a relaxation term was added to the model. The aim of this term is to keep velocities from SLIM close enough to velocities from HYCOM in areas where HYCOM is more accurate than SLIM. Those areas mainly correspond to deep areas where a 2D model using shallow water equations is not sufficiently precise [18]. The global circulation forcing $\mathbf{F}_{gc}$ is:

$$\mathbf{F}_{gc} = \gamma(\mathbf{u}_* - \mathbf{u}) \tag{2.7}$$

where $\mathbf{u}_*$ is the depth-averaged velocity obtained from the addition of velocities from HYCOM with velocities from the tidal data and γ is equal to $1/\tau$ where τ is the relaxation time. In the deep ocean, τ is defined such as it is longer than the timescale of the dominant tidal wave [35].

The parameter γ giving the strength of the relaxation term was defined as follows:

- $\gamma = 0$ in areas shallower than 50 meters. It means that there is no relaxation in these areas and that SLIM is assumed to be precise enough.
- In deeper areas, γ is a function of the depth (see figure 2.5).

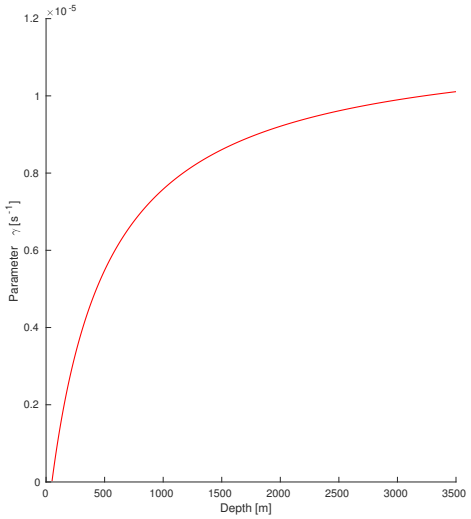

Figure 2.5: Value of the parameter γ in areas deeper than 50 meters.

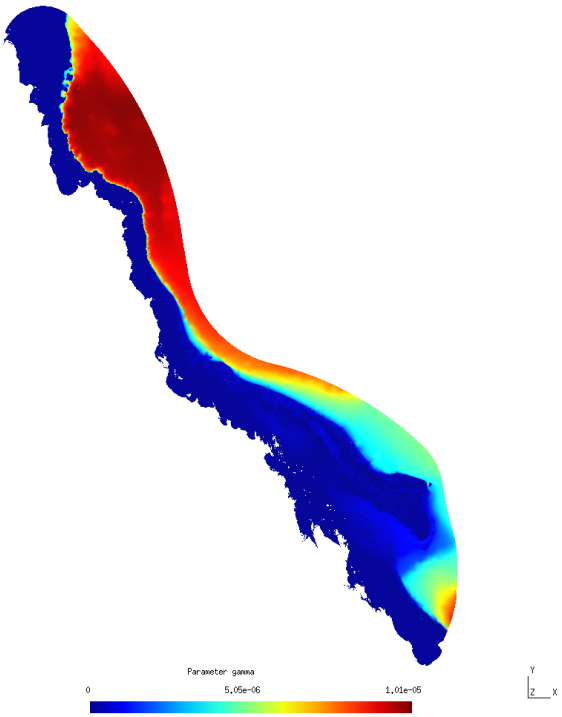

Figure 2.6: Value of the parameter γ giving the strength of the relaxation term. In areas deeper than 50 meters, γ varies with the depth. This map is indeed similar to the figure 2.2 showing the bahymetry of the GBR.

2.5 Validation of the hydrodynamics

The water elevation η and depth-integrated veclocity $\mathbf{u}$ are the outputs of the hydrodynamic model. An illustration of these outputs is shown on figures 2.7 and 2.8.

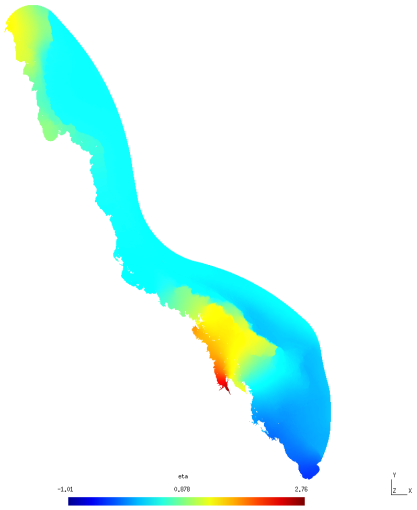

(a) Water elevation on 01/12/2010 at 00:00

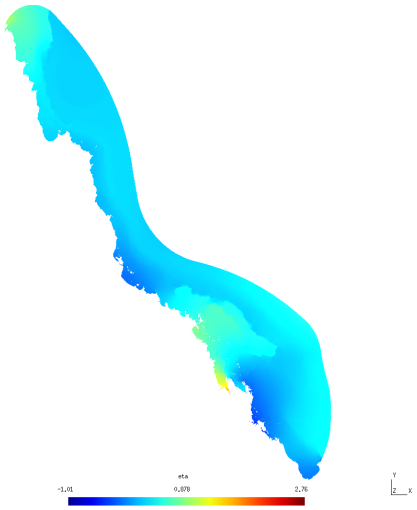

(b) Water elevation on 01/12/2010 at 02:00

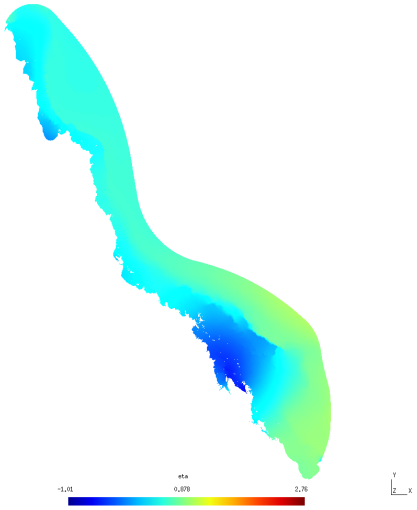

(c) Water elevation on 01/12/2010 at 04:00

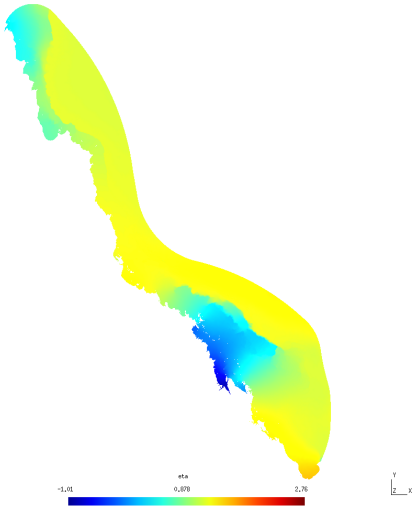

(d) Water elevation on 01/12/2010 at 06:00

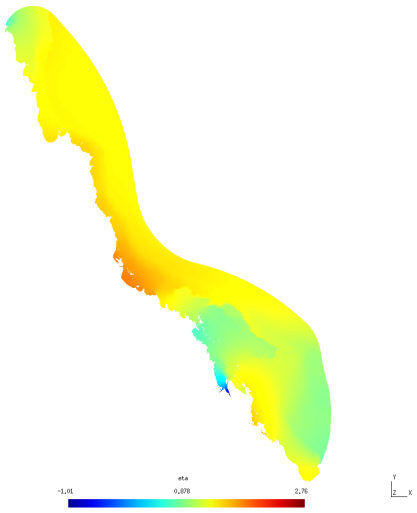

(e) Water elevation on 01/12/2010 at 08:00

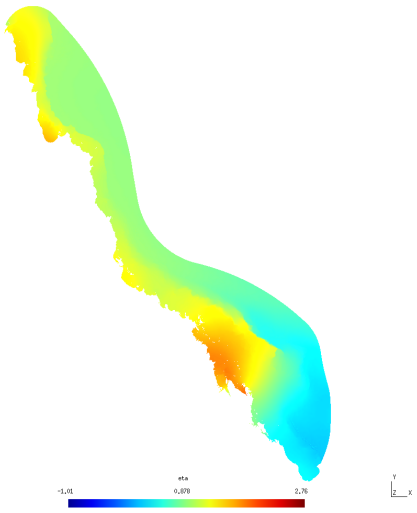

(f) Water elevation on 01/12/2010 at 10:00

Figure 2.7: Pictures showing the water elevation in the GBR at 6 different points in time.

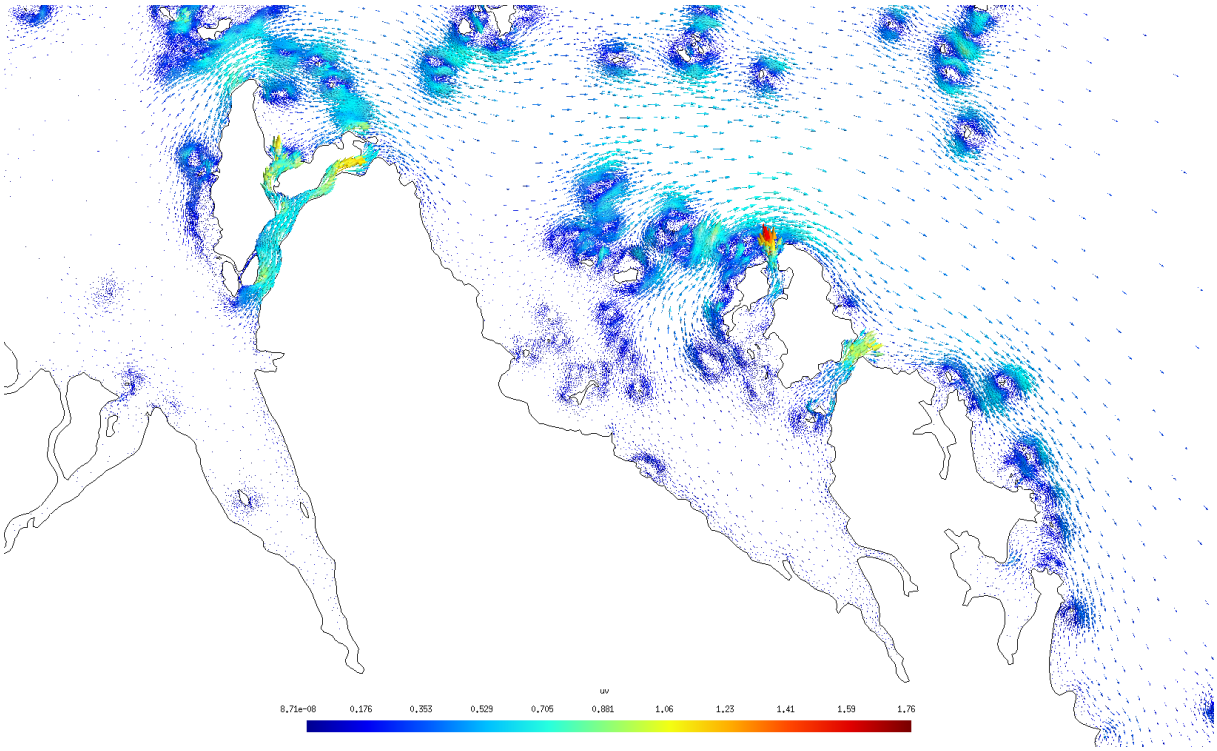

Figure 2.8: Depth-integrated velocity on 01/12/2010 at 00:00. Only a part of the south of the GBR is shown to better visualise the amplitude and the direction of the depth-integrated velocity on each element of the mesh.

However, before using these outputs of the hydrodynamic model as inputs of the Lagrangian particle tracker (see section 3), we need to ensure that the depth-integrated velocity and water elevation, $\mathbf{u}$ and $H = h + \eta$, are realistic. In order to do that, the hydrodynamics simulated by the model were validated with respect to time-series data of observed currents and/or HYCOM. The positions of the mooring sites is shown on figure 2.9.

The outputs of the hydrodynamic model are compared with observation data, HYCOM data and/or HYCOM data coupled with tides data for each mooring site. The comparisons include current speeds, current amplitudes, current directions and water elevations. The 2012 results can be seen on figures 2.10, 2.11, 2.12, 2.13, 2.14 and 2.15. The 2008 and 2010 results are included in the appendices (see section A.1).
Generally, the south of the GBR is well modelled and the model can be considered as reliable in this region. Indeed, there is a good agreement between currents from the hydrodynamic model and real hydrodynamics in this region. Although there are more pronounced differences between currents from SLIM and real observations in the center of the GBR, the middle region has also acceptable results. However, the north of the GBR is not well modelled and currents from SLIM do not replicate the real hydrodynamics of the north region.

Number	Name	Code
1	Lizard Shelf	LSH
2	Palm Passage	PPS
3	Yongala	YON
4	Capricorn Channel	CCH
5	One Tree East	OTE
6	Heron South	HIS

Table 2.1: Name of the validation points (see figure 2.9).

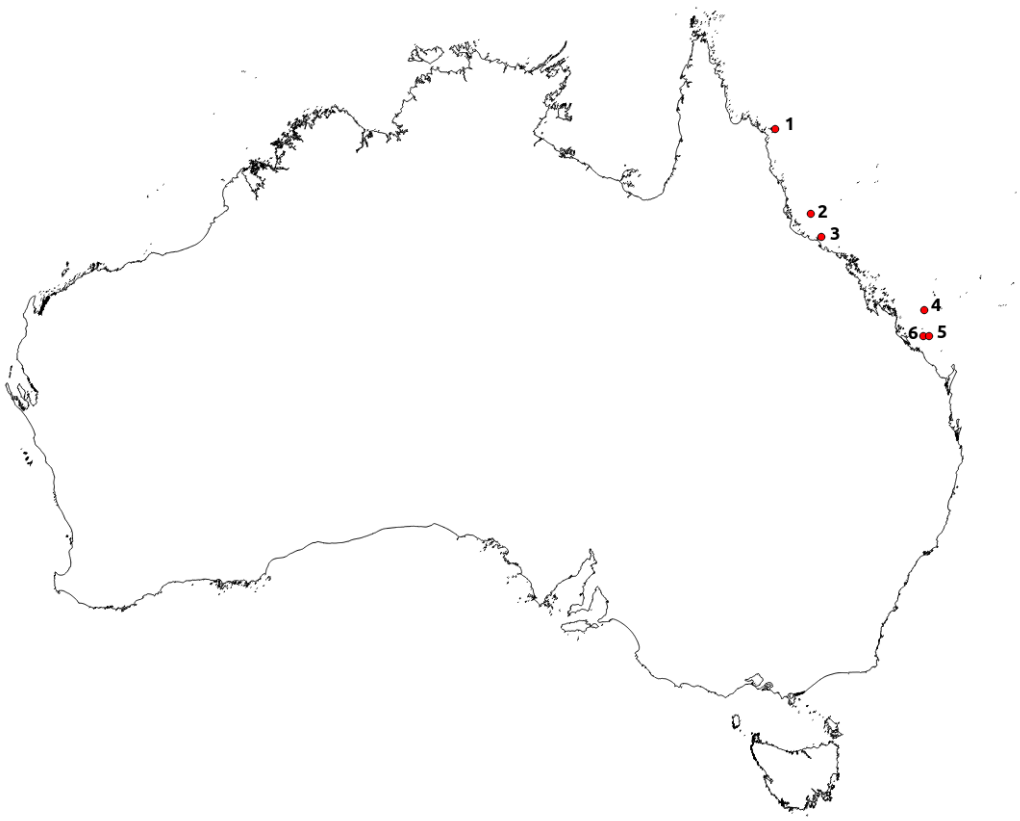

Figure 2.9: Location of the validation points.

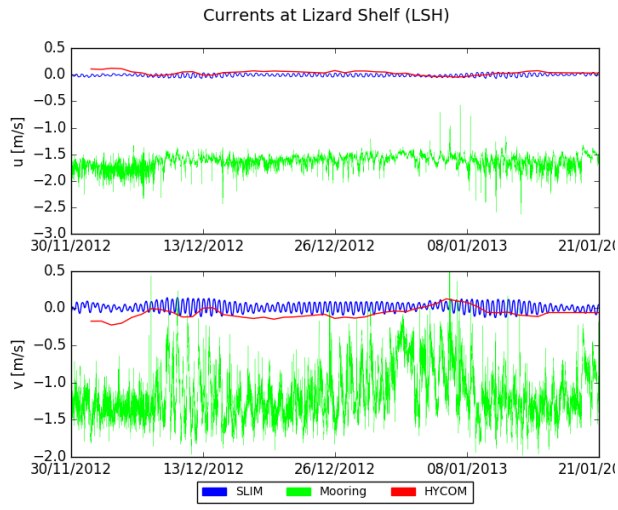

(a) Current speeds

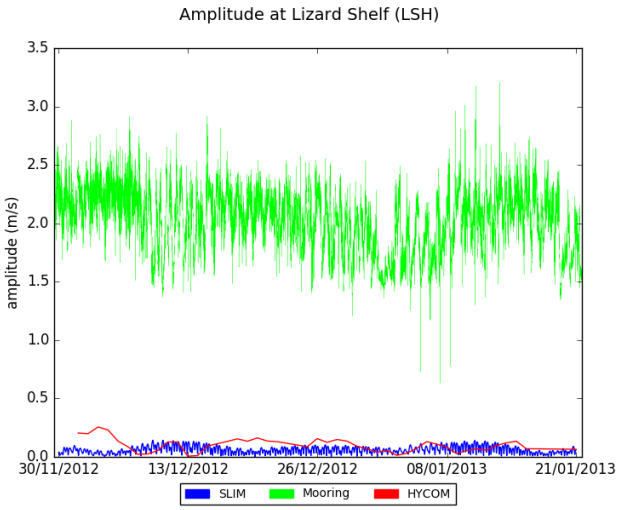

(b) Current amplitudes

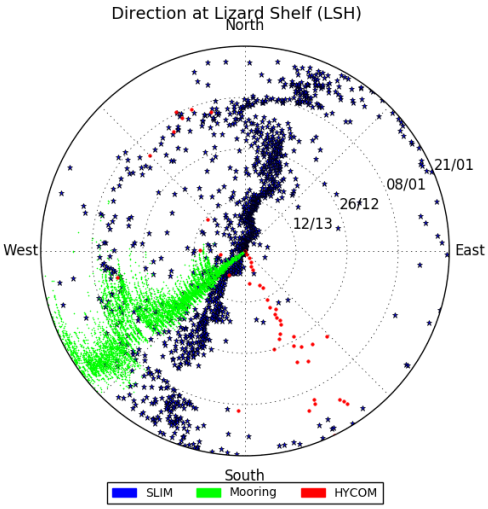

(c) Current directions

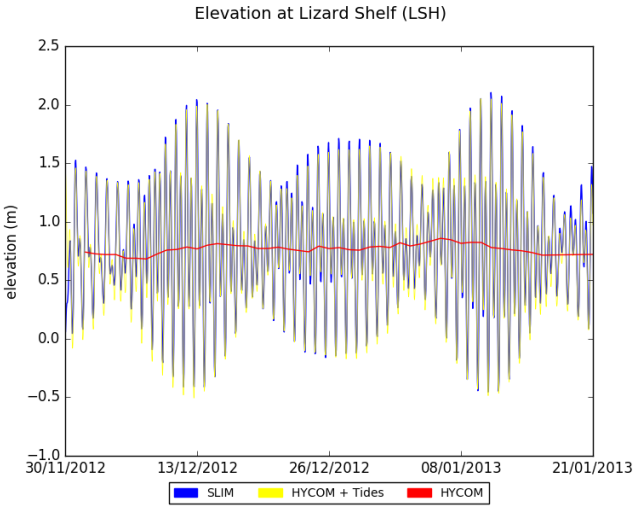

(d) Water elevations

Figure 2.10: Current speeds, current amplitudes, current directions and water elevations of validation point 1 (Lizard Shelf) in 2012. The first validation point located in the north of the GBR is not well modelled by SLIM. Indeed, currents from the hydrodynamic model are weak with almost zero speed while real observations show that there are strong currents having a speed of approximately 1.5 [m/s] in this region. Furthermore, observation data show a marked tendency for the current directions while currents from SLIM do not follow this trend. The hydrodynamic model clearly does not replicate the real hydrodynamics of the region. This is partly due to the fact that HYCOM data are not correct in this region.

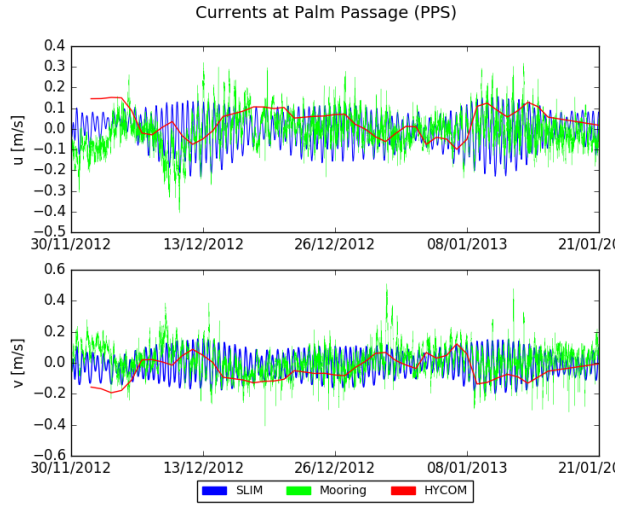

(a) Current speeds

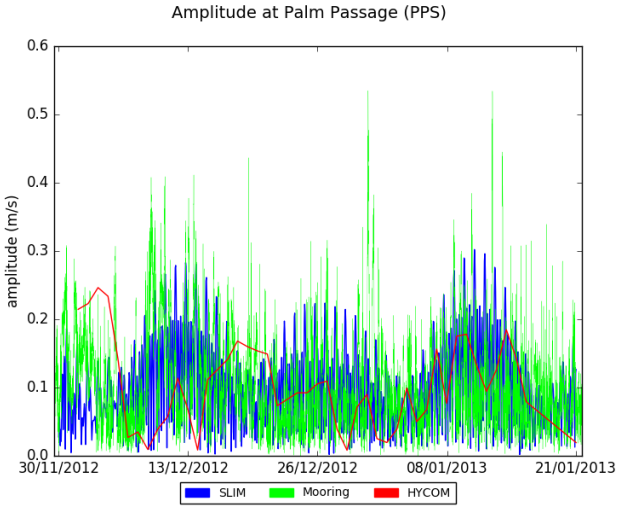

(b) Current amplitudes

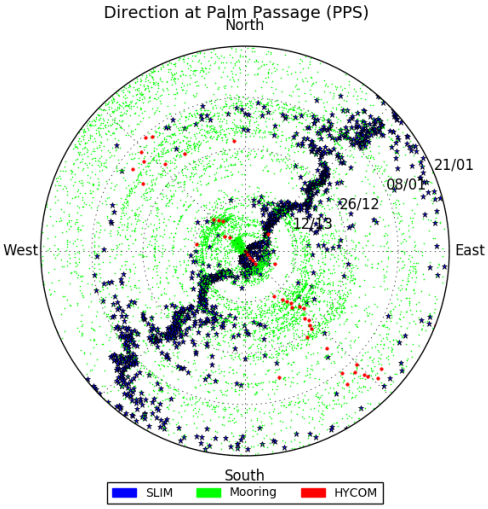

(c) Current directions

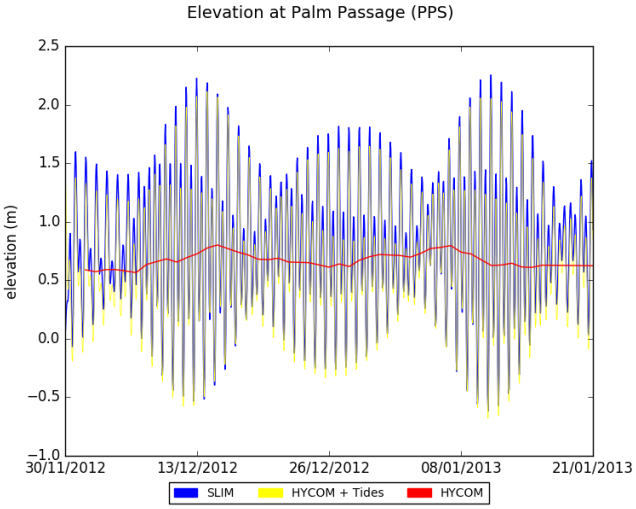

(d) Water elevations

Figure 2.11: Current speeds, current amplitudes, current directions and water elevations of validation point 2 (Palm Passage) in 2012. The second validation point located in the center of the GBR is better modelled than the first one. Figures show a relatively good agreement between currents from SLIM and real currents although current amplitudes from SLIM are sometimes a bit weaker than real amplitudes. Nevertheless, current directions from SLIM show a more marked tendency than the real current directions.

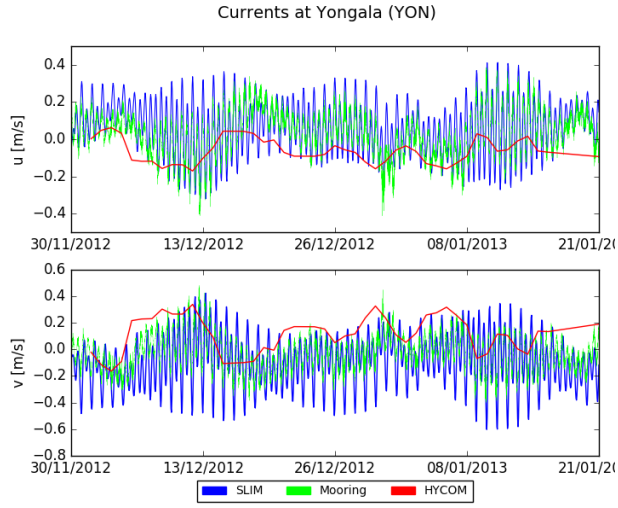

(a) Current speeds

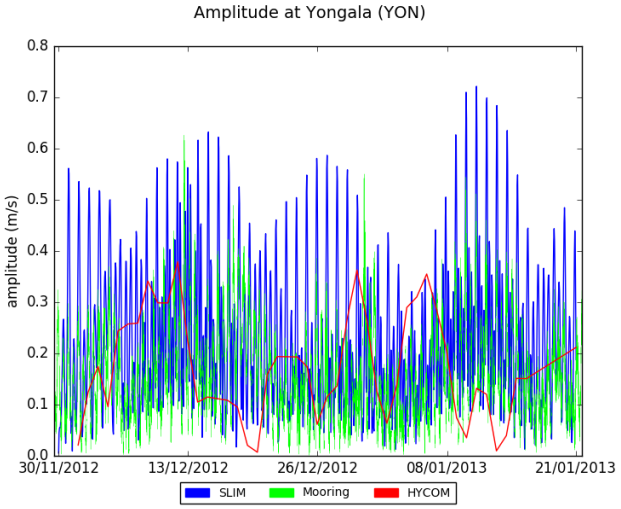

(b) Current amplitudes

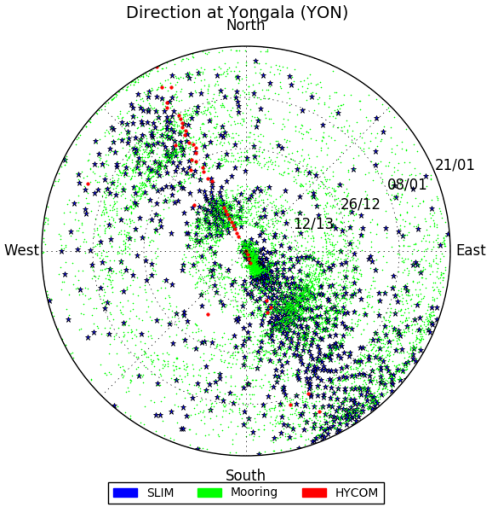

(c) Current directions

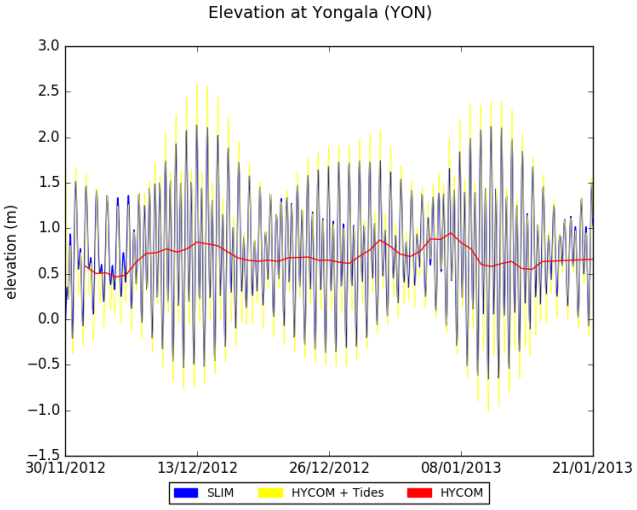

(d) Water elevations

Figure 2.12: Current speeds, current amplitudes, current directions and water elevations of validation point 3 (Yongala) in 2012. Figures of the third validation point located in the center of the GBR show a similar level of agreement than the second validation point. Unlike the second validation point, current amplitudes from SLIM seem to be a bit stronger than real current amplitudes.

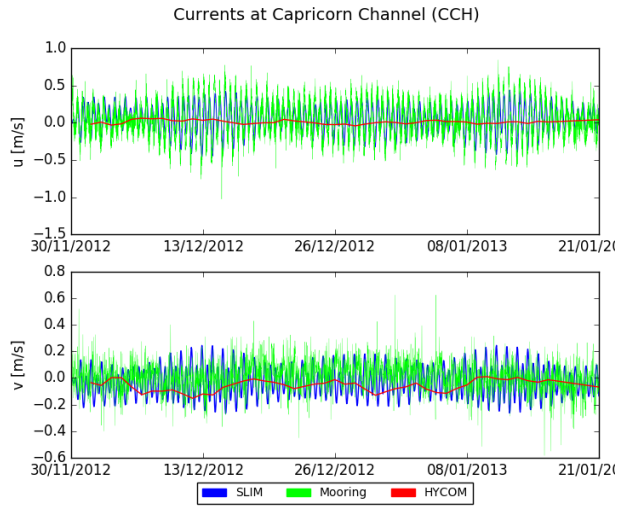

(a) Current speeds

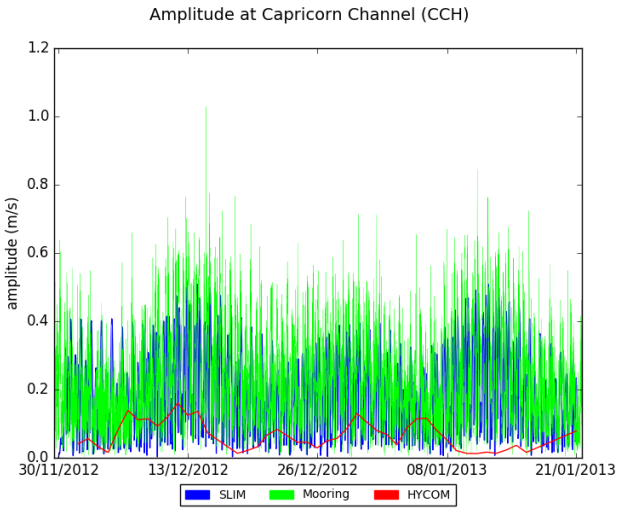

(b) Current amplitudes

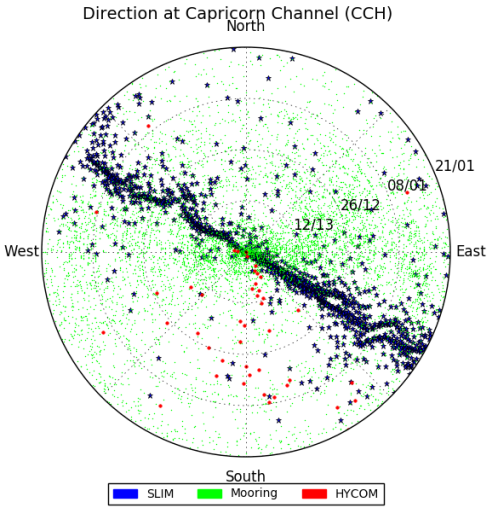

(c) Current directions

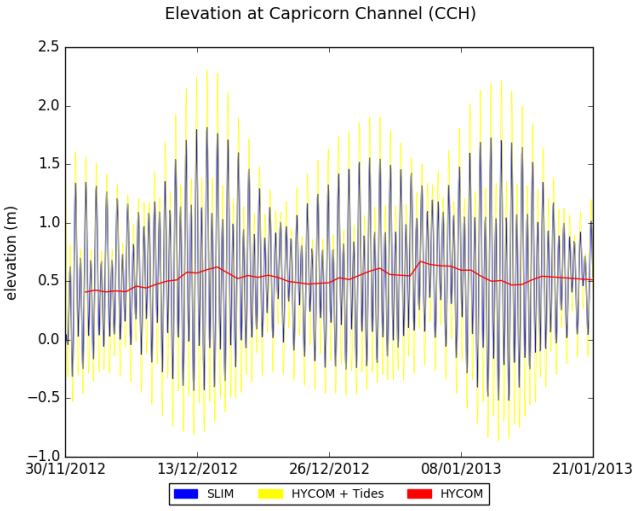

(d) Water elevations

Figure 2.13: Current speeds, current amplitudes, current directions and water elevations of validation point 4 (Capricorn Channel) in 2012. The fourth validation point located in the south of the GBR is well modelled. Current speeds and amplitudes from SLIM roughly correspond to real observations. Nevertheless, current directions from SLIM still show a too marked tendency.

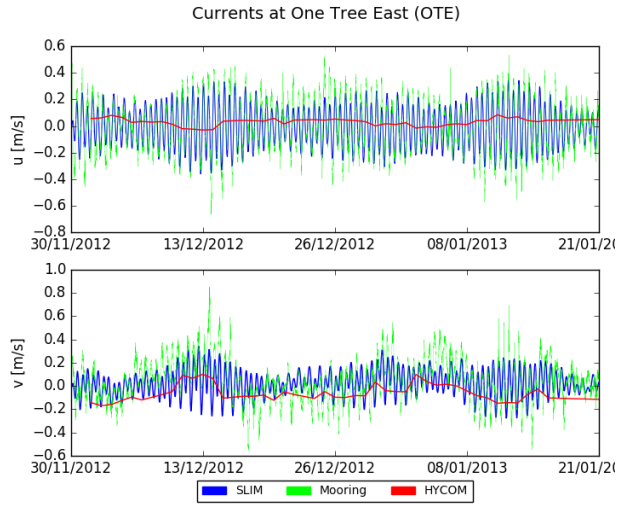

(a) Current speeds

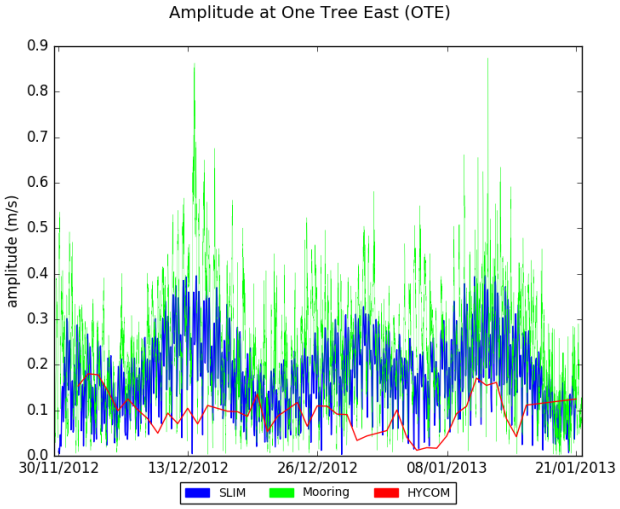

(b) Current amplitudes

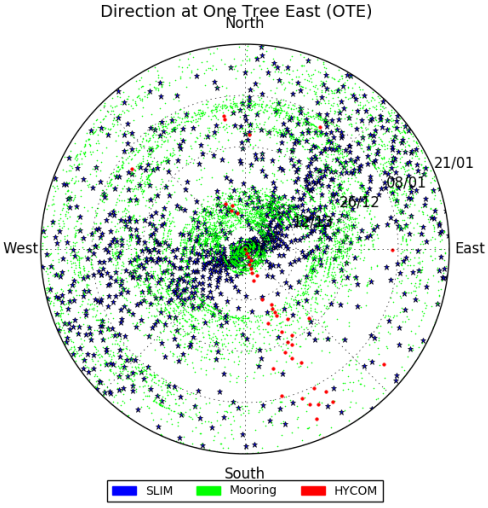

(c) Current directions

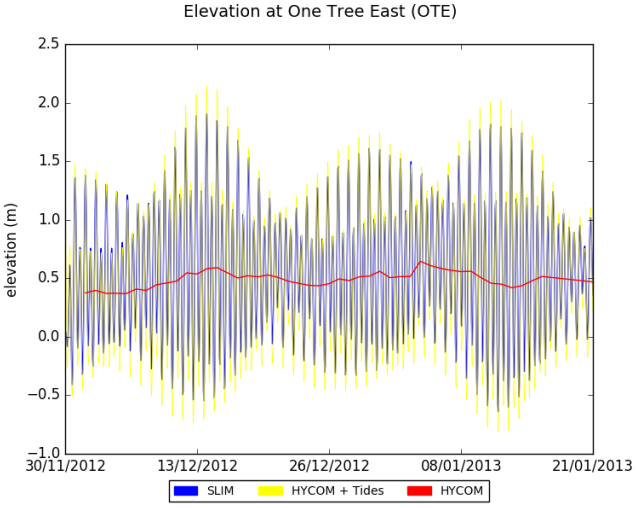

(d) Water elevations

Figure 2.14: Current speeds, current amplitudes, current directions and water elevations of validation point 5 (One Tree East) in 2012. The fifth validation point located in the south of the GBR is relatively well modelled. However, current amplitudes from SLIM seem to be weaker than the real current amplitudes.

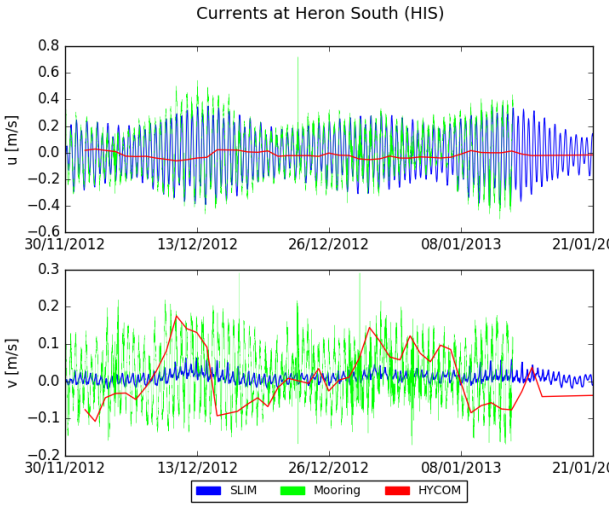

(a) Current speeds

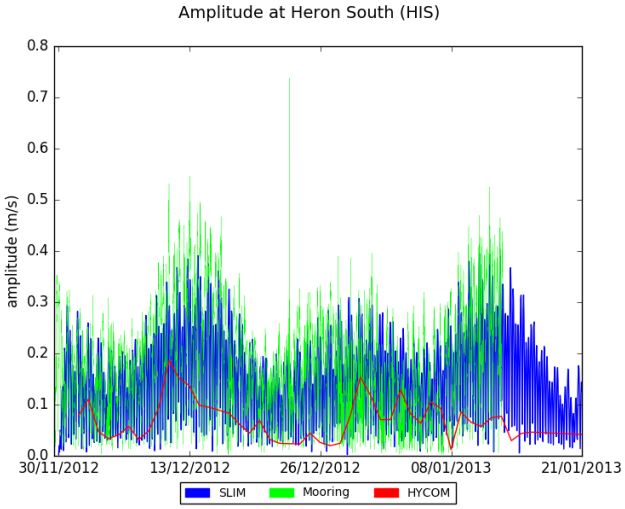

(b) Current amplitudes

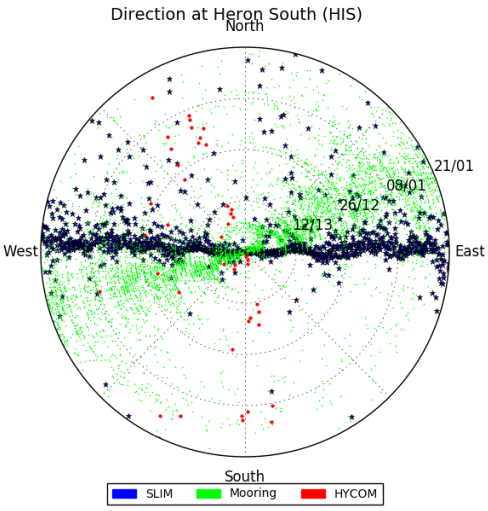

(c) Current directions

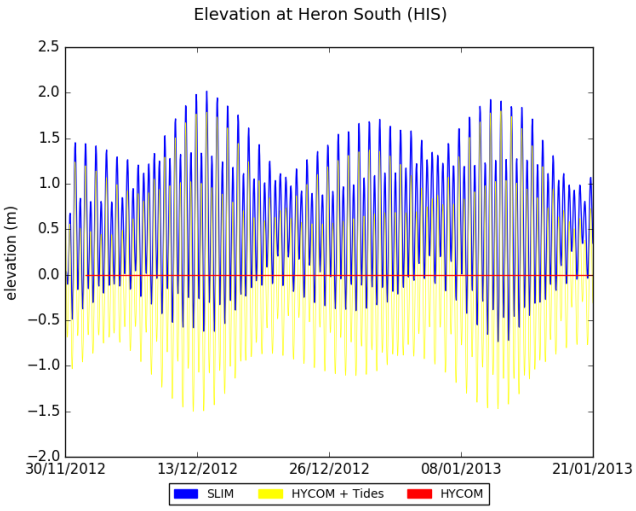

(d) Water elevations

Figure 2.15: Current speeds, current amplitudes, current directions and water elevations of validation point 6 (Heron South) in 2012. All features of the last validation point located in the south of the GBR are well modelled except the northward velocity v. There is also a slight difference between the current directions from SLIM and real current directions.

3 Simulating larval dispersal with a Lagrangian particle tracker

The dispersal and settlement of larvae was modelled by considering many "virtual larvae" released into the domain as autonomous, buoyant, individual organisms, passively transported by the ocean currents and subject to some very simple biological processes [36].

3.1 Physical parameters

Transport of larvae was modelled using a random walk formulation of the 2D advection-diffusion equation [37] [38]:

$$\mathbf{x}_{n+1} = \mathbf{x}_n + \mathbf{v}_n \Delta t + \frac{\mathbf{R}_n}{\sqrt{r}} \sqrt{2K\Delta t} \tag{3.1}$$

$$\mathbf{v}_n = \left(\mathbf{u} + \frac{K}{H} \nabla H + \nabla K \right) |_{\mathbf{x}_n} \tag{3.2}$$

where $\mathbf{x}_n$ and $\mathbf{x}_{n+1}$ are the particle positions at time iterations n annd $n+1$ respectively, Δt is the time difference between iterations, $\mathbf{R}_n$ is a horizontal vector of zero-mean random numbers with variance $r \equiv < R^2 >$ $\left(\frac{\mathbf{R}_n}{\sqrt{r}} \right.$ is a vector of random numbers with unit variance$\Big)$, K is the horizontal diffusivity coefficient, H denotes water depth and $\mathbf{u}$ is the depth-averaged horizontal water velocity supplied by the ocean model.

The horizontal diffusivity coefficient K is calculated as follows:

$$K = \alpha \Delta^{1.15} \qquad \text{where } \alpha = 0.041 m^{0.85} s^{-1} \text{ and } \Delta \text{ is the local element size} \tag{3.3}$$

The parameter α is calibrated for coastal waters in the GBR [27]. This parametrisation of diffusivity has a dependence on the local mesh resolution. As larger elements have a greater range of unresolved water motion, the horizontal diffusivity coefficient K is bigger for these elements [7].

The position $\mathbf{x}_{n+1}$ of a particle is found by adding two terms to the previous position $\mathbf{x}_n$ of the particle [18]:

- The first term $\mathbf{v}_n \Delta t$ corresponds to the movement resulting from the currents calculated with SLIM. $\mathbf{v}_n$ does not only depend on the instantaneous depth-averaged horizontal water velocity. $\mathbf{v}_n$ is calculated by adding a correction velocity $\mathbf{u}' = \mathbf{v} - \mathbf{u}$ depending on the diffusivity and water depth gradients. This correction velocity tends to transport particles towards region of increasing depth and diffusivity [37].
- The second term $\frac{\mathbf{R}_n}{\sqrt{r}} \sqrt{2K\Delta t}$ is a stochastic term that characterises the effect of turbulence of the movement for particles. This effect tends to increase where the diffusivity coefficient is higher (i.e. in larger elements).

The Lagrangian particle tracker is a module of SLIM which uses the outputs of the hydrodynamic model (i.e. the depth-integrated velocity and water elevation, $\mathbf{u}$ and $H = h + \eta$) as inputs.

3.2 Biological parameters

Corals can reproduce asexually and sexually. The asexual reproduction occurs when the coral reaches a certain size and divides. This process continues throughout the animal's life [39]. This kind of reproduction corresponds to a coral cloning which expands the existing colony on a same reef. The asexual reproduction does not concern the larval dispersal.

The sexual reproduction occurs once a year as a mass synchronised event when entire colonies of coral reefs simultaneously release their gametes into the ocean. After this event called mass coral spawning, the gametes rise slowly to the ocean surface where the process of fertilisation occurs to give coral larvae. The mass coral spawning occurs on the Great Barrier Reef during summer, generally in November or December (see table 3.1). The exact spawning date depends on several parameters such as the water temperature and the lunar cycle (spawning occurs around full moon) [40].

Year	Spawning date	Simulation period
2008	17^{th} of November	17/11/2008 - 17/12/2008
2010	26^{th} of November	26/11/2010 - 26/12/2010
2012	4^{th} of December	04/12/2012 - 03/01/2013

Table 3.1: Spawning dates and period of larval dispersal simulations

Coral larvae are then transported by currents. After floating at the surface they swim back down to the bottom where they will settle onto a reef if conditions are favorable. Larvae usually settle within a time frame of two days to three weeks [41]. Once settled larvae grow into a new coral colony.

In addition to physical parameters modelling the transport of particles, a few biological parameters are used to complete the model and to account for the life histories of the virtual larvae [7]. The coral species chosen for the modelling is *Acropora millepora* (see figure 3.1).

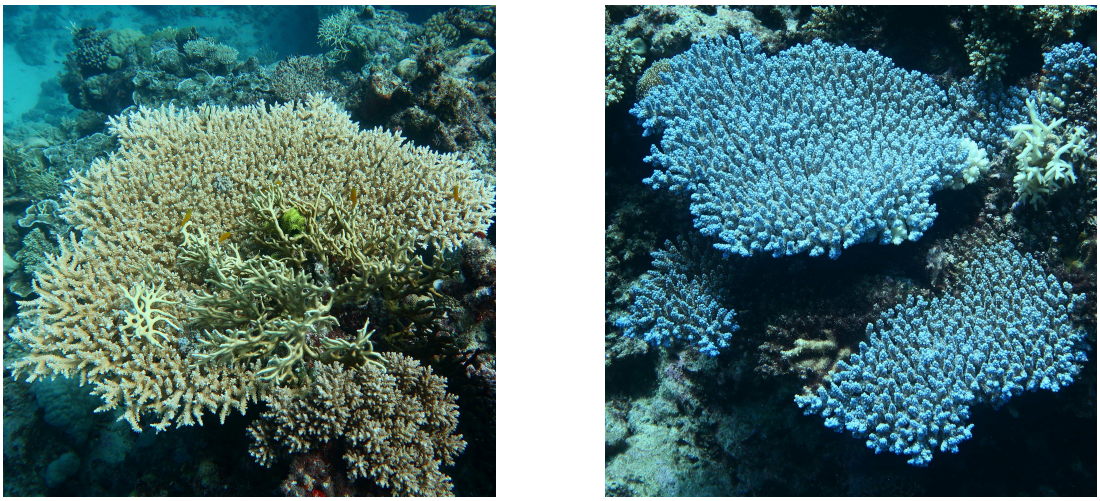

Figure 3.1: *Acropora millepora*

The following life history traits are implemented in the model [42]:

- **Mortality**: Each larva has a probability of dying at each time step. This probability is calculated by assuming a constant mortality rate. The mortality rate can follow another distribution, it depends on the coral species.
- **Competence**: It represents the ability of a larva to settle onto a reef. After a certain period of time, a larva has a certain probability of acquiring competence following a constant competence acquisition rate, and once they are competent, a certain probability of losing competence following a constant competence loss rate [7] [43]. By lack of information this last feature is assumed to be equal to 0. The pre-competency period corresponds to the number of days before larvae could become competent while the post-competency period corresponds to the number of days after which larvae are no longer competent.
- **Settlement**: Once a larva becomes competent, it will then settle onto the first reef it travels over. This behavioural trait reflects the fact that once they are competent, coral larvae are known to be able to change their buoyancy to sink down to the reef surface and settle onto it if conditions are favorable [44].

Acropora millepora	
Mortality Rate	0.054 day^{-1}
Pre-competency period	3.526 days
Post-competency period	100 days
Competence acquisition rate	0.348 day^{-1}
Competence loss rate	0

Table 3.2: Life history traits for *Acropora millepora* [42]

3.3 Biophysical particle transport

The virtual larvae were released over all reefs in the GBR. The number of larvae released over each reef was a proportional function of the reef's surface area, with greater numbers of larvae released over larger reefs [7]. Furthermore, it is assumed that *Acropora millepora* always covers the entire area of each reef and is present on each reef in the GBR.

Larvae were then tracked for 30 days since the spawning date for each year. Once a larva had acquired competency, it was considered to settle onto the first reef it travelled over. As soon as a larva settled onto a reef it was immediately removed from the remainder of the simulation [7]. The evolution of the larval dispersal simulation can be seen on figures 3.2 and 3.3.

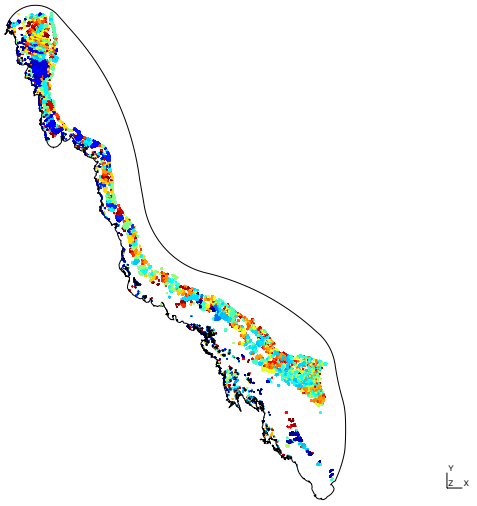

(a) Initial particle positions

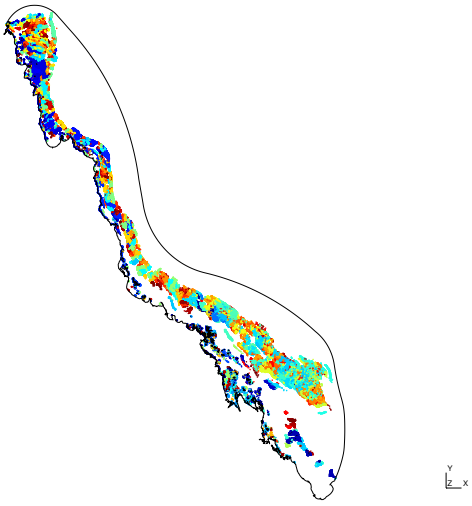

(b) Positions after 6 days

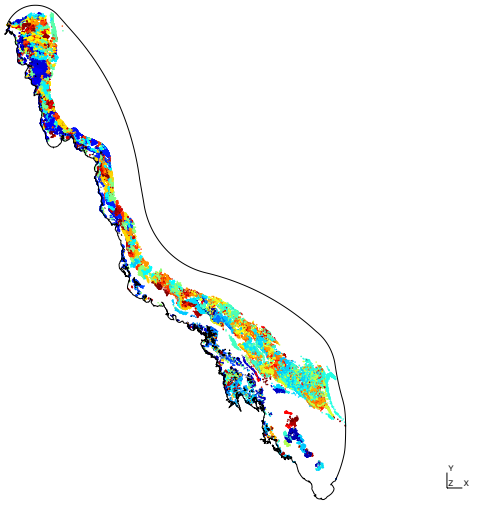

(c) Positions after 12 days

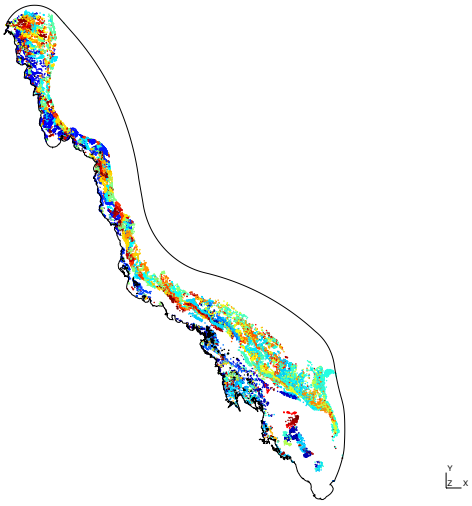

(d) Positions ater 18 days

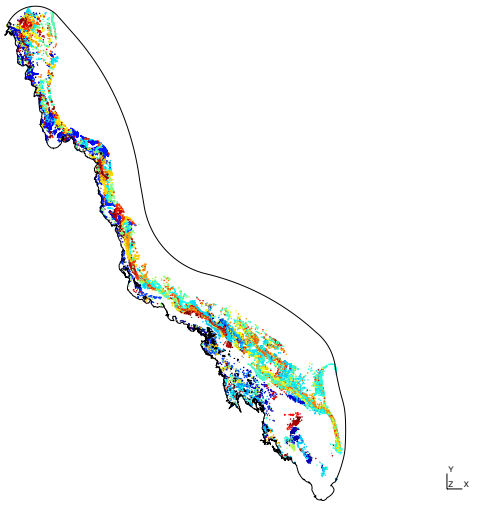

(e) Positions after 24 days

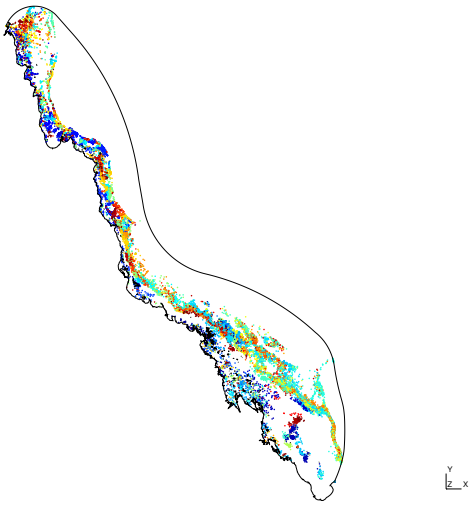

(f) Positions after 30 days

Figure 3.2: Pictures showing the dispersal of particles over 30 days in the entire GBR in 2010

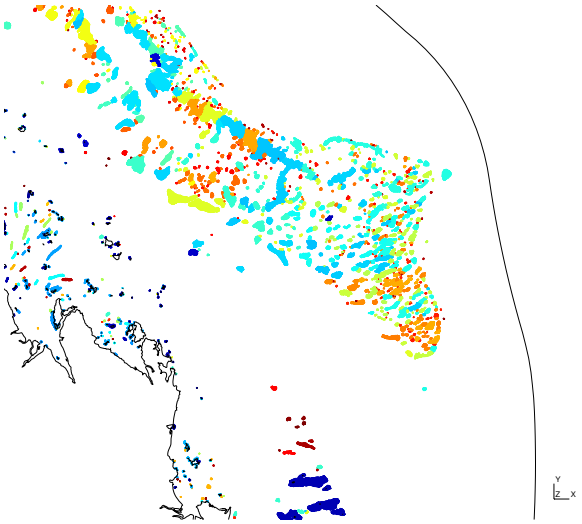

(a) Initial particle positions

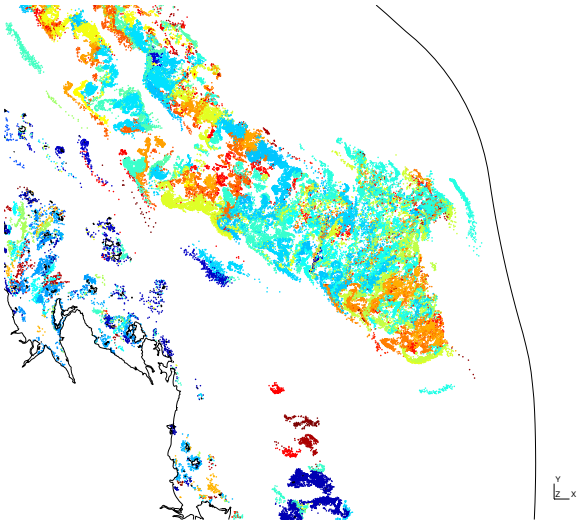

(b) Positions after 6 days

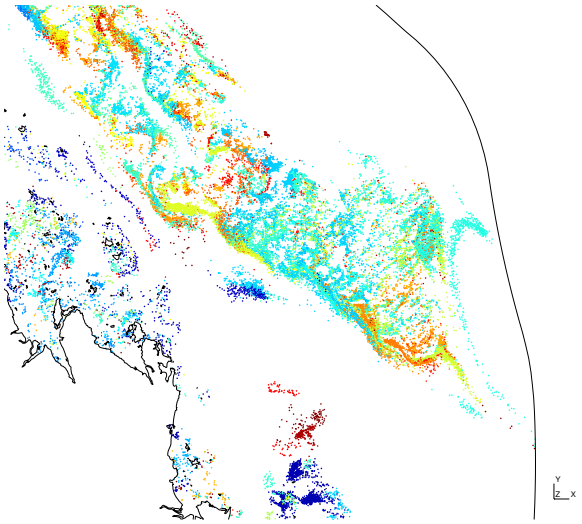

(c) Positions after 12 days

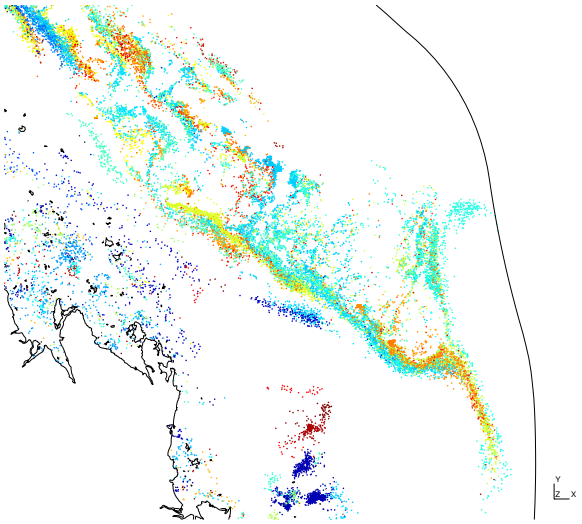

(d) Positions after 18 days

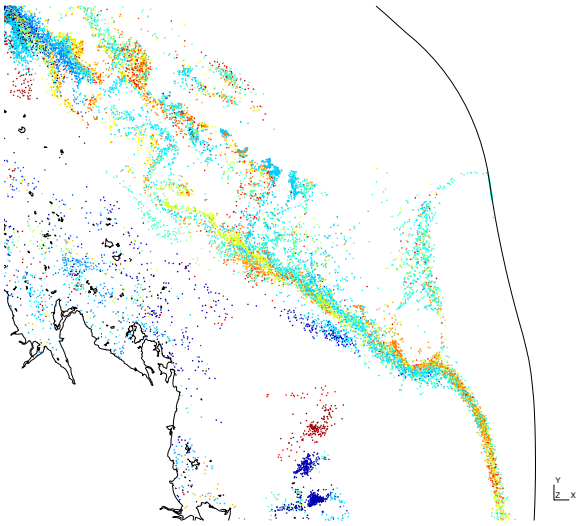

(e) Positions after 24 days

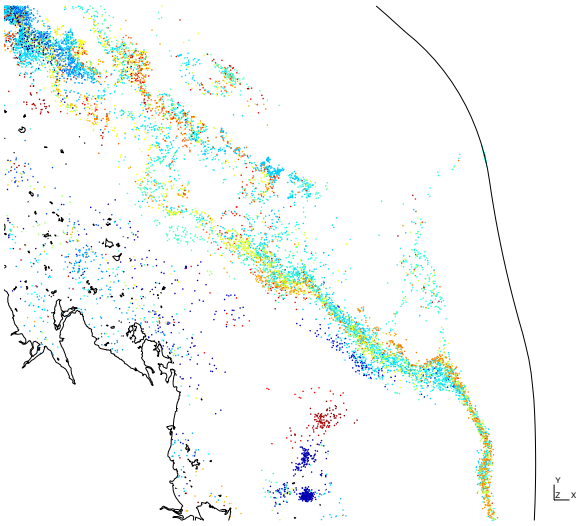

(f) Positions after 30 days

Figure 3.3: Pictures showing the dispersal of particles over 30 days in the south of the GBR in 2010

3.4 Connectivity matrix

The output of the biophysical model is a large connectivity matrix whose elements give the strength of the connectivity between every pair of reefs in the domain, where the connectivity strength C_{ij} is defined as the number of larvae released over a source reef i which settle onto a sink reef j. The connectivity matrix encapsulates then all of the relevant output from the Lagrangian particle tracking simulation (see figure 3.4) [7].

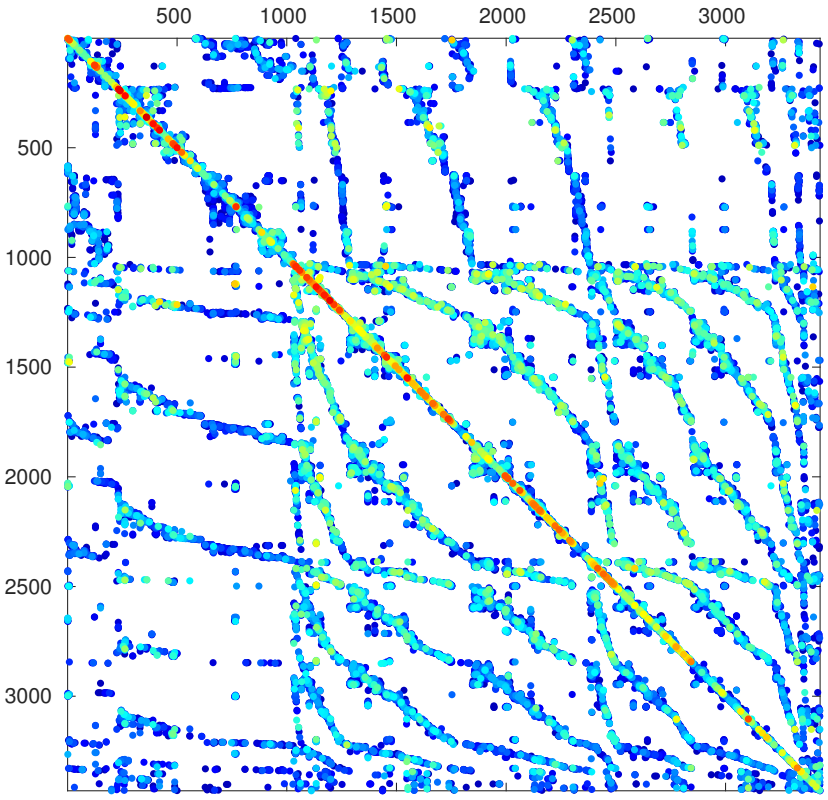

Figure 3.4: Connectivity matrix of the GBR in 2010

A more visual representation of the connectivity matrix is the connectivity graph (see figures 3.5, 3.6 and 3.7). The connectivity graph shows all connections between reefs.

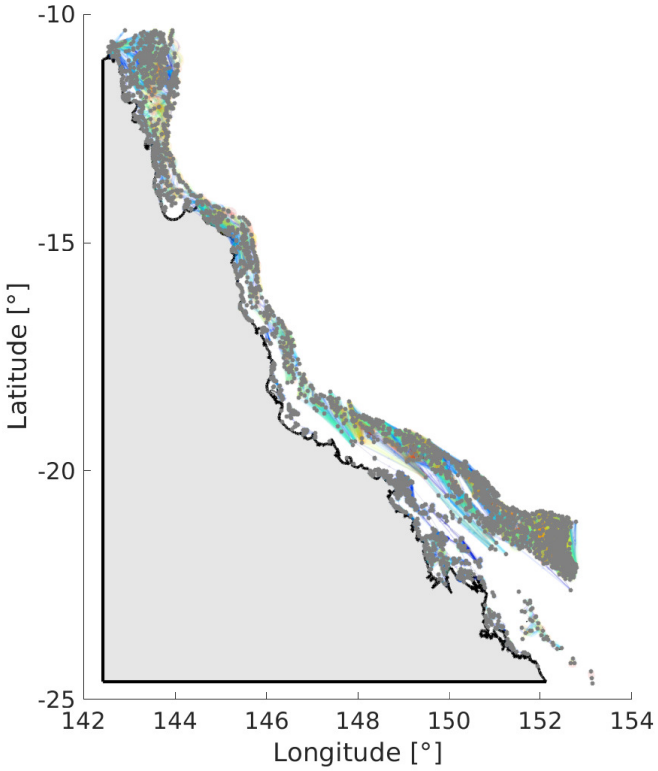

Figure 3.5: Illustration of the connectivity graph of the GBR in 2010

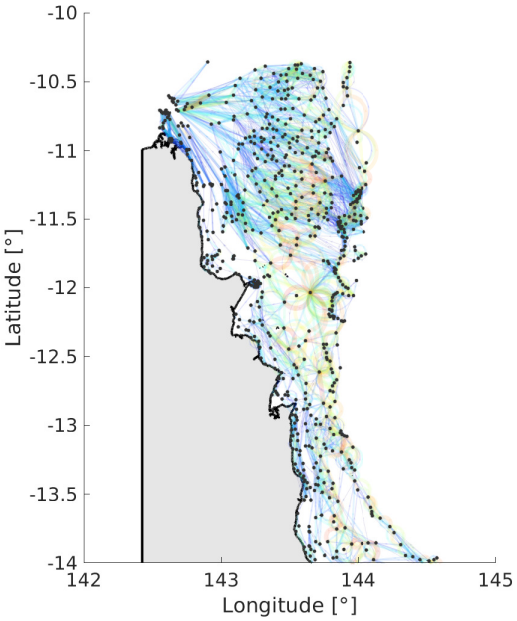

Figure 3.6: Overview of the connectivity graph in the north of the GBR in 2010

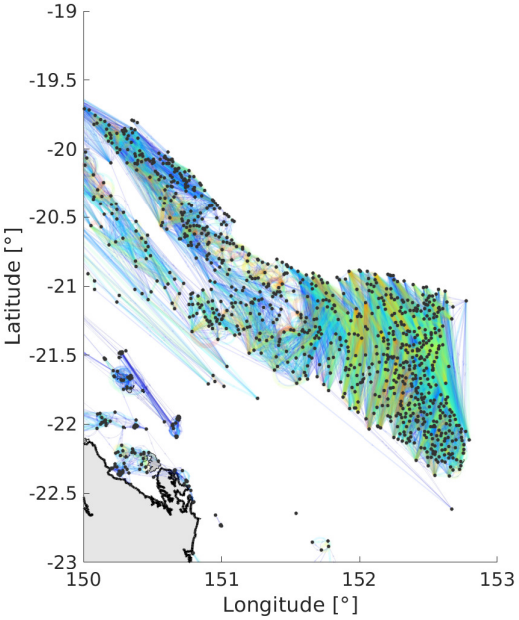

Figure 3.7: Overview of the connectivity graph in the south of the GBR in 2010

4 Studying connectivity with graph theory tools

To study the connectivity in the GBR, we need to extract useful information from the connectivity matrix. This can be made by using some graph theory tools. The analysis is divided in three parts and realised for the three periods considered (2008, 2010 and 2012). The first part describes different connectivity measures used to identify connectivity patterns and important reefs. The second part defines some protection and restoration measures based on the indicators described in the first part. Finally, the third part consists of the identification of reef clusters.

In sections 4.1 and 4.2, each indicator is illustrated by two graphs. The first one shows the value of the indicator of all coral reefs while the second one highlights the 1% reefs having the highest value for the indicator in question.
The figures are shown only for 2010 to avoid redundancy. The figures for 2008 and 2012 are included in the appendices (see sections A.2, A.3 and A.4). Furthermore, as the purpose of this thesis is to study the variability of the connectivity through three different years, the graphs of this section are not commented. All conclusions are made in section 5 which gathers the results of the three periods considered.

4.1 Connectivity measures

To interpret all data encapsulated in the connectivity matrix, we need to define some connectivity measures. Those connectivity measures are applied to every reef in the GBR to identify some connectivity patterns and important reefs.

4.1.1 Local retention

This connectivity measure is defined as the proportion of larvae released by a reef which settle onto the same reef.

$$\lambda_i = \frac{C_{ii}}{S_i} \tag{4.1}$$

The local retention of a reef i represents then the proportion of larvae released by the reef i which settle on the same reef i (C_{ii}) to the total amount of larvae released by the reef i (S_i). This describes the ability of a reef to be its own source of larvae compared to the total number of larvae released by this reef [18].

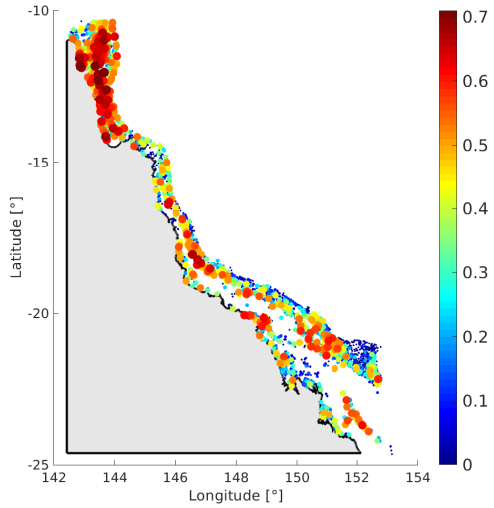

Figure 4.1: Local retention in 2010

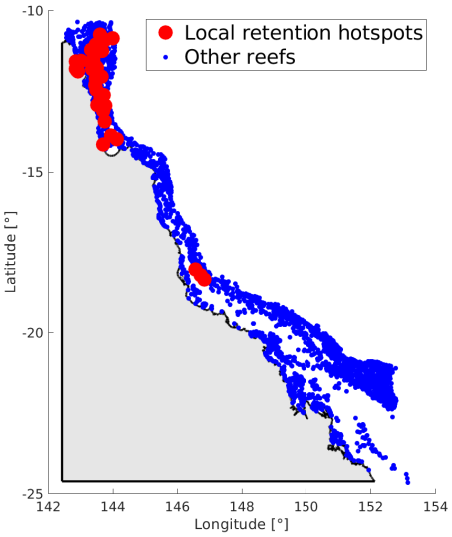

Figure 4.2: Local retention hotspots in 2010

4.1.2 Self-recruitment

This connectivity measure is defined as the proportion of larvae returning to and settling in their natal population [45].

$$\sigma_i = \frac{C_{ii}}{\sum_j C_{ji}} \tag{4.2}$$

The self-recruitment of a reef i represents then the proportion of larvae released by the reef i which settle onto the same reef i (C_{ii}) to the total amount of larvae settled onto the reef i received from other reefs j (C_{ji}). This describes the ability of a reef to be its own source of larvae compared to what it receives from other reefs [18].

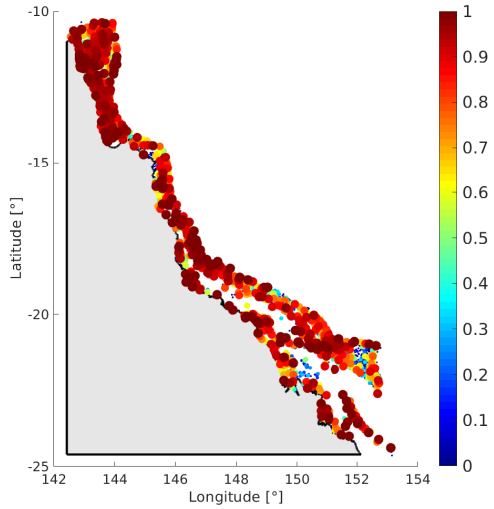

Figure 4.3: Self-recruitment in 2010

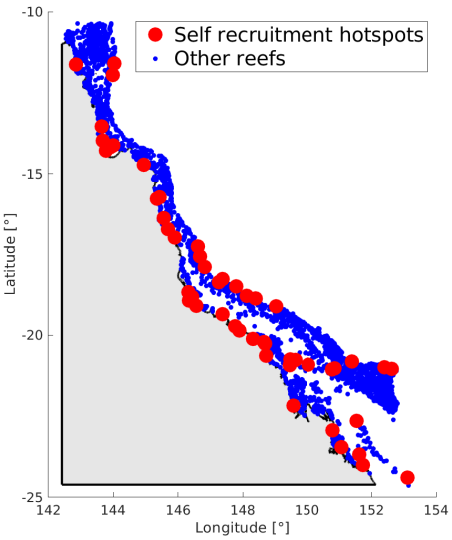

Figure 4.4: Self-recruitment hotspots in 2010

4.1.3 Degree centrality

The degree centrality indicator takes into account for each reef the number of its connections and their strength. This indicator is then calculated by multiplying the number of incoming/outgoing connections ($K_i^{in/out}$) by the number of incoming/outgoing larvae ($N_i^{in/out}$) for each reef i.

This analysis is made for each reef for incoming and outgoing connections.

4.1.3.1 Incoming degree centrality

A reef with a high incoming degree centrality indicator means that it receives many larvae from several different reefs. This kind of reef can be qualified as resilient since it is supplied with many larvae.

$$S_i^{in} = K_i^{in} \times N_i^{in} \tag{4.3}$$

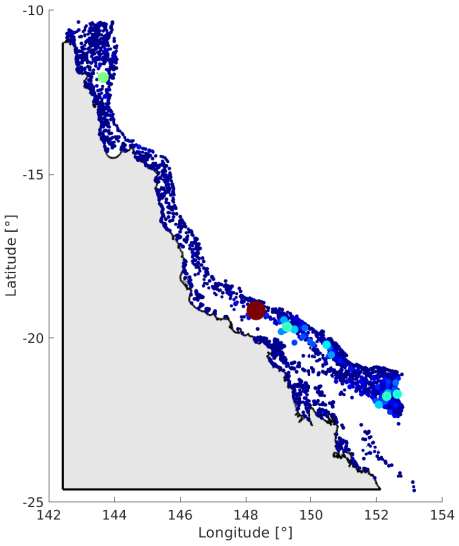

Figure 4.5: Incoming degree centrality in 2010

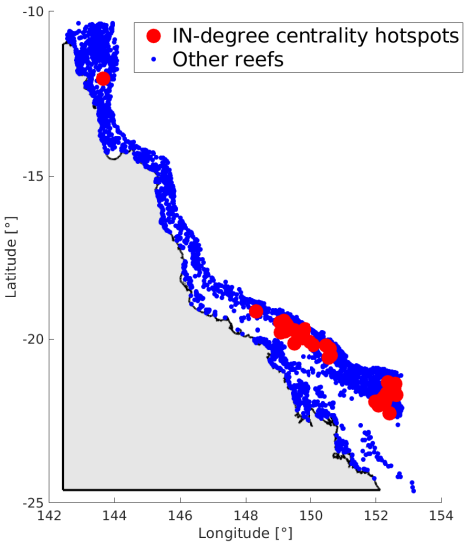

Figure 4.6: Incoming degree centrality hotspots in 2010

4.1.3.2 Outgoing degree centrality

A reef with a high outgoing degree centrality indicator means that it gives many larvae to several different reefs. This kind of reef is useful for the resilience of its neighbours since it supplies them with many larvae.

$$S_i^{out} = K_i^{out} \times N_i^{out} \tag{4.4}$$

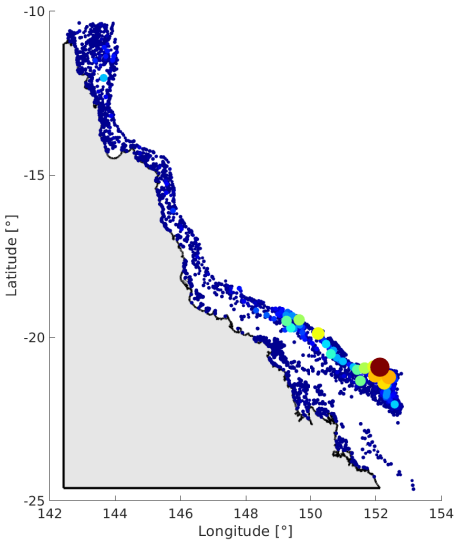

Figure 4.7: Outgoing degree centrality in 2010

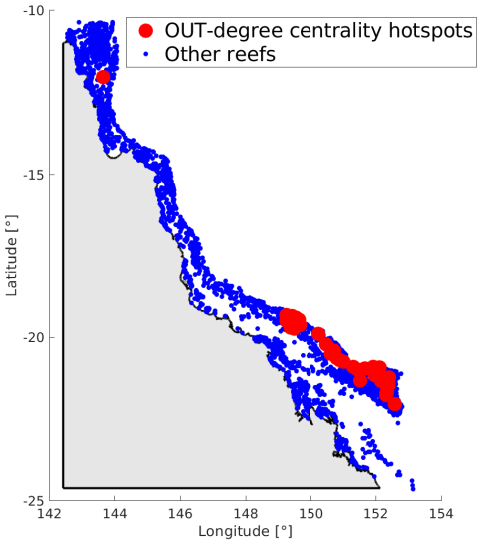

Figure 4.8: Outgoing degree centrality hotspots in 2010

4.1.4 PageRank

PageRank is initially a method for computing a ranking for every web page based on the graph of the web. This algorithm is used by Google in order to measure the relative importance of web pages (from the most important to the least important) [46]. Two main factors are taken into consideration to determine the PageRank of a web page:

- The number of links leading to this web page
- The importance of the pages linking to this web page

This algorithm can be applied to calculate the PageRank of a reef. It results from a random walk where at each reef, the next one is chosen with a probability from the set of successors of the current reef. A successor is simply a reef connected to the current reef. If a reef has no successor, the next reef is chosen from all the reefs. The final score is the average time spent at each node during the random walk. The weights of the connections affect how the algorithm chooses the successors [18].

The PageRank indicator is similar to the degree centrality one but the difference is that the PageRank indicator takes into account the whole graph. While the degree centrality indicator of a reef is only influenced by its connections with its neighbours, the PageRank indicator includes the influence of the connections with its predecessors/successors.

As above, this analysis is made for each reef for incoming and outgoing connections.

4.1.4.1 Incoming PageRank

The indicator π_i^{in} measures the importance of a sink reef. A reef i with a high π_i^{in} indicator means that its predecessors give it many larvae and were provided with many larvae.

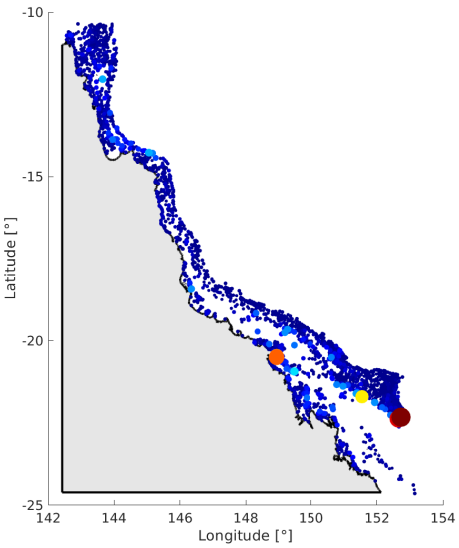

Figure 4.9: Incoming PageRank in 2010

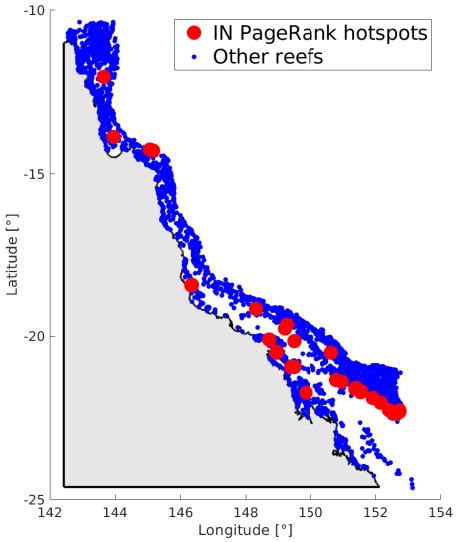

Figure 4.10: Incoming PageRank hotspots in 2010

4.1.4.2 Outgoing PageRank

This indicator π_i^{out} measures the importance of a source reef. A reef i with a high π_i^{out} indicator means that the successors of the reef i provide many larvae to other reefs.

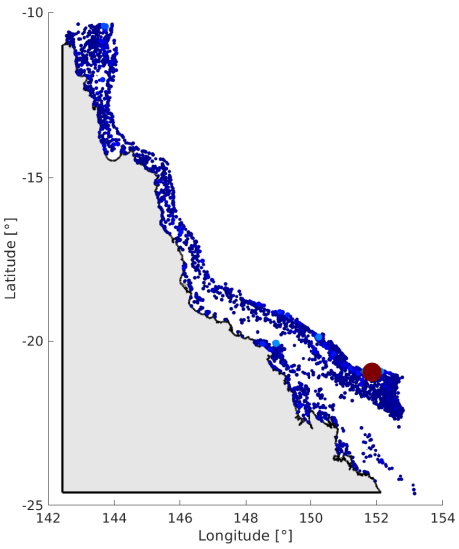

Figure 4.11: Outgoing PageRank in 2010

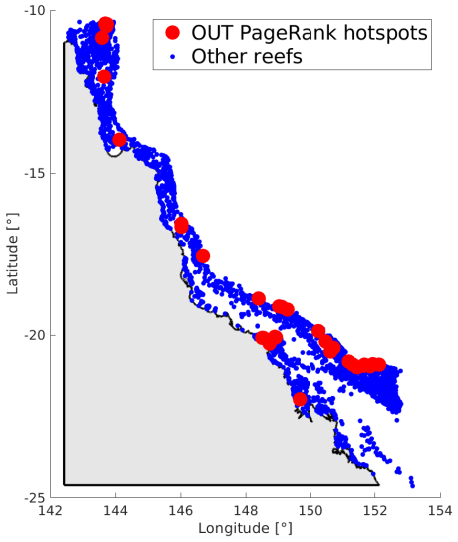

Figure 4.12: Outgoing PageRank hotspots in 2010

4.2 Protection and restoration measures

Some protection and restoration measures can be defined based on the different indicators calculated in the section 4.1. From a management and conservation perspective, it is indeed important to determine which reefs play a major role in the conservation of the GBR. Those reefs are either good exporters of larvae or both good importers and good exporters of larvae. The PageRank and degree centrality indicators are used to define the protection and restoration measures because they show how good a reef export or import some larvae.

4.2.1 Protection measures

The protection measures concern the source reefs. Those reefs are useful for the resilience of the GBR because they provide many larvae to connected reefs. Nevertheless, those reefs may be vulnerable because they are not well supplied or due to other external reasons. By constantly protecting those reefs, they could help the recovery of many other connected reefs.

4.2.1.1 Degree centrality protection

The degree centrality protection indicator is defined as the difference between the indicators S_i^{out} and S_i^{in} normalised by their sums.

$$S_i^{out-in} = \frac{S_i^{out} - S_i^{in}}{S_i^{out} + S_i^{in}} \tag{4.5}$$

This indicator varies from -1 to +1. A reef with a low value corresponds to reef that receives many larvae but does not provide much while a reef with a high value corresponds to a reef that gives many larvae to other reefs but not well supplied. In other words, a value close to -1 characterises a sink reef and a value close to +1 characterises a source reef. Therefore the reefs that would need some protection are the reefs with a value close to +1.

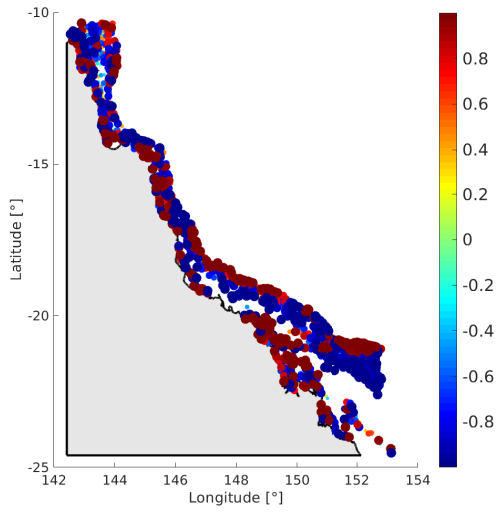

Figure 4.13: Degree centrality protection in 2010

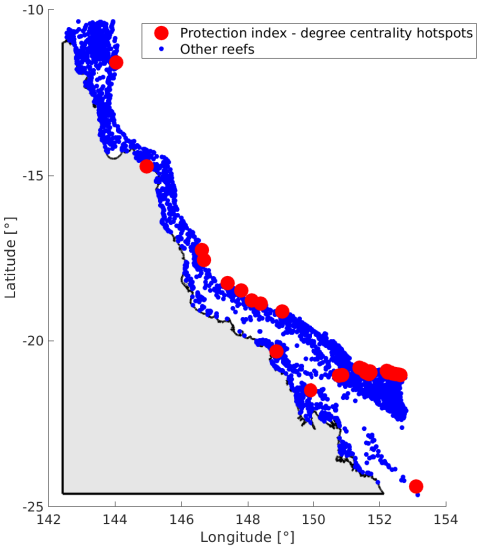

Figure 4.14: Degree centrality protection hotspots in 2010

4.2.1.2 PageRank protection

The PageRank protection indicator is defined in the same way as above.

$$\pi_i^{out-in} = \frac{\pi_i^{out} - \pi_i^{in}}{\pi_i^{out} + \pi_i^{in}} \tag{4.6}$$

The interpretation of the PageRank protection indicator is the same as the degree centrality one considering the fact that the PageRank algorithm takes into account all connections of a reef and not only the connections with its neighbours.

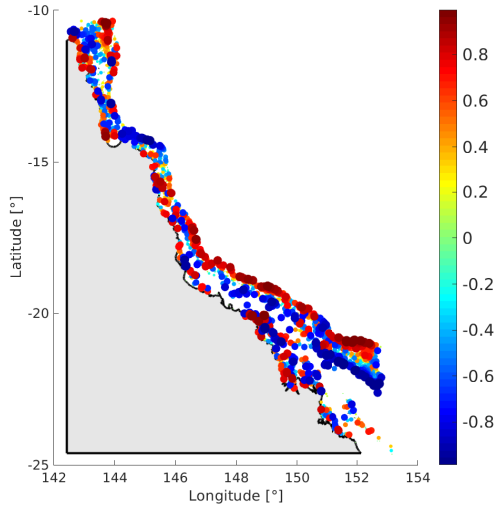

Figure 4.15: PageRank protection in 2010

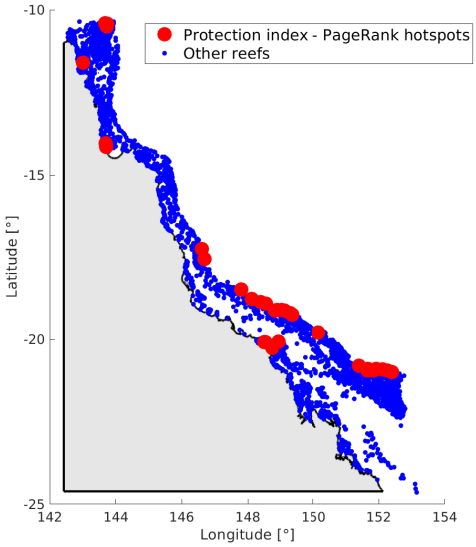

Figure 4.16: PageRank protection hotspots in 2010

4.2.2 Restoration measures

The restoration measures concern the reefs that are both good exporters and good importers. Those reefs are useful for the resilience of the Great Barrier Reef and also self-sufficient. Once they would have been properly restored those reefs could help the recovery process of connected reefs while keeping themselves safe.

4.2.2.1 Degree centrality restoration

The degree centrality restoration indicator is obtained by multiplying S_i^{out} by S_i^{in}.

$$S_i^{out \times in} = S_i^{out} \times S_i^{in} \tag{4.7}$$

The reefs that would be the most suitable for restoration practices are the reefs with the highest value of $S_i^{out \times in}$. Those reefs are both good exporters and good importers. However, no conclusion can be drawn for reefs with a low value.

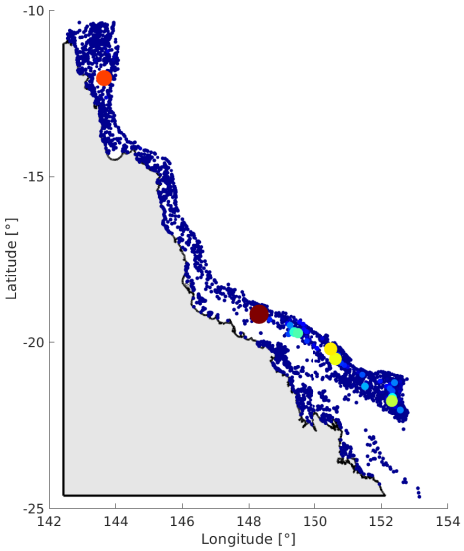

Figure 4.17: Degree centrality restoration in 2010

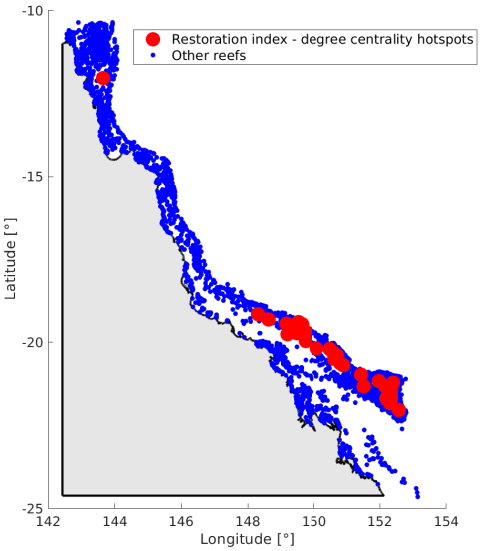

Figure 4.18: Degree centrality restoration hotspots in 2010

4.2.2.2 PageRank restoration

The PageRank restoration indicator is defined in the same way as above.

$$\pi_i^{out \times in} = \pi_i^{out} \times \pi_i^{in} \tag{4.8}$$

Again, the interpretation of the PageRank restoration indicator is the same as the degree centrality one with the fact that the PageRank analysis is performed a bit further.

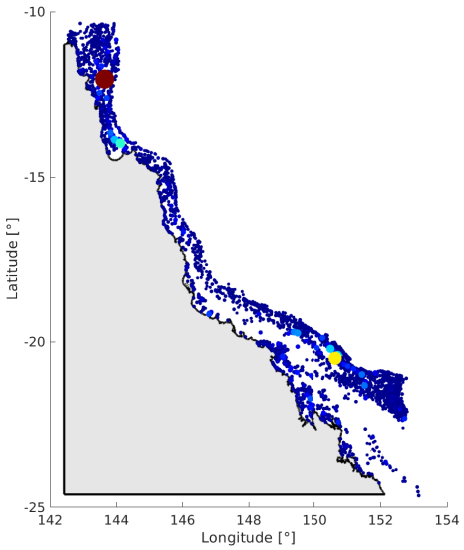

Figure 4.19: PageRank restoration in 2010

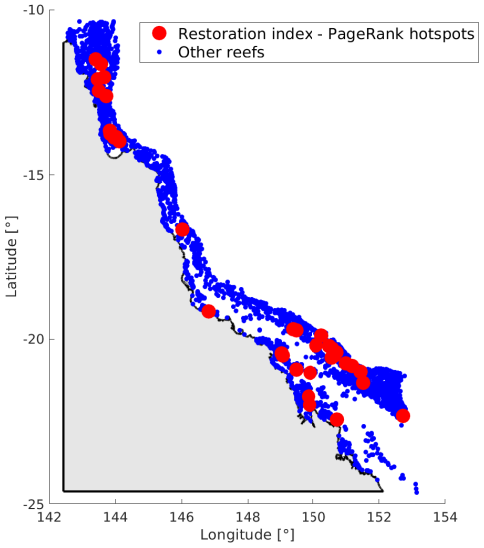

Figure 4.20: PageRank restoration hotspots in 2010

4.3 Identification of reef clusters

The protection and restoration measures give good information about which reefs play an important role in the conservation of the GBR. However, although this information is helpful, it is not sufficient. Indeed, it does not provide information about the scope of the action of the most important reefs. This section deals with this issue.

By identifying the reef clusters we could get an overview of reefs strongly connected to each other and weakly connected to reefs outside their cluster. From management and conservation perspectives, these additional data coupled with the protection and restoration indicators give a more realistic view of the area of influence of the reefs with high protection or restoration indicators.

The identification of reef clusters is realised with 2 different methods namely the strongly connected components and the community detection.

4.3.1 Strongly connected components

The strongly connected components (SCC) method does not focus on the strengh of the connections but simply on the presence of connections going in both directions. Therefore, two reefs are in the same cluster if there are paths connecting them in both directions. The advantage of this method is that it allows to visualise reefs that are either not connected at all, or connected only by one-way conections.

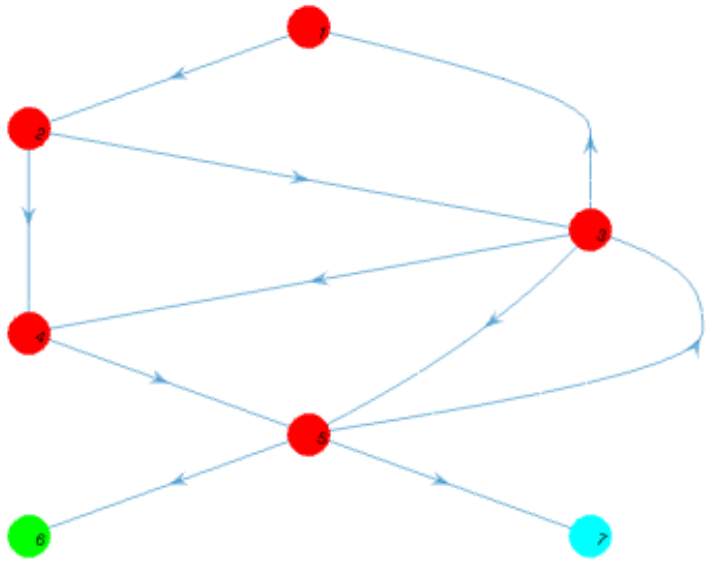

Figure 4.21: Illustration of the SCC method. All red nodes are included in the same cluster because they are all connected to each other in both directions while the green one and the blue one are in different clusters because there are not connected with other nodes in both directions. Credit: [18]

A cluster contains at least one reef. It means that this reef is connected to itself and provides itself with its own larvae. However, as the GBR contains more than 3000 reefs, detecting clusters with only one or just a few reefs is not that relevant. Therefore, in order to get consistent results, this method was applied several times with different lower bounds. These lower bounds correspond to the minimum number of reefs that must be present in the cluster. The method

then computes the strongly connected components and removes the components whose the total number of reefs is lower than the lower bound.

Furthermore, to get even more relevant results, a criterion on weight connections can be added to the initial method. This can be done by considering only connections that are demographically significant and thus by not taking into account connections below a certain weight. In order to do that, only connections having weights larger than 0.1% of the total amount of larvae released over the source reef are considered [18]. This percentage has obviously an impact on the number of reefs included in a certain cluster.

The results are shown on figures 4.22, 4.23, 4.24, 4.25, 4.26 and 4.27.

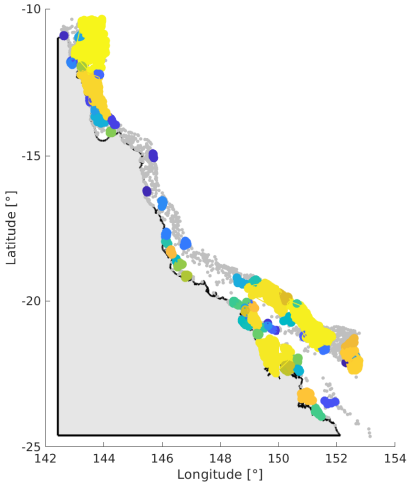

Figure 4.22: Number of strongly connected components with more than 5 reefs in 2010: 64

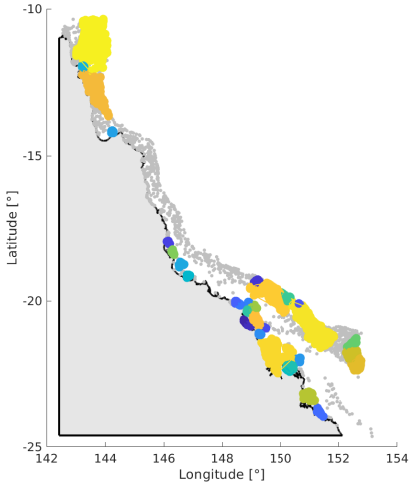

Figure 4.23: Number of strongly connected components with more than 10 reefs in 2010: 33

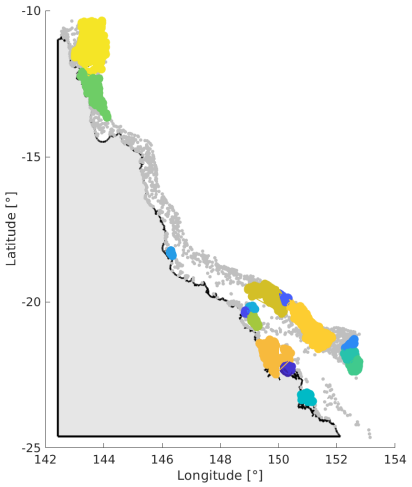

Figure 4.24: Number of strongly connected components with more than 20 reefs in 2010: 17

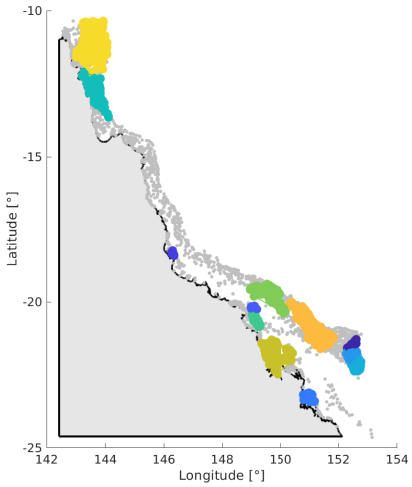

Figure 4.25: Number of strongly connected components with more than 35 reefs in 2010: 12

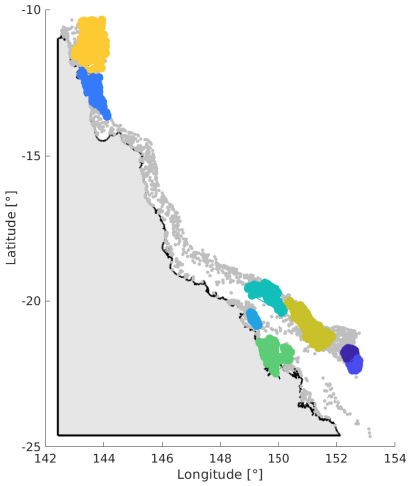

Figure 4.26: Number of strongly connected components with more than 50 reefs in 2010: 8

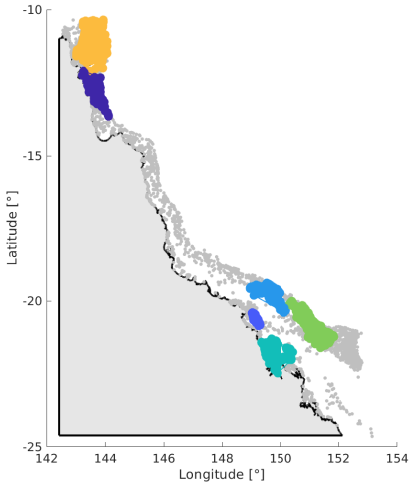

Figure 4.27: Number of strongly connected components with more than 75 reefs in 2010: 6

4.3.2 Community detection

The clustering based on this second method was made by using the Constant Potts Model (CPM) [47] [48] and an optimisation algorithm called the Louvain Method algorithm [49].

This method contains an additional parameter γ which allows to detect reef communities at different spatial scales. This parameter has an influence on how much inter- and intra-community connectivity there is. Choosing a low value of γ implies that the connectivity between any two communities will be small, but the internal connectivity may also be low and the size of the communities will tend to be large. Instead, choosing a larger value of γ implies that the connectivity between any two communities may be higher, but the internal connectivity will also be higher and communities will tend to be smaller and boundaries more permeable (see figure 4.28) [36]. There is no optimal value of γ. The figure 4.29 shows a graph comparing the number of communities detected in 2010 by the model with different values of γ.

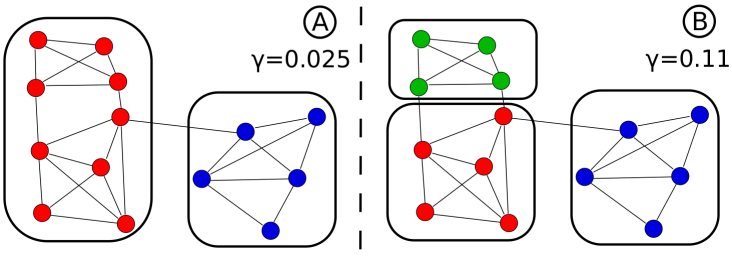

Figure 4.28: Illustration of the community detection method. Diagrams A and B show two identical graphs. The community detection method is applied with two different values of γ, which leads to different results. Using a lower value of γ results in fewer communities being detected. Credit: [36]

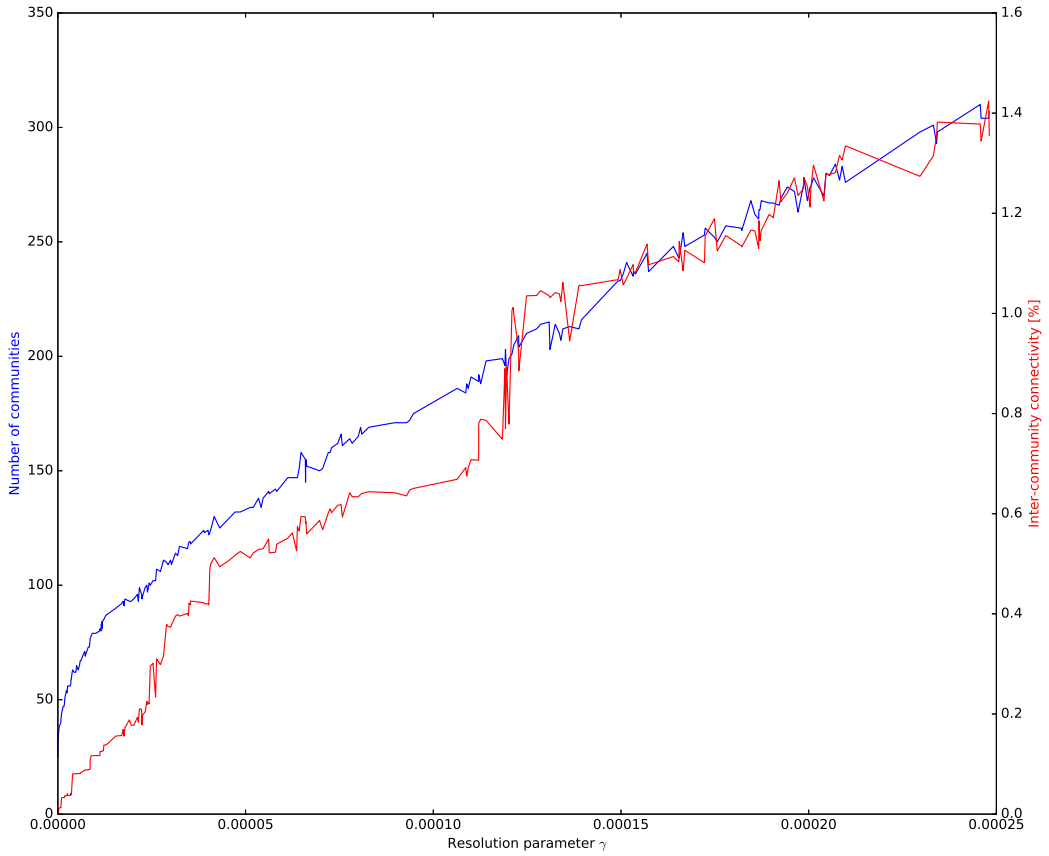

Figure 4.29: Number of communities and percentage of inter-community connectivity in 2010 as a function of the resolution parameter γ

5 Results and pratical implications

The section 4 describes different tools and methods which can be used to study connectivity patterns for any given spawning season. However annual variations in oceanographic conditions may modify larval dispersal patterns year-on-year. By comparing the figures for 2010 in section 4 with the figures for 2008 and 2012 (see sections A.2, A.3 and A.4), some variations can indeed be seen.

It is thus crucial to analyse the variability of the connectivity in the GBR between the different years. This analysis will lead to more reliable and sustainable results which could be used to inform marine management for achieving effective restoration and protection of the GBR.

5.1 Variability of the connectivity

This section gathers the results of the three spawning seasons considered by following the same structure as the section 4.

Firstly, data are gathered by calculating the mean value of each connectivity measure for the three spawning seasons. Secondly, while the mean provides a useful information about an indicator, it is not sufficient. It must be supported by another indicator such as the variance or the standard deviation. Those indicators give information about which reefs have the highest values for the indicator in question and about how much these values vary from one year to another.

Statistics used to study the connectivity are [50]:

- **Mean**: The mean refers to the central value of a discrete set of numbers and is simply defined as follows:

$$\mu = \frac{1}{n}\sum_{i=1}^{n} x_i \tag{5.1}$$

- **Standard deviation**: The standard deviation is a measure that is used to quantify the dispersion of a set of data values. A low standard deviation means that the data tend to be close to the mean value of the set of data, while a high standard deviation means that the data are spread out over a wider range of values.
  The standard deviation is defined as the positive square root of the variance which is defined as follows (for a set of n equally likely values):

$$\sigma^2 = \frac{1}{n}\sum_{i=1}^{n} (x_i - \mu)^2 \tag{5.2}$$

The standard deviation is thus equal to:

$$\sigma = \sqrt{\sigma^2} = \sqrt{\frac{1}{n}\sum_{i=1}^{n}(x_i - \mu)^2} \tag{5.3}$$

- **Coefficient of variation**: The coefficient of variation is also known as the relative standard deviation and is defined as follows:

$$c_v = \frac{\sigma}{\mu} \tag{5.4}$$

The coefficient of variation is a useful dimensionless number because the standard deviation of data must always be understood in the context of the mean of the data.

Indeed, for example, let us take two standard deviations $\sigma_1 = 10$ and $\sigma_2 = 5$. These standard deviations have little meaning unless we can compare them to something else such as their respective means μ_1 and μ_2. If $\mu_1 = 1000$ and $\mu_2 = 10$, the respective coefficients of variation are $c_{v_1} = 0.01$ and $c_{v_2} = 0.5$. Therefore, although σ_1 is higher than σ_2, c_{v_1} is lower than c_{v_2} and then the data set 2 is more spread out. The data set 2 has thus a greater variability than the data set 1.

In the next sections, the connectivity is mainly analysed with the mean and the coefficient of variation.

5.1.1 Connectivity measures

The aim of this section is to identify the reefs with the highest value for each connectivity measure. In order to do that, statistics are calculated for each connectivity measure and then each indicator is illustrated by two figures (other figures are in the appendices, see section A.5). The first one on the left side shows the hotspots for each connectivity measure. These hotspots highlight the 1% reefs having the highest mean for the indicator in question. The second one on the right side shows the coefficient of variation of these hotspots to determine if these hotspots can be considered as reliable hotspots or not. Hotspots with a high coefficient of variation are unreliable because it means that these reefs are more likely to have a different value for the indicator every year. However, hotspots with a low coefficient of variation can be considered as reliable because it means that these reefs are more likely to have a high value for the indicator every year.

In terms of local retention, the reefs that tend to have high values are mainly located in the north of the GBR although a few reefs in the center of the GBR have also a high value (see figure 5.1). All these hotspots can clearly be considered as reliable in view of their low coefficient of variation. This may be due to the "sticky water effect". This phenomenon occurs in regions with a high reef density where tidal currents are steered around these regions during spring tides but not during neap tides. This occurs because in very shallow waters, when the water speed is high, a higher proportion of the flow's energy is dissipated through friction with the sea bed than when the speed is low [51]. Therefore, as the currents are steered around the regions with a high reef density, it could stimulate the local retention in these regions. However it should also be noted that the local retention hotspots are located around Lizard Shelf and this area and its surroundings is not well modelled by SLIM (see figure 2.10). Currents from SLIM are weak with almost zero speed while real observations show that there are strong currents having a speed of approximately 1.5 [m/s] in this region. These strong currents might have a significant effect on

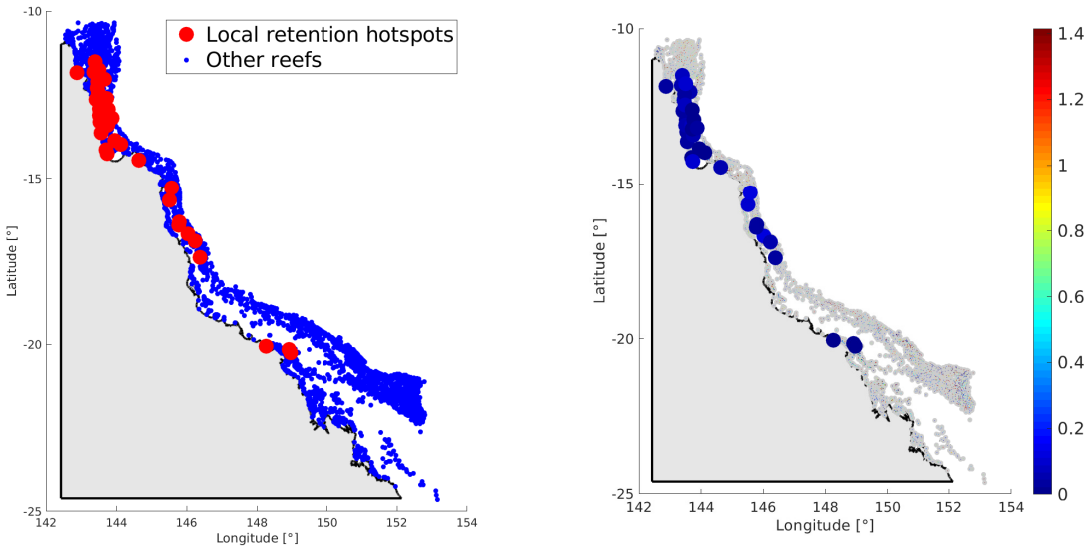

Figure 5.1: Local retention in the GBR

local retention in this area.

In terms of self-recruitment, the reefs having the highest value are spread around the whole GBR but located near the coasts or, on the contrary, in the outer shelf of the GBR (see figure 5.2). Similarly as for the local retention, the coefficients of variation of the hotspots are low. Generally, the reefs with a high self-recruitment value correspond to isolated reefs. Otherwise, a few reefs in the north and in the center of the GBR have a high self-recruitment value thanks to their high local retention value. This is why these reefs are local retention hotspots as well as self-recruitment hotspots.

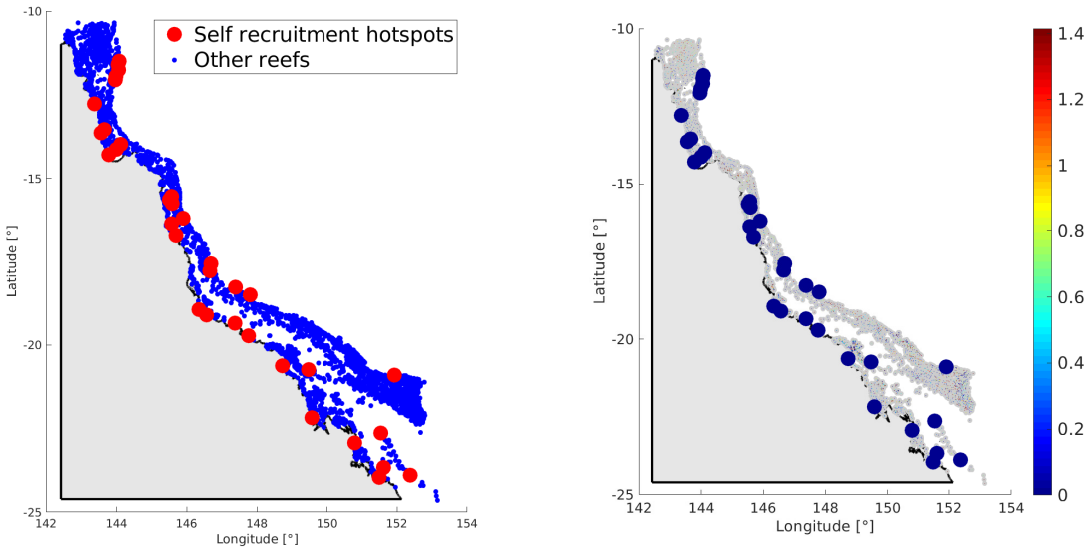

Figure 5.2: Self-recruitment in the GBR

The incoming degree centrality hotspots as well as the outgoing degree centrality hotspots are almost all located in the south of the GBR and more specifically in the outer shelf (see figures 5.3 and 5.4). Most of them can be considered as reliable in view of their low coefficient of variation. Some hotspots are common between the two indicators. It means that the reefs in the outer shelf in the south of the GBR receive and give many larvae. Considering these results, some of these reefs are probably degree centrality restoration hotspots as well. Furthermore, as most of the hotspots are located in the same region and are good source reefs as well as good sink reefs, these hotspots should belong to a same reef cluster.

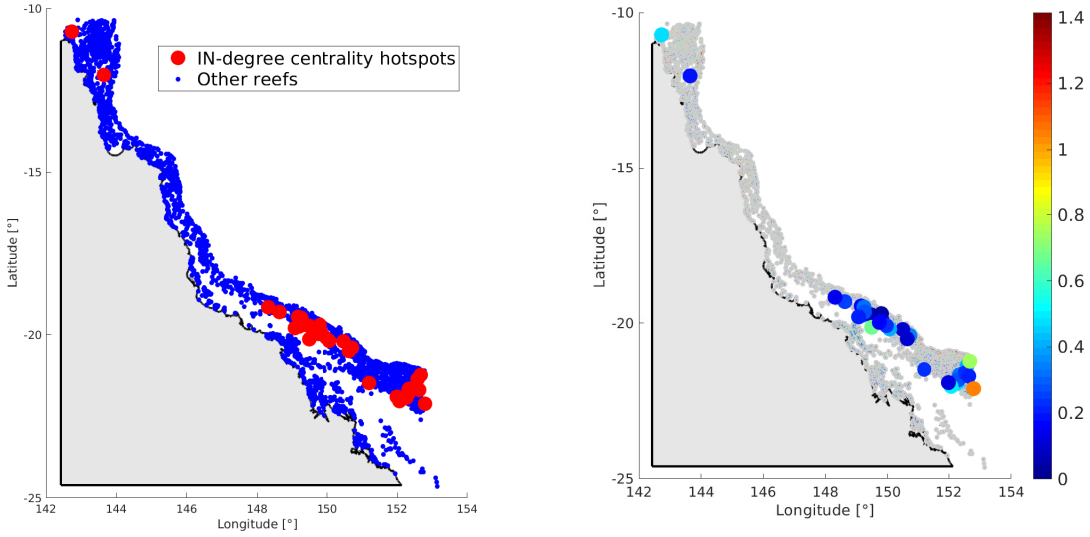

Figure 5.3: Incoming degree centrality in the GBR

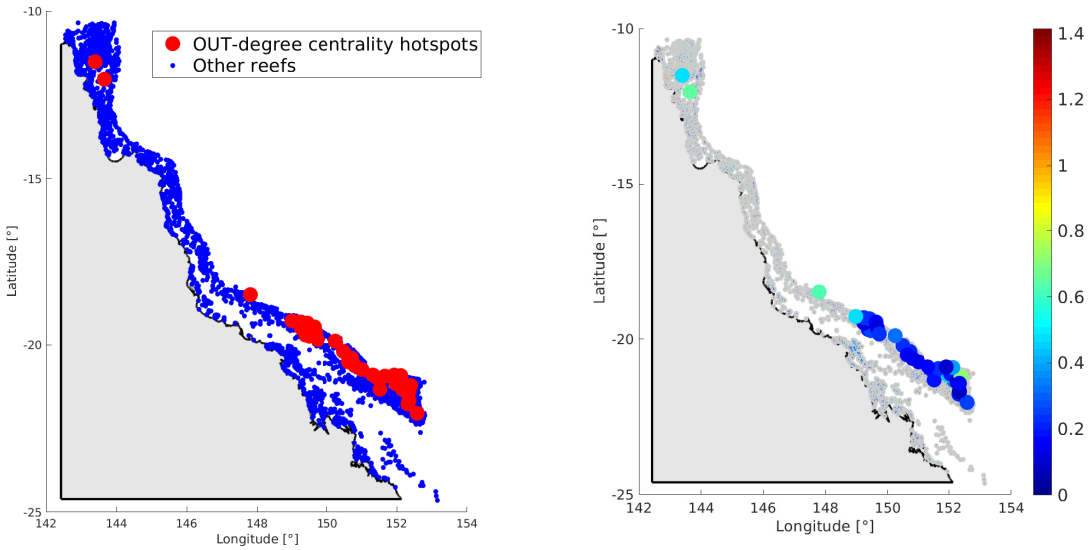

Figure 5.4: Outgoing degree centrality in the GBR

Finally, as explained in section 4.1.4, the PageRank indicators are similar to the degree centrality ones. The difference is that the PageRank indicators take into account the whole graph. While the degree centrality indicators of a reef are only influenced by its connections with its neighbours, the PageRank indicators include the influence of the connections with its predecessors/successors. Therefore, the incoming PageRank and outgoing PageRank hotspots roughly correspond to the degree centrality ones. The coefficients of variation are still quite low, especially in the south of the GBR. Similarly, some of the PageRank hotspots are probably PageRank protection or restoration hotspots as well.

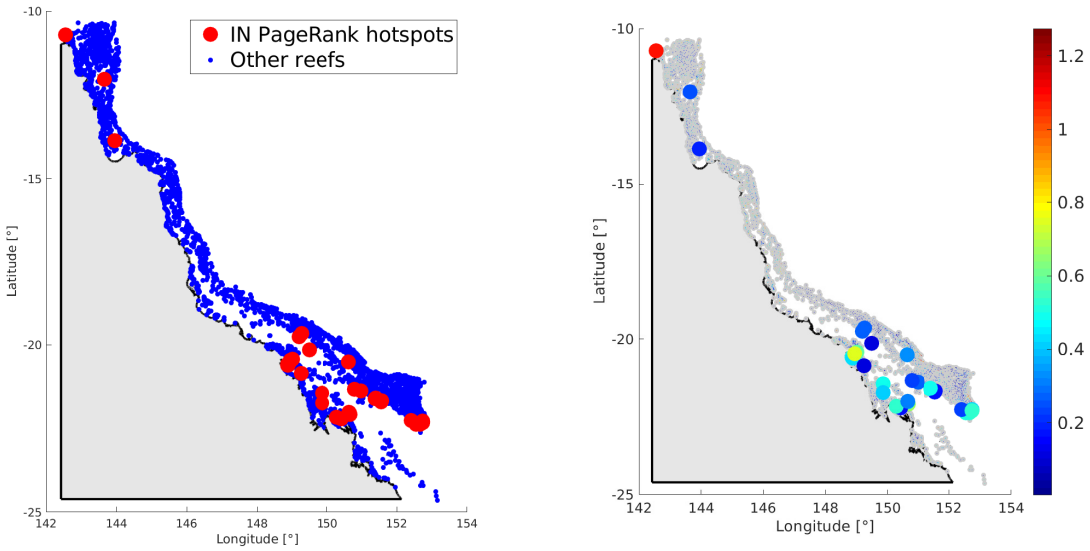

Figure 5.5: Incoming PageRank in the GBR

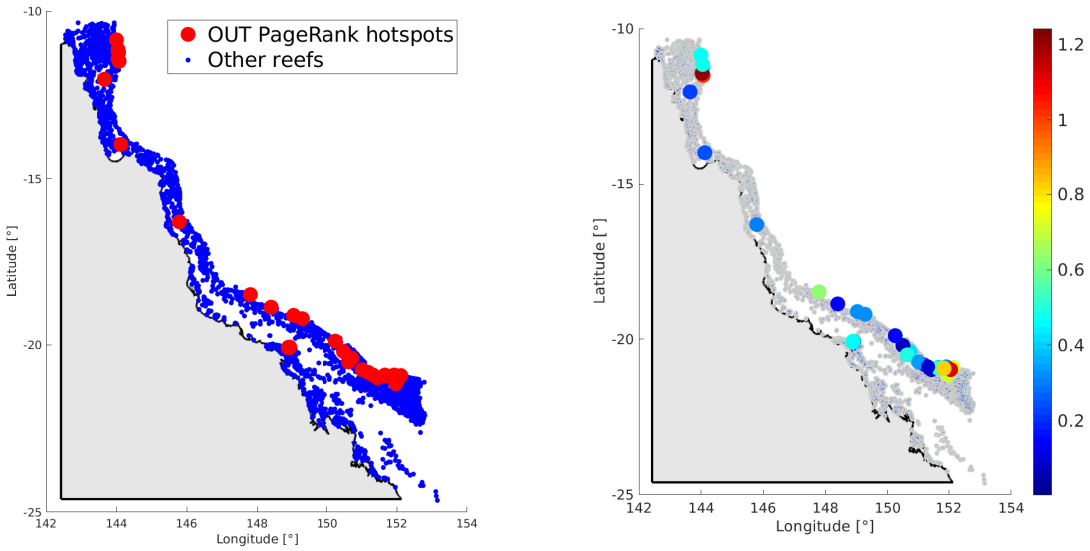

Figure 5.6: Outgoing PageRank in the GBR

5.1.2 Protection and restoration measures

The aim of this section is to identify the reefs with the highest values for the protection and restoration indicators. Figures 5.7, 5.8, 5.9 and 5.10 show the protection and restoration hotspots. The protection measures concern the source reefs. Those reefs are useful for the resilience of the GBR because they provide many larvae to connected reefs. Nevertheless, those reefs may be vulnerable because they are not well supplied. The protection hotspots are mainly located in the south of the GBR near the coasts or in the outer shelf for both indicators. Generally, these good source reefs thus correspond to isolated reefs.
The restoration measures concern the reefs that are both good exporters and good importers. As already mentioned above, the degree centrality restoration hotspots approximately correspond to the incoming and outgoing degree centrality hotspots. This also applies for the PageRank restoration hotspots.

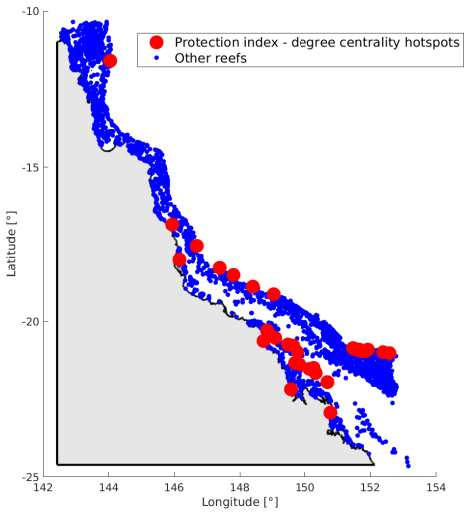

Figure 5.7: Degree centrality protection hotspots

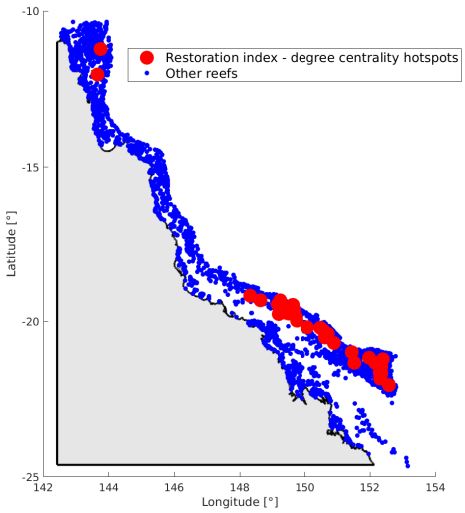

Figure 5.8: Degree centrality restoration hotspots

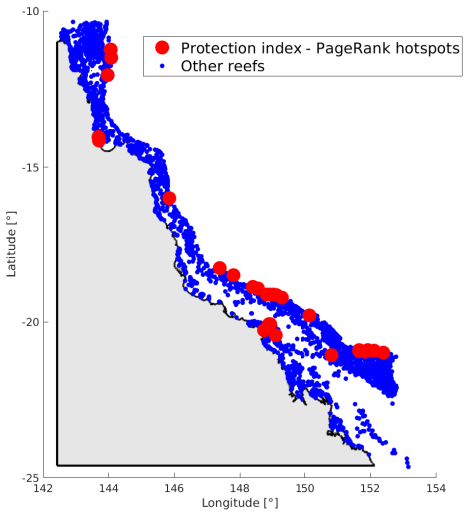

Figure 5.9: PageRank protection hotspots

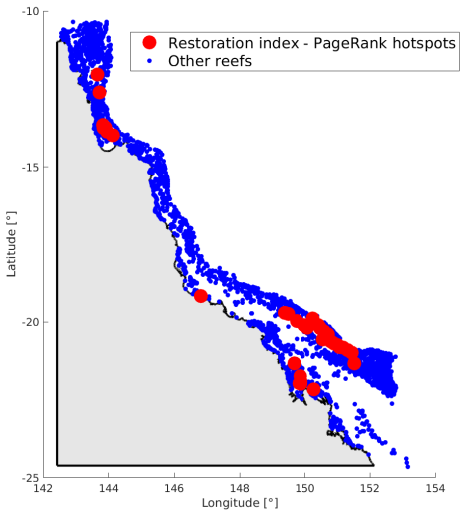

Figure 5.10: PageRank restoration hotspots

5.1.3 Identification of reef clusters

The aim of this section is to identify global reef clusters by taking account of data of every year.

5.1.3.1 Strongly connected components

In order to determine the global strongly connected components, the connectivity matrix of each year are merged into a single connectivity matrix. The SCC method is then applied as before by using this new matrix. The results are shown on figures 5.11, 5.12, 5.13, 5.14, 5.15 and 5.16.

As described in section 4.3.1, only connections that are demographically significant are considered. Only connections having weights larger than 1% of the total amount of larvae released over the source reef are considered.

Most of the significant reef clusters are located in the south of the GBR and more specifically in the outer shelf. Some medium-sized reef clusters with approximately 15 reefs are also located in the south of the GBR but rather near the coasts. The north of the GBR contains one major reef cluster with more than 50 reefs. The center of the GBR contains a few medium-sized reef clusters including approximately 10 reefs.

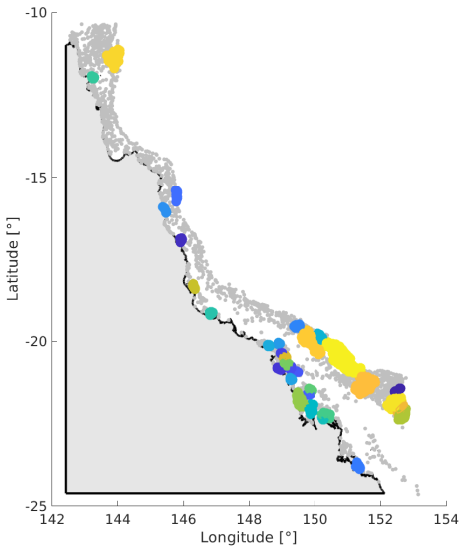

Figure 5.11: Number of strongly connected components with more than 10 reefs: 32

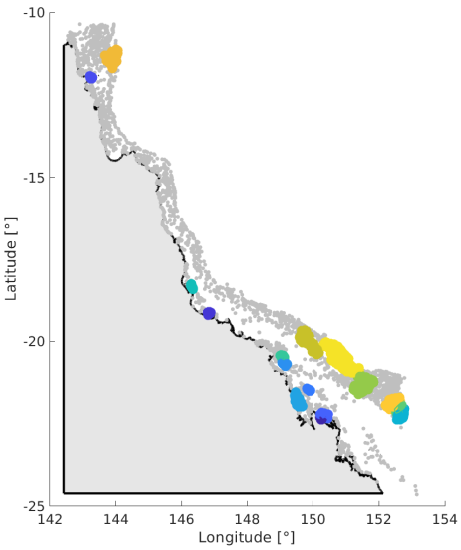

Figure 5.12: Number of strongly connected components with more than 15 reefs: 16

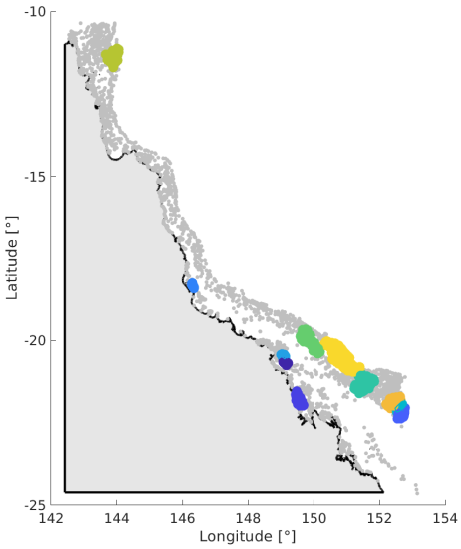

Figure 5.13: Number of strongly connected components with more than 20 reefs: 11

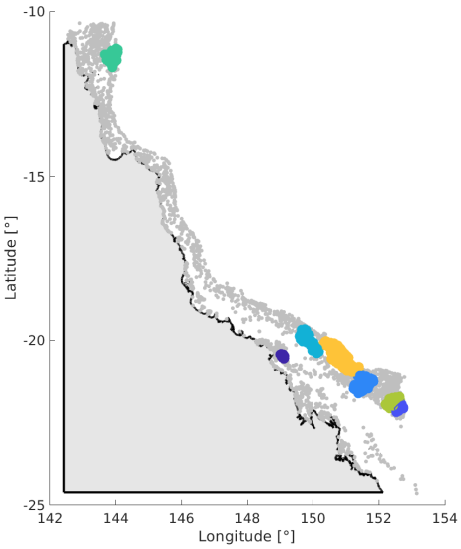

Figure 5.14: Number of strongly connected components with more than 35 reefs: 7

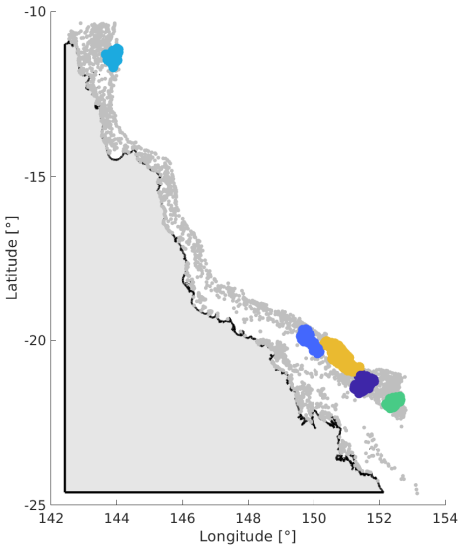

Figure 5.15: Number of strongly connected components with more than 50 reefs: 5

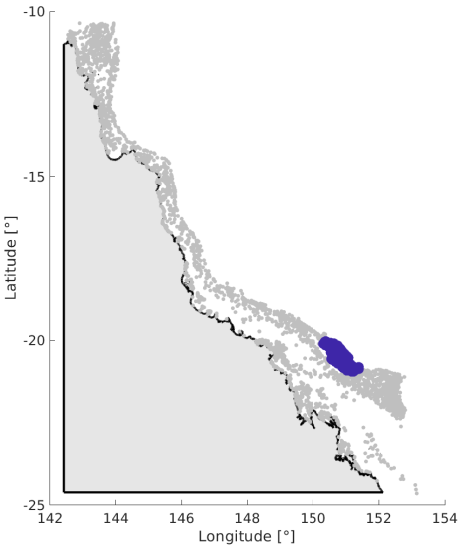

Figure 5.16: Number of strongly connected component with more than 75 reefs: 1

5.1.3.2 Community detection

Figures 5.17 and 5.18 present respectively the number of communities and the percentage of inter-community connectivity in 2008, 2010 and 2012 as a function of the resolution parameter γ. The two graphs show similar trends for every year. It means that the number of communities obtained by using the community detection method for a given resolution parameter γ is approximately the same for every year. The variability of the number of communities for a given resolution parameter γ is then small. However, it does not mean that these communities are the same every year.

Figures 5.19, 5.20 and 5.21 present the community detection results on the map of the GBR for every year. The resolution parameter γ was set at 0.00013. This value implies a percentage of inter-community connectivity of about 1%. The number of communities detected by the community detection method is about 200 every year but only the five main communities are shown for the sake of clarity. Generally, the five main communities are quite similar every year. One or two communities are located in the north of the GBR. Another community is located in the center of the GBR except in 2012 and the remaining communities are located in the south of the GBR, especially in the outer shelf.

It is interesting to note that reef clusters obtained with the community detection method rougly correspond to reef clusters obtained with the SCC method. Nevertheless, reef clusters obtained with the community detection method are generally larger and contain more reefs than reef clusters obtained with the SCC method. This is due to the fact that creating a cluster with the community detection method does not require two-way connections.

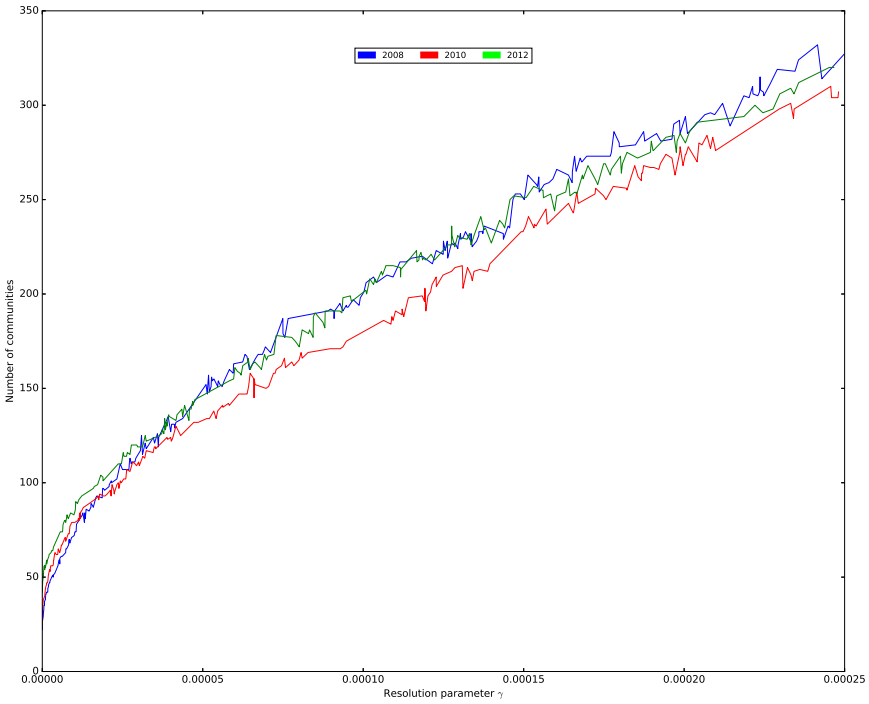

Figure 5.17: Number of communities in 2008, 2010 and 2012 as a function of the resolution parameter γ

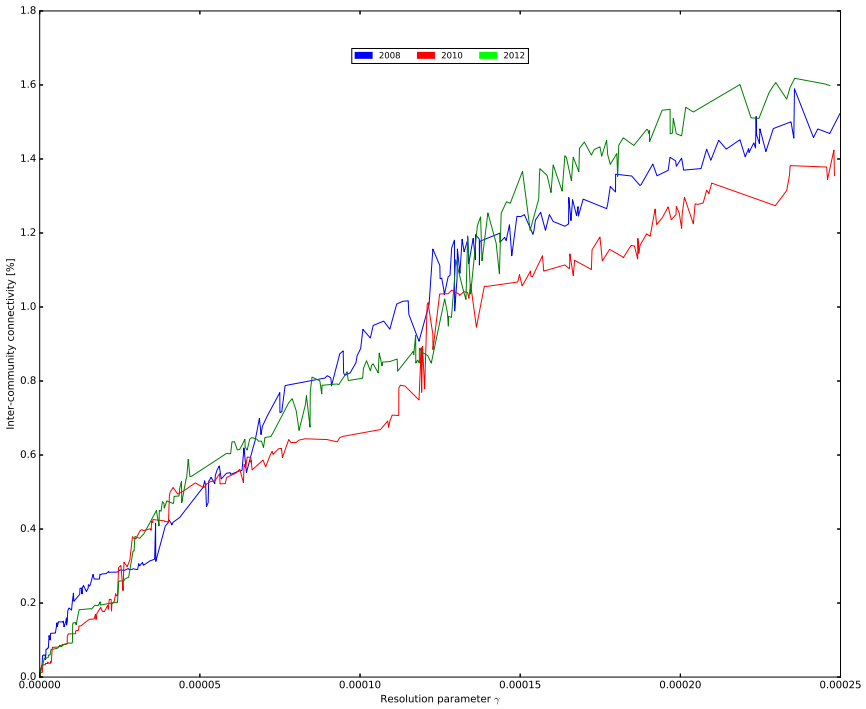

Figure 5.18: Percentage of inter-community connectivity in 2008, 2010 and 2012 as a function of the resolution parameter γ

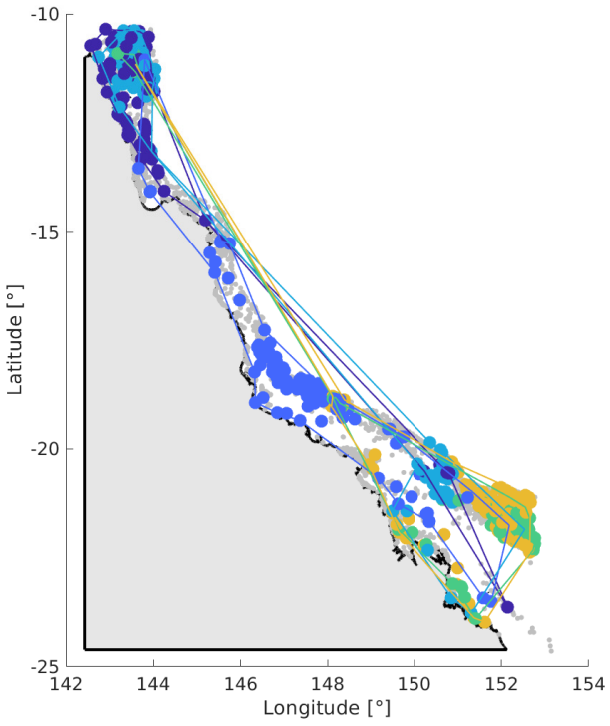

Figure 5.19: Five main communities in 2008 (for $\gamma = 0.00013$)

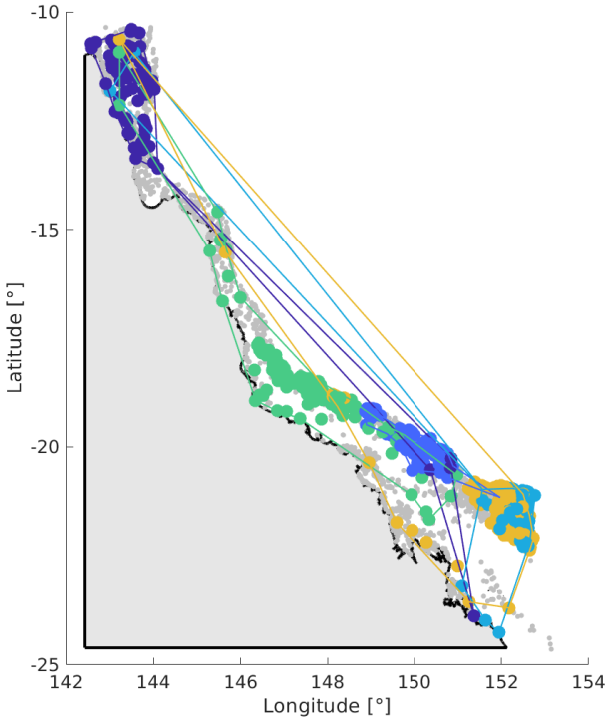

Figure 5.20: Five main communities in 2010 (for $\gamma = 0.00013$)

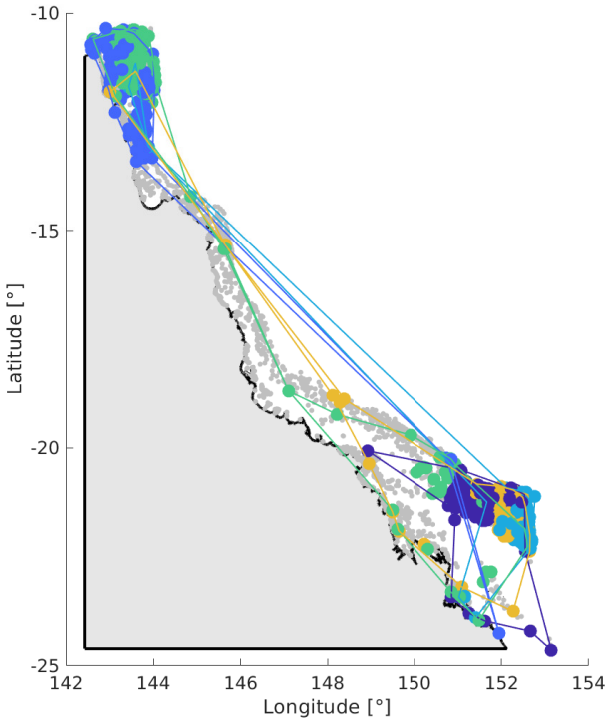

Figure 5.21: Five main communities in 2012 (for $\gamma = 0.00013$)

5.2 Pratical implications

All results from section 5.1 can be used to draw meaningful conclusions. These conclusions give an overview of the connectivity in the GBR and they could be used to inform marine management strategies for achieving restoration and protection of the GBR.

First of all, the analysis can be performed by interpreting the connectivity measures. This analysis reveals that the GBR is divided in three distinct regions. The first one corresponds to the north of the GBR which is a region with a high reef density. This region is characterised by a high local retention notably due to the high "sticky water" effect. This area has also a high self-recruitment indicator which is a consequence of the high local retention indicator. Although the reefs in the north region are still connected to each other, the main source of larvae for a reef seem to be itself. The second region corresponds to the center of the GBR. This region is also characterised by high local retention and self-recruitment indicators. However, this trend is less pronounced. The third region corresponds to the south of the GBR. This region is characterised by a high level of connectivity. The reefs in the south regions are well connected to each other and thus they give many larvae to their neighbours and receive many larvae from them as well. This is due to high degree centrality and PageRank indicators in this area. The reefs in the outer shelf are even more connected to each other. Furthermore, it should be noted that the coefficients of variation of each indicator are generally low for most of the hotspots. It means that these hotspots are consistent and can be considered as reliable from one year to another.

Secondly, in terms of protection, the reefs that would need some protection are mainly located in the southern part of the center of the GBR and in the northern part of the south of the GBR (see figure 5.22). These reefs have the highest protection indicators as they provide many larvae to downstream reefs. Larvae from reefs that would need protection are indeed transported from most northern areas to most southern areas (see figures 5.23 and 5.24). This is notably due to the East Australian Current (see figure 1.4). Because of the net transport southward, the reefs located in the center of the GBR and in most northern areas of the south of the GBR are not well supplied. Therefore, the reefs that would need more protection are the hotspots located in the center of the GBR and in the northern part of the south of the GBR.

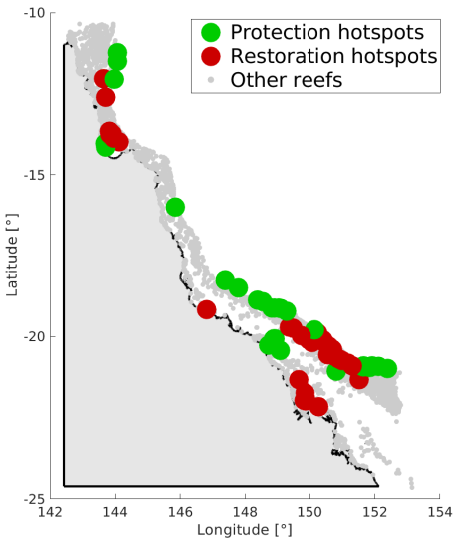

Figure 5.22: Reefs in the GBR that would need protection or restoration based on the PageRank indicators

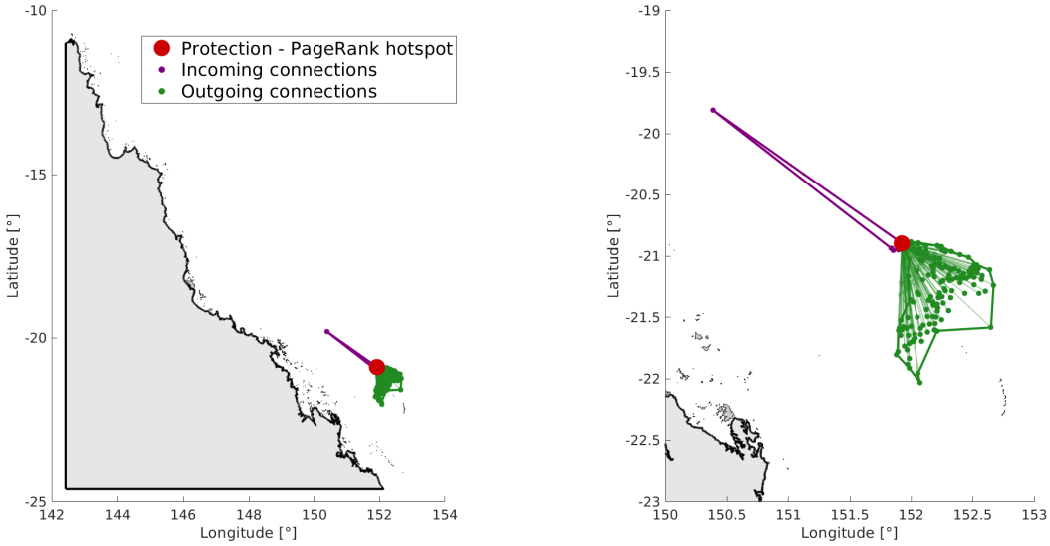

Figure 5.23: A reef with a high PageRank protection indicator located in the south of the GBR. This reef corresponds to a protection hotspot (see figure 5.22)

.

Thirdly, in terms of restoration, the reefs that would need some restoration are mainly located downstream of reefs that would need protection. These restoration hotspots are thus located in the south of the GBR. These reefs have the highest restoration indicators as they receive many larvae from upstream reefs and give many larvae to downstream reefs. As already mentioned above, below the bifurcation point, larvae are transported from most northern areas to most southern areas due to the East Australian Current (see figures 1.4, 5.23 and 5.24).

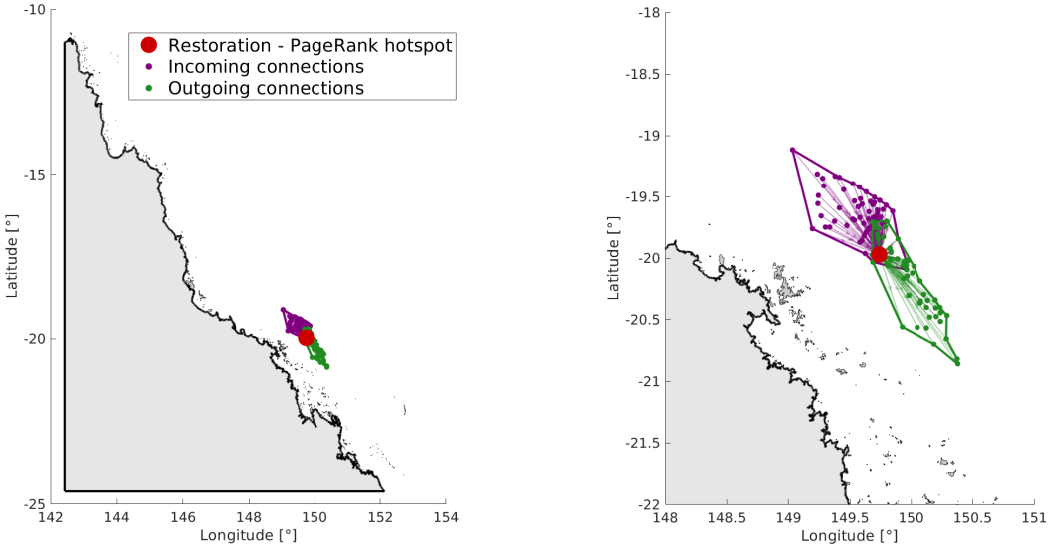

Figure 5.24: A reef with a high PageRank restoration indicator located in the south of the GBR. This reef corresponds to a restoration hotspot (see figure 5.22)

.

Furthermore, most of the protection and restoration hotspots are located inside reef clusters obtained by the SCC method (see section 5.1.3.1) and the community detection method (see section 5.1.3.2). The overall effect of these protection and restoration reefs is then expected to be very positive. The size of the reef clusters gives an idea about the scope of the action of the most important reefs (i.e. the protection and restoration hotspots).

Finally, although the reefs with the highest protection and restoration values are mainly located in the south of the GBR, those with lower values that are located in the north of the GBR or in the northern part of the center of the GBR should not be neglected. Indeed, only local retention might be not sufficient for the recovery of the north region of the GBR.

5.3 Limitations

The whole modelling process is not free from errors of course and have some limitations. Here is a non-exhaustive list of points that could be improved:

- The reliability of the larval dispersal results depends directly on the quality of the hydrodynamics modelled by SLIM. However, as shown in section 2.5, currents from SLIM in some regions of the GBR do not replicate the real hydrodynamics. Therefore, the modelling effort should be improved to get more relevant outputs, especially in the north of the GBR.
- The aim of this master thesis is to study the variability of marine connectivity in the GBR between 2008, 2010 and 2012. However, in order to get more reliable results, the study should be conducted on a larger sample of spawning seasons.
- The dispersal of coral larvae is modelled only for the coral species *Acropora millepora*. To get a broader overview, this study should also be conducted for other coral species.
- A homogeneous repartition of the coral species *Acropora millepora* is assumed over the whole GBR but it is far from reality. Therefore, a deeper knowledge of biological aspects such as the exact repartition and density of *Acropora millepora* in the GBR could significantly improve the biophysical model.
- The biophysical model includes a few biological parameters in order to account for the life histories of the virtual larvae. However, many assumptions are made about these biological processes and thus the biophysical model does not reflect the reality.
- The aim of this master thesis is to identify the reefs most likely to support regional recovery processes due to their high connectivity. These reefs are classified as those would need some protection and those would need some restoration. However, to ensure an effective and sustainable action of the most important reefs, other criteria such as the probability to have a lower risk of exposure to coral bleaching or starfish outbreaks should be taken into account.
- The connectivity in the GBR was studied by using six different connectvity measures but other connectivity measures could give additional useful information about connectivity in the GBR.
- ...

6 Conclusion

The aim of this thesis was to study the variability of the connectivity in the GBR between 2008, 2010 and 2012. In order to do that, the study presented an effort to model the dispersal of coral larvae, of the species *Acropora millepora*, for the whole Great Barrier Reef (GBR) in each of the three years considered. In order to carry out this analysis of the variability of the connectivity in the GBR, several steps were achieved. Firstly, a high resolution ocean model was devised to simulate ocean currents in the whole GBR. The hydrodynamic model used is a 2D version of SLIM, an unstructured mesh ocean model. This allowed to increase the model's resolution close to reefs where small scale flow features were important and decrease the resolution in deeper areas where flow features were thought to be more uniform. Validation of the model showed a good agreement with real observations in the south of the GBR while the currents in the north of the GBR would still need improvements to replicate the real hydrodynamics of the region. Secondly, a Lagrangian particle tracker was used to simulate the transport of particles over the currents generated by the ocean model. It generated a connectivity matrix giving for each reef the number of larvae settled onto it and their origin. To interpret all data encapsulated in the connectivity matrix, some connectivity measures were described. Moreover, some protection and restoration measures were defined based on previous connectivity measures and two clustering methods were used. The analysis was made for the three spawning seasons and gave a picture of the connectivity patterns linking the different reefs in the GBR for every year. Finally, in order to have a broader overview of the connectivity in the GBR and to get more relevant and reliable results, data of the three years considered were gathered by using statistics such as the mean and the coefficient of variation. A few pratical conclusions could then be drawn from this statistical study.

The statistical analysis reveals that the GBR is divided in three distinct regions. The first one corresponds to the north of the GBR which is a region with a high reef density. This region is characterised by a high local retention and self-recruitment. Although the reefs in the north region are still connected to each other, the main source of larvae for a reef seem to be itself. The second region corresponds to the center of the GBR. This region is also characterised by high local retention and self-recruitment even though the trend is less pronounced. The third region corresponds to the south of the GBR which is characterised by a high level of connectivity. This implies high degree centrality and PageRank indicators in this area. The reefs in the outer shelf are even more connected to each other. Furthermore, it should be noted that the coefficients of variation of each indicator are generally low for most of the hotspots. It means that these hotspots are consistent and can be considered as reliable from one year to another.

In terms of protection, the reefs that would need some protection are mainly located in the southern part of the center of the GBR and in the northern part of the south of the GBR. Larvae from these reefs are transported from most northern areas to most southern areas. In terms of restoration, the reefs that would need some restoration are mainly located downstream of previous reefs that would need some protection. These restoration hotspots are thus located in the south of the GBR. These reefs receive many larvae from upstream reefs and give many larvae to downstream reefs. Most of the protection and

restoration hotspots are located inside reef clusters. The overall effect of these protection and restoration reefs is then expected to be very positive for reefs inside those clusters. Finally, the reefs with lower protection and restoration indicators that are located in the north of the GBR or in the northern part of the center of the GBR should not be neglected because only local retention might be not sufficient for the recovery of the north region of the GBR.

All these meaningful results could be used to inform marine management strategies for achieving restoration and protection of the GBR because they determine which reefs play a major role in the conservation of the GBR. These marine management strategies could consist of the placement of Marine Protected Areas (MPAs).

Bibliography

[1] Jonathan Lambrechts. *Finite Element Methods for Coastal Flows: Application to the Great Barrier Reef.* PhD thesis, Université Catholique de Louvain, 2011.

[2] Eric Deleersnijder. Msc thesis subjects (co-)submitted by Eric Deleersnijder to students of the Louvain School of Engineering for the academic year 2017-2018. *Optimal placement of corals restoration projects to enhance reef resilience*, 2017.

[3] Karlo Hock, H. Wolff Nicholas, C. Ortiz Juan, A. Condie Scott, G. Blackwell Paul R.N. Anthony Kenneth, and J. Mumby Peter. Connectivity and systemic resilience of the Great Barrier Reef. *PLOS | Biology*, 2017.

[4] John O'Mahony, Dr. Ric Simes, David Redhill, Kelly Heaton, Claire Atkinson, Emily Hayward, and Mai Nguyen. At what price ? The economic, social and icon value of the Great Barrier Reef. *Deloitte. Access Economics*, 2017.

[5] Wolanski E. *Physical Oceanographic Processes of the Great Barrier Reef.* Boca Raton, FL: CRC Press, 1994.

[6] Andrews J.C. and L. Bode. The tides of the central Great Barrier Reef. *Continental shelf research*, 1988.

[7] Christopher Thomas. *Modelling marine connectivity in the Great Barrier Reef and exploring its ecological implications.* PhD thesis, Université Catholique de Louvain, 2015.

[8] Redondo-Rodriguez A., S.J. Weeks, R.Berkelmans, O. Hoegh-Guldberg, and J.M. Lough. Climate variability of the Great Barrier Reef in relation to the tropical Pacific and El Niño-southern oscillation. *Marine and Freshwater Research*, 2012.

[9] Wolanski Eric, Richard Brinkman, Simon Spagnol, Felicity McAllister, Craig Steinberg, William Skirving, and Eric Deleersnijder. Merging scales in models of water circulation: perspectives from the Great Barrier Reef. *Advances in coastal modeling*, 2003.

[10] Middleton J.H. Steady coastal circulation due to oceanic longshore pressure gradients. *Journal of physical oceanography*, 1987.

[11] Brinkman R., E. Wolanski, E. Deleersnijder, F. McAllister, and W. Skirving. *Oceannic inflow from the Coral Sea into the Great Barrier Reef.* Estuarine, Coastal ad Shelf Science, 2002.

[12] Cowen R.K., G. Gawarkiewicz, J. Pineda NAD S.R. Thurrold, and F.E. Werner. Population connectivity in marine systems: an overview. *Oceanography*, 2007.

[13] Gaylord B. and S.D. Gaines. Smelling home can prevent dispersal of reef fish larvae. *The american naturalist*, 2000.

[14] Trakhtenbrot A., R. Nathan, G. Perry, and D.M. Richardson. The importance of long-distance dispersal in biodiversity conservation. *Diversity and distributions*, 2005.

[15] Cowen R.K., C.B. Paris, and A. Srinivasan. Scaling of connectivity in marine populations. *Science*, 2006.

[16] Hughes T.P. and J.E. Tanner. Recruitment failure, life histories, and long-term decline of Caribbean corals. *Ecology*, 2000.

[17] Palumbi S.R. Population genetics and demographic connectivity and the design of marine reserves. *Ecological Applications*, 2003.

[18] Charles Frys. Modeling marine connectivity in the Florida Coral Reef Tract. Master's thesis, Université Catholique de Louvain, Faculty of Bioscience Engineering, 2017.

[19] White J.W., A.J. Scholz, A. Rassweiler, C. Steinback, L.W. Botsford, S. Kruse, C. Costello, S. Mitarai, D.A. Siegel, P.T. Drake, and C.A. Edwards. A comparison of approaches used for economic analysis in marine protected area network planning in California. *Ocean and coastal management*, 2013.

[20] Almany G.R., S.R. Connolly, D.D. Heath, J.D. Hogan, G.P. Jones, L.J. McCook, M.Mills, R.L. Pressey, and D.H. Williamson. Connectivity biodiversity conservation and the design of marine reserve networks for coral reefs. *Coral Reefs*, 2009.

[21] Drew J.A. and P.H. Barber. Comparative phylogeography in fijian coral reef fishes: a multi-taxa approach towards marine reserve design. *PLOS | Biology*, 2009.

[22] Hughes T.P., D.R. Bellwood, C. Folke, R.S. Steneck, and J. Wilson. New paradigms for supporting the resilience of marine ecosystems. *Trends in ecology and evolution*, 2005.

[23] Christie M.R., B.N. Tissot, M.A. Albins, J.P. Beets, Y. Jia, D.M. Ortiz, S.E. Thompson, and M.A. Hixon. Larval connectivity in an effective network of Marine Protected Areas. *PLOS One*, 2010.

[24] Kininmonth S., M. Berger, M. Bode, E. Peterson, V.M. Adams, D. Dorfman, D.R. Brumbaugh, and H.P. Possingham. Dispersal connectivity and reserve selection for marine conservation. *Ecological modelling*, 2011.

[25] Olivier Gourgue. *Finite element modeling of sediment dynamics in the Scheldt*. PhD thesis, Université Catholique de Louvain, 2011.

[26] de Brye B., A. de Brauwere, O. Gourgue, T. Karna, J. Lambrechts, R. Comblen, and E. Deleersnijder. A finite-element, multi-scale of the scheldt tributaries, river, estuary and rofi. *Coastal Engineering*, 2010.

[27] Andutta F.P., P.V. Ridd, and E. Wolanski. Dynamics of hypersaline coastal waters in the Great Barrier Reef. *Estuarine, coastal and shelf science*, 2011.

[28] Cushman-Roisin B. and J.M. Beckers. *Introduction to geophysical fluid dynamics*. Elsevier, 2011.

[29] Smith S.D. and E.G. Banke. Variation of the sea surface drag coefficient with wind speed. *Quarterly journal of the Royal Meteorological Society*, 1975.

[30] Geenaert G.L. On the importance of the drag coefficient in air-sea interactions. *Dynamics of atmospheres and oceans*, 1987.

[31] Smagorinsky J. General circulation experiments with the primitive equations. *Monthly weather review*, 1963.

[32] Lambrechts J., E. Hanert, E. Deleersnijder, P.E. Bernard, V. Legat, J.F. Remacle, and E. Wolanski. A multi-scale model of the hydrodynamics of the whole Great Barrier Reef. *Estuarine, coastal and shelf science*, 2008.

[33] Introduction to the SLIM model. `http://sites.uclouvain.be/slim/index.php?id=24`.

[34] Geuzaine C. and J.F. Remacle. Gmsh: a 3-D finite element mesh generator with built-in pre- and post- processing facilities. *International journal for numerical metods in engineering*, 2009.

[35] Le Bars Y., V. Vallaeys, E. Deleersnijder, E. Hanert, L. Carrere, and C. Channelière. Introduction to geophysical fluid dynamics. 2016.

[36] Christopher J. Thomas, Jonathan Lambrechts, Eric Wolanski, Vincent A. Traag, Vincent D. Blondel, Eric Deleersnijder, and Emmanuel Hanert. Numerical modelling and graph theory tools to study ecological connectivity in the Great Barrier Reef. *Elsevier*, 2013.

[37] Spagnol S., E. Wolanski, E. Deleersnijder, R. Brinkman, F. McAllister, B. Cushman-Roisin, and E. Hanert. An error frequently made in the evaluation of advective transport in two-dimensional lagrangian modles of advection-diffusion in coral reef waters. *Marine ecology progress series*, 2002.

[38] Hunter J.R., P.D. Craig, and H.E. Phillips. On the use of random walk models with spatially variable diffusivity. *Journal of computational physics*, 1993.

[39] Barnes and Hughes. *An introduction to marine ecology.* Blackwell Science, 1999.

[40] Veron JEN. *Corals of the world.* Australian Institute of Marine Sciences, 2000.

[41] Jones O.A. and R. Endean. *Biology and geology of coral reefs.* New York: Harcourt Brace Jovanovich, 1973.

[42] Joana Figueiredo, Andrew H. Baird, and Sean R. Connolly. Synthesizing larval competence dynamics and reef-scale retention reveals a high potential for self-recruitment in corals. *Ecological society of America*, 2013.

[43] Connolly S.R. and A.H. Baird. Estimating dispersal potential for marine larvae: dynamic models applied to scleractinian corals. *Ecology*, 2010.

[44] Price N. Habitat selection, facilitation, and biotic settlement cues affect distribution and performance of coral recruits in french polynesia. 2010.

[45] Jones G., G. Almany, G. Russ, P. Sale, and R. Steneck. Larval retention and connectivity among populations of corals and reef fishes: history, advances and challenges. *Coral Reefs*, pages 307–325, 2009.

[46] Lawrence Page, Sergey Brin, Rajeev Motwani, and Terry Winograd. The PageRank Citation Ranking: Bringing order to the web. Technical report, Stanford InfoLab, 1999.

[47] Traag V.A., P.Van Dooren, and Y. Nesterov. Narrow scope for resolution-limit-fere community detection. *Physical review*, 2011.

[48] Ronhovde P. and Z. Nussinov. Local resolution-limit-free Potts model for community detection. *Physical review*, 2010.

[49] Blondel V.D., J.L. Guillaume, R. Lambiotte, and E. Lefebvre. Fast unfolding of communities in large networks. *Journal of Statistical Mechanics: theory and experiment*, 2008.

[50] Wackerly D., W. Mendenhall III, and R. Scheaffer. *Mathematical Statistics with applications*. Thomson Brooks/Cole, 2008.

[51] Wolanski E. and S. Spagnol. "sticky Waters" in the Great Barrier Reef. *Estuarine, COastal and Shelf Science*, 2000.

A Appendices

The appendices mainly contain the figures of the two periods not shown in the main text.

A.1 Validation of the hydrodynamics

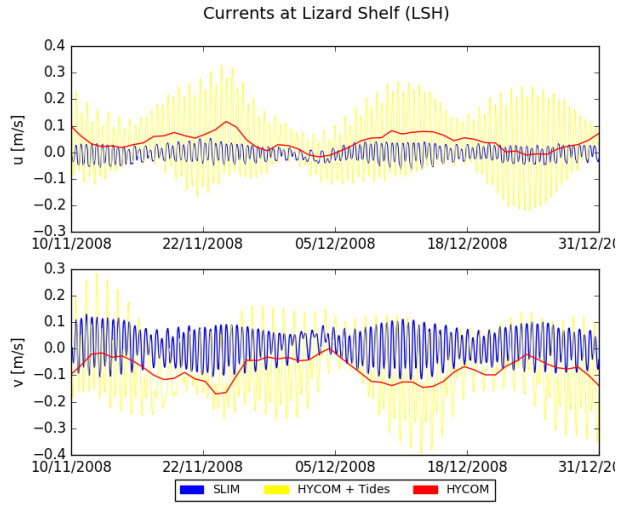

(a) Current speeds

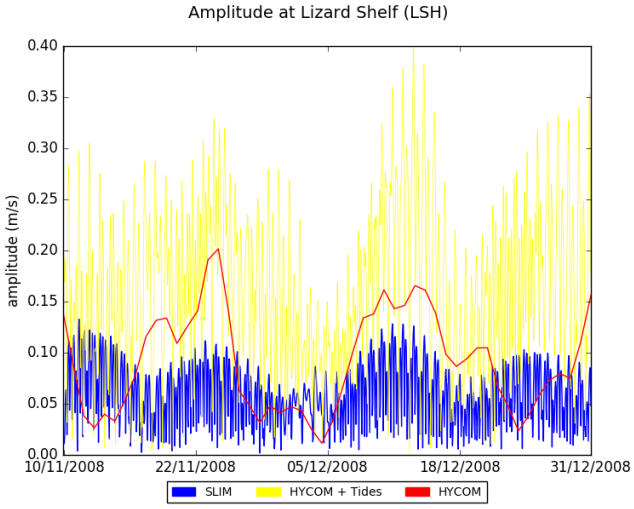

(b) Current amplitudes

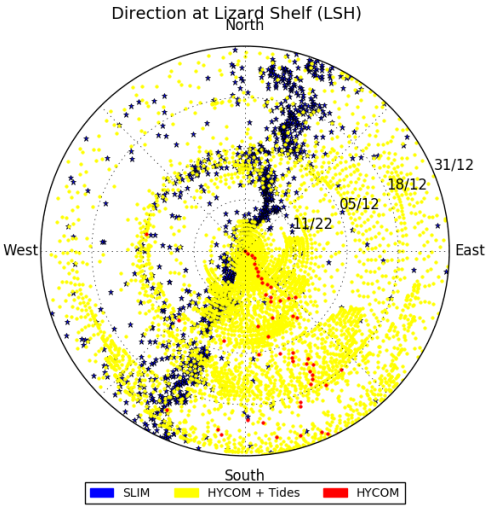

(c) Current directions

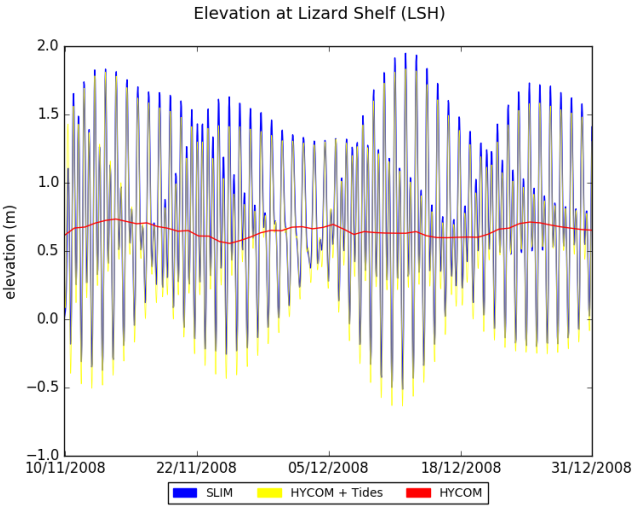

(d) Water elevations

Figure A.1: Current speeds, current amplitudes, current directions and water elevations of validation point 1 (Lizard Shelf) in 2008.

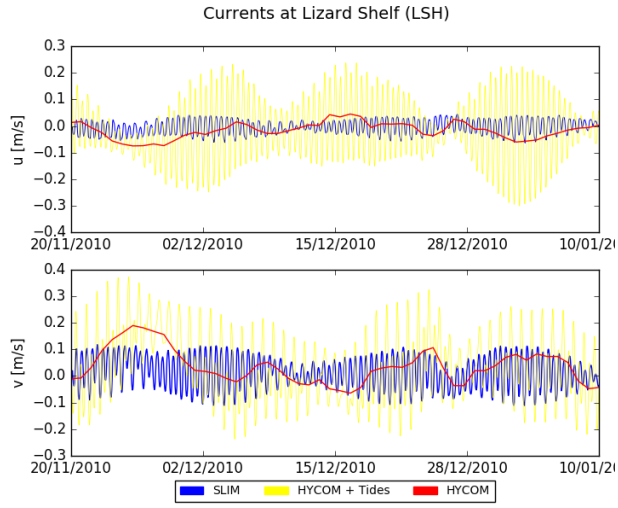

(a) Current speeds

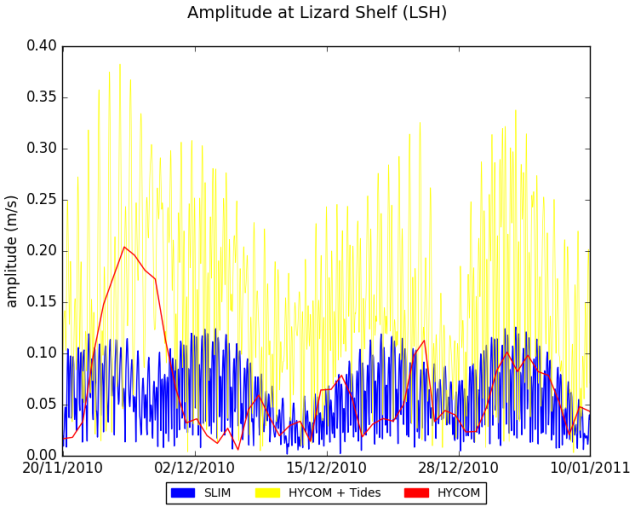

(b) Current amplitudes

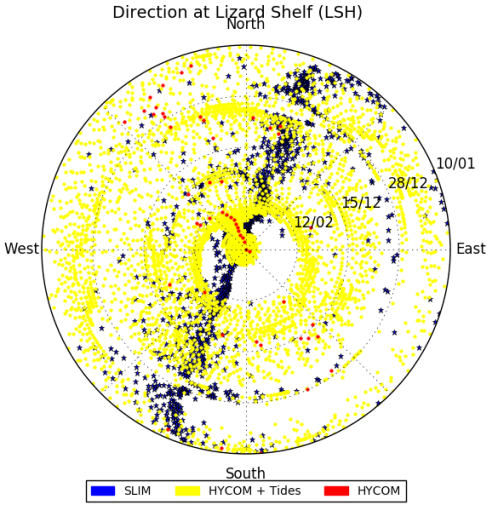

(c) Current directions

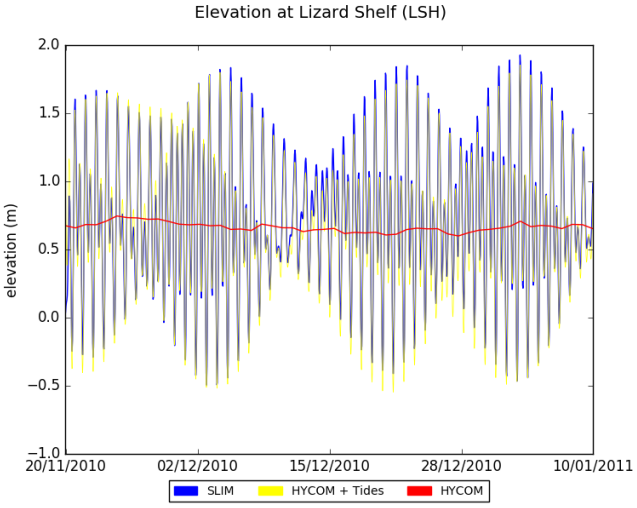

(d) Water elevations

Figure A.2: Current speeds, current amplitudes, current directions and water elevations of validation point 1 (Lizard Shelf) in 2010.

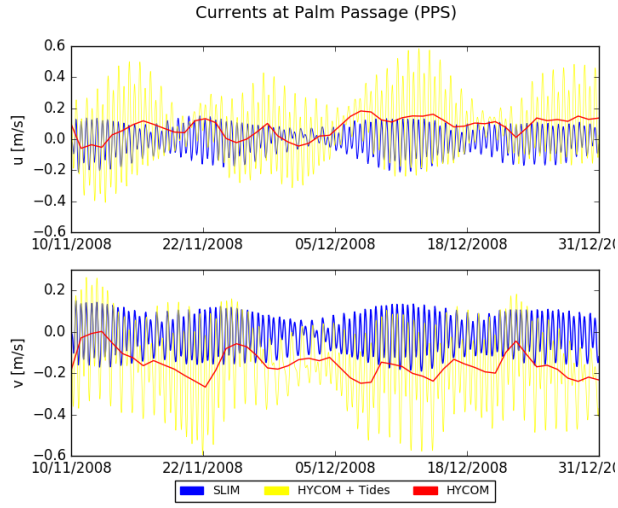

(a) Current speeds

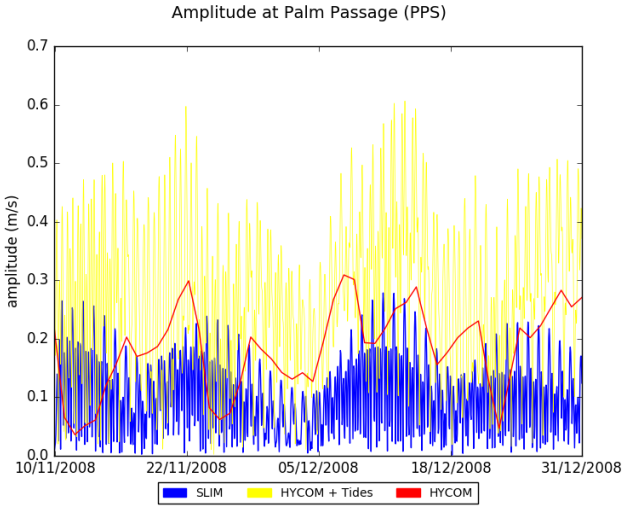

(b) Current amplitudes

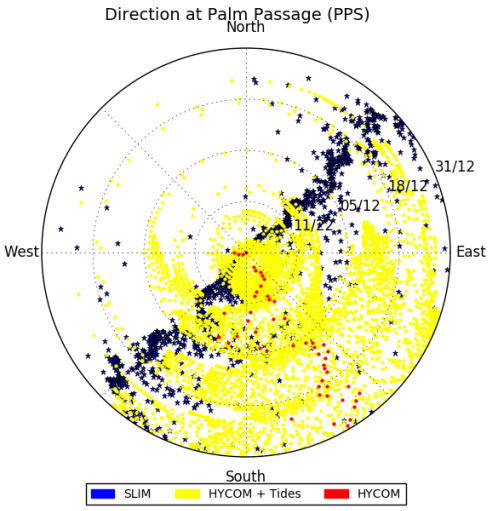

(c) Current directions

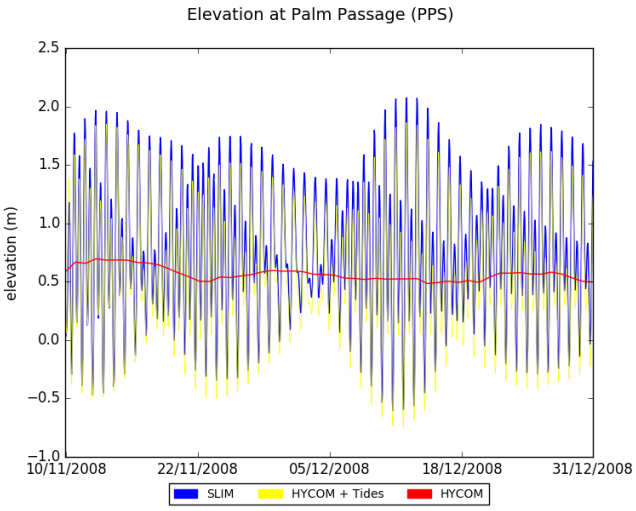

(d) Water elevations

Figure A.3: Current speeds, current amplitudes, current directions and water elevations of validation point 2 (Palm Passage) in 2008.

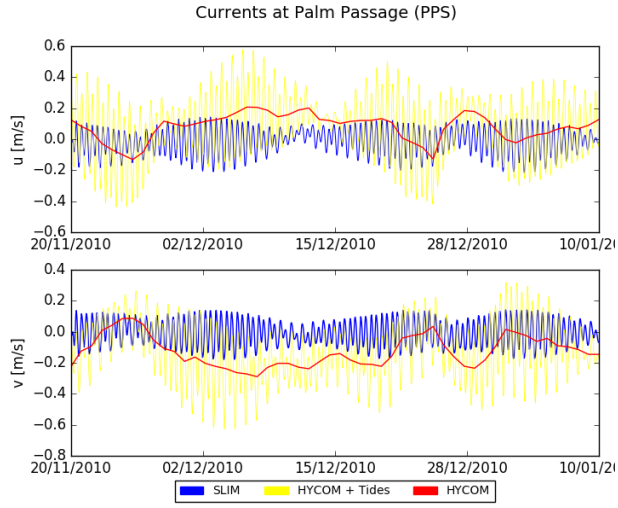

(a) Current speeds

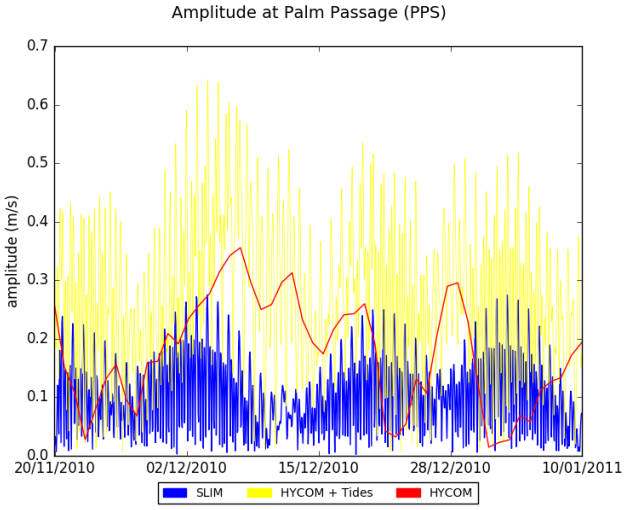

(b) Current amplitudes

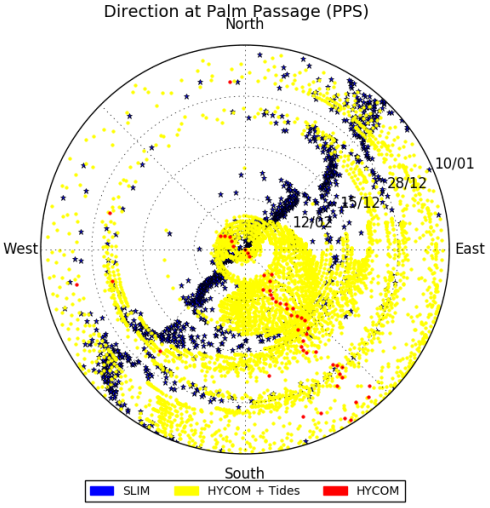

(c) Current directions

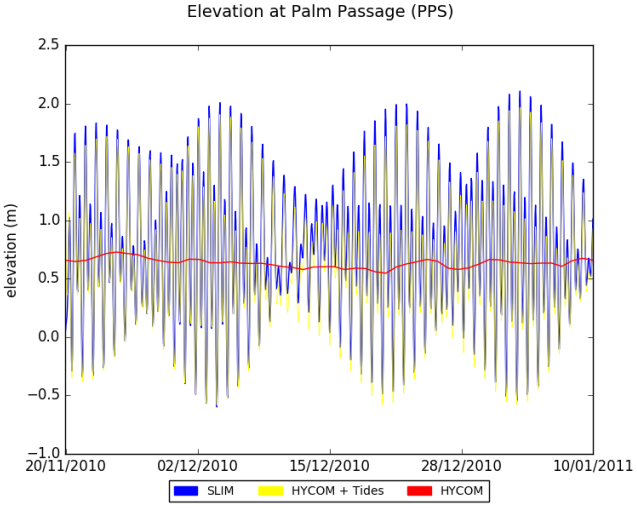

(d) Water elevations

Figure A.4: Current speeds, current amplitudes, current directions and water elevations of validation point 2 (Palm Passage) in 2010.

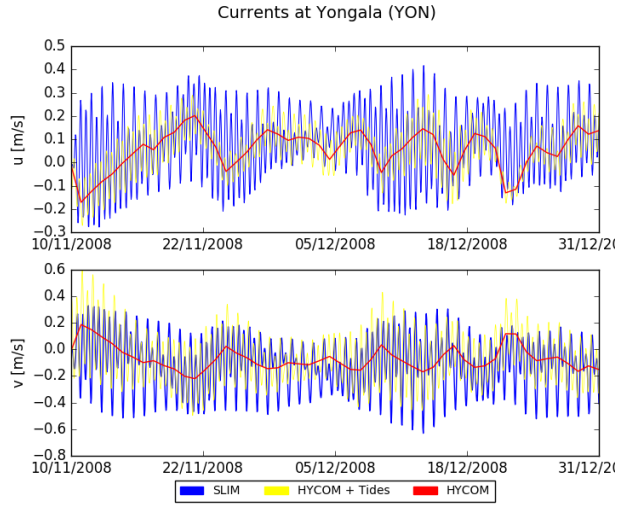

(a) Current speeds

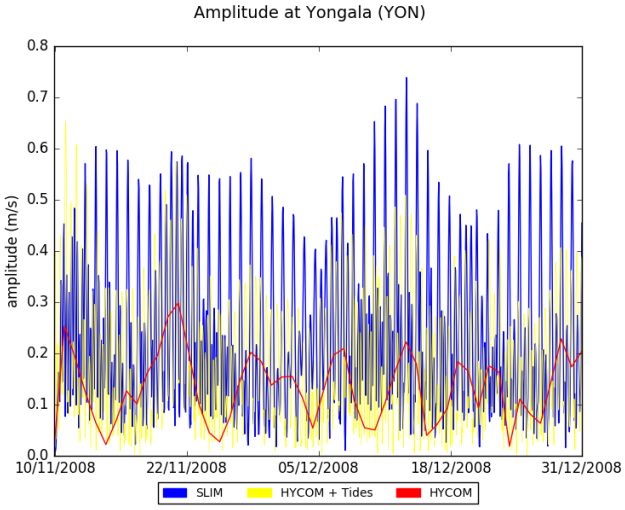

(b) Current amplitudes

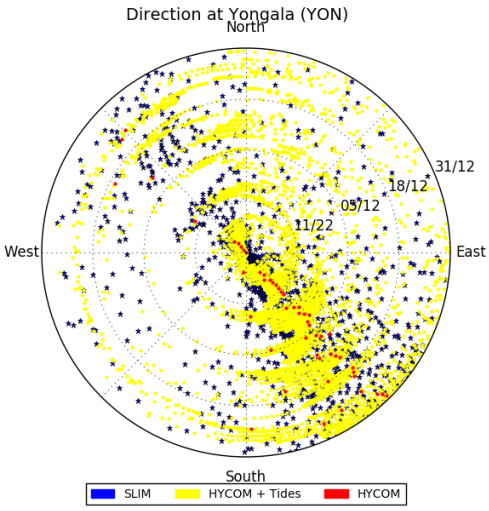

(c) Current directions

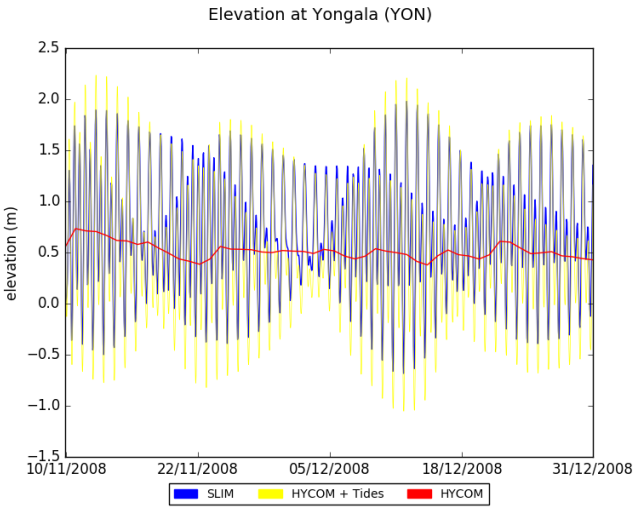

(d) Water elevations

Figure A.5: Current speeds, current amplitudes, current directions and water elevations of validation point 3 (Yongala) in 2008.

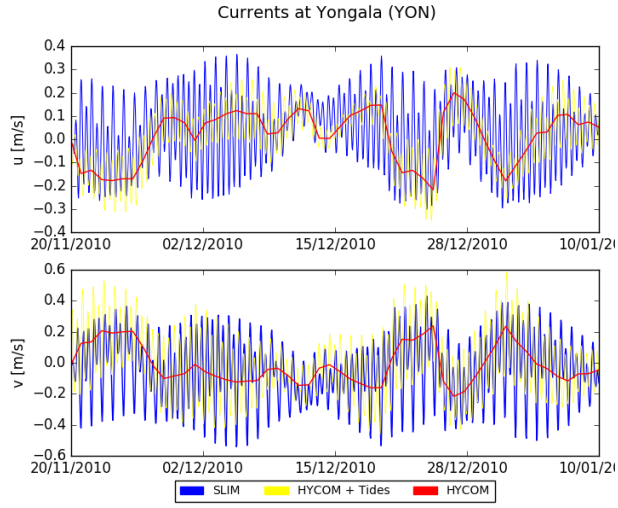

(a) Current speeds

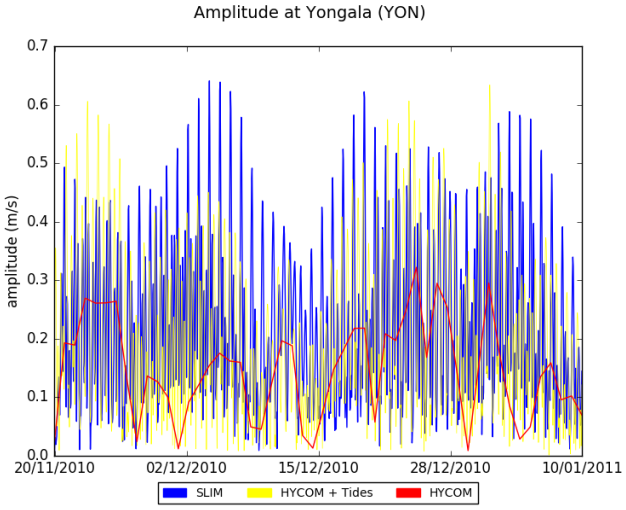

(b) Current amplitudes

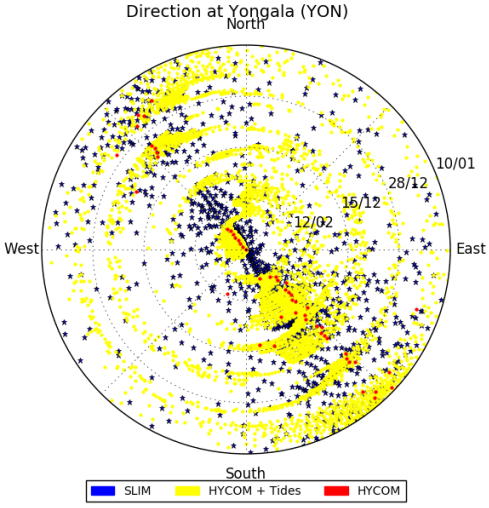

(c) Current directions

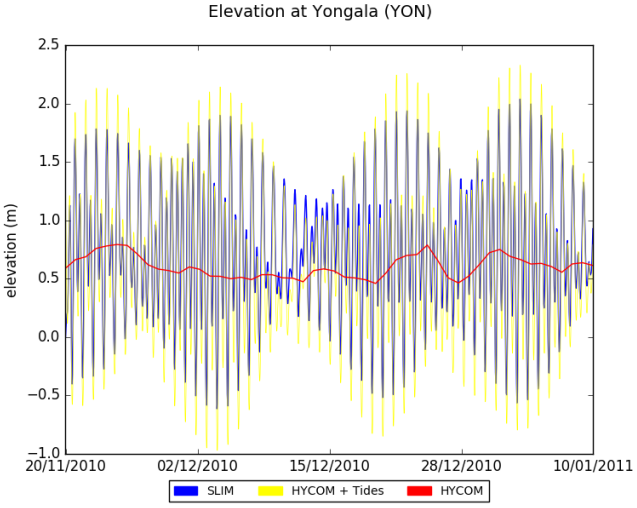

(d) Water elevations

Figure A.6: Current speeds, current amplitudes, current directions and water elevations of validation point 3 (Yongala) in 2010.

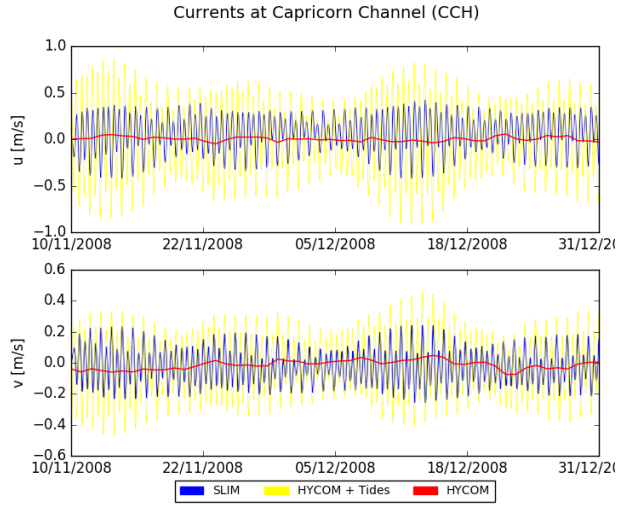

(a) Current speeds

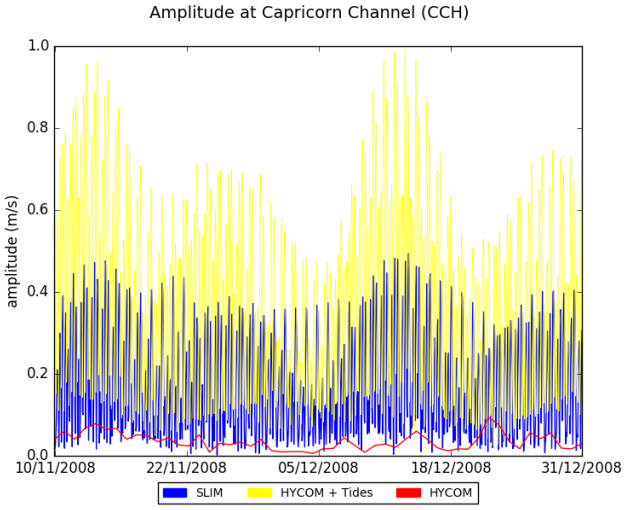

(b) Current amplitudes

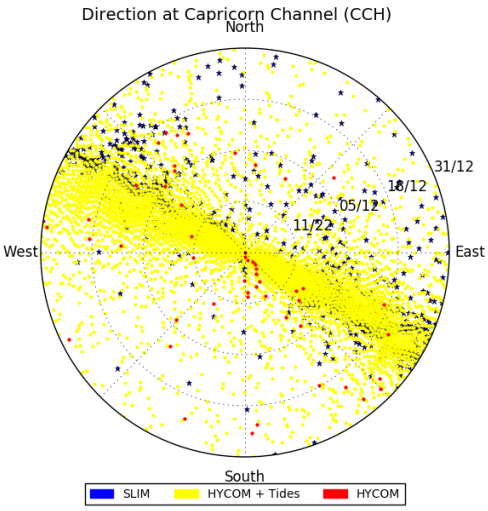

(c) Current directions

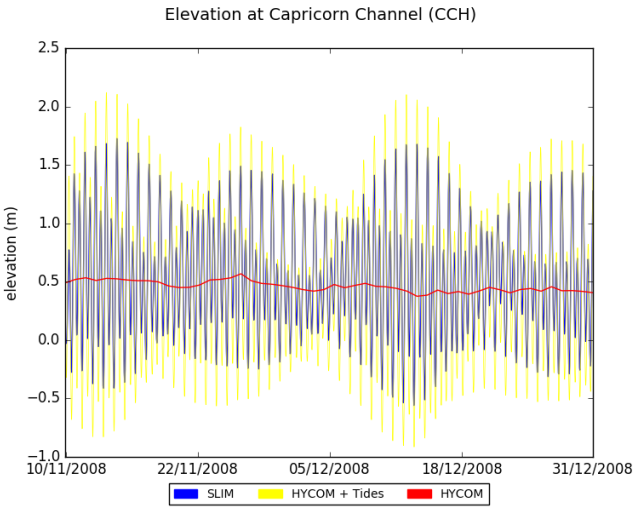

(d) Water elevations

Figure A.7: Current speeds, current amplitudes, current directions and water elevations of validation point 4 (Capricorn Channel) in 2008.

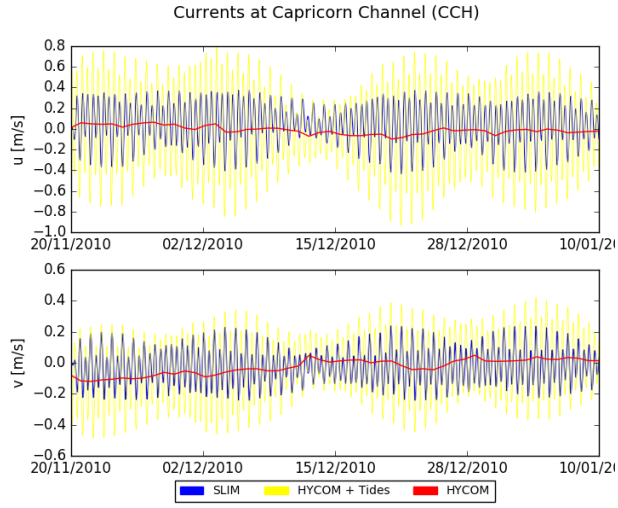

(a) Current speeds

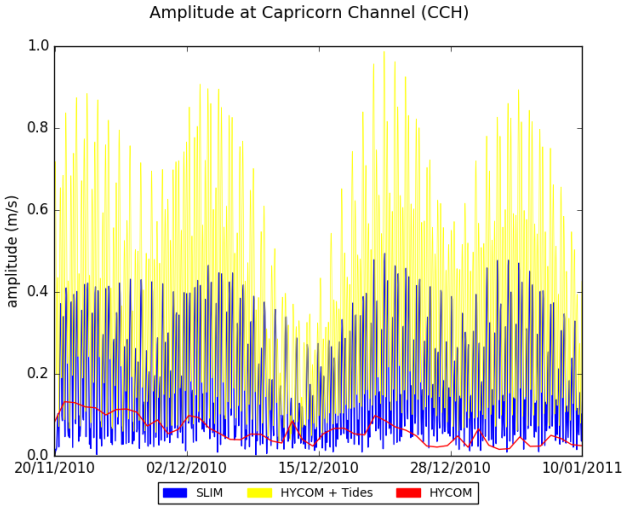

(b) Current amplitudes

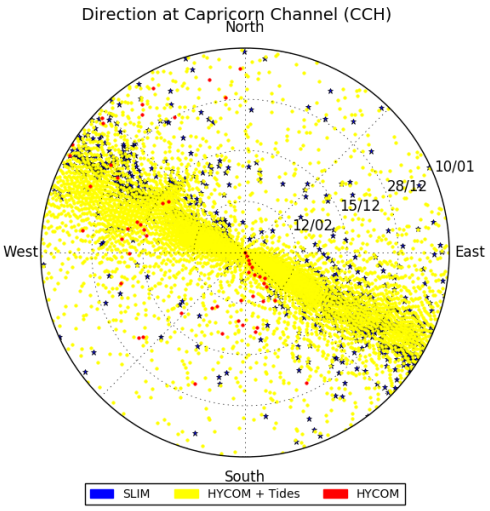

(c) Current directions

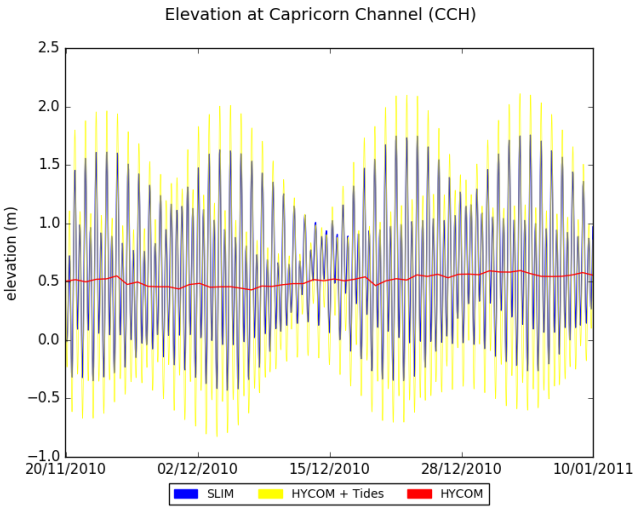

(d) Water elevations

Figure A.8: Current speeds, current amplitudes, current directions and water elevations of validation point 4 (Capricorn Channel) in 2010.

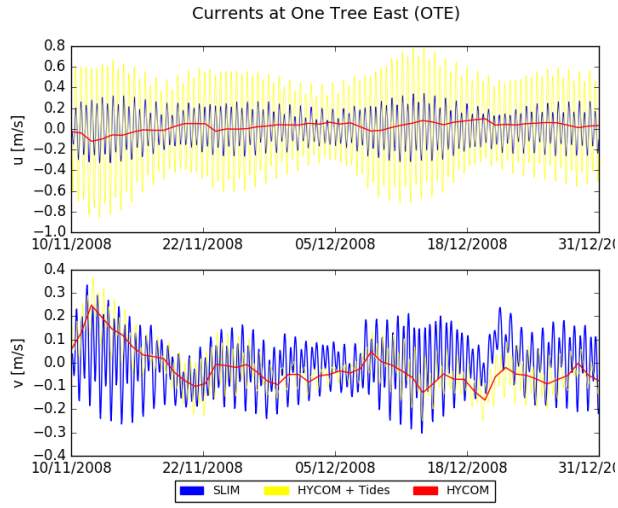

(a) Current speeds

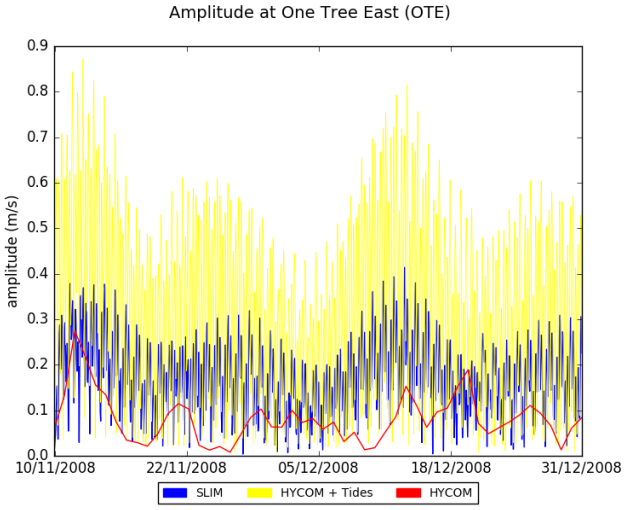

(b) Current amplitudes

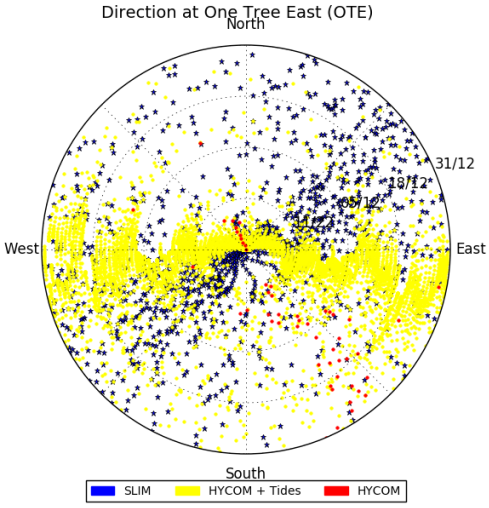

(c) Current directions

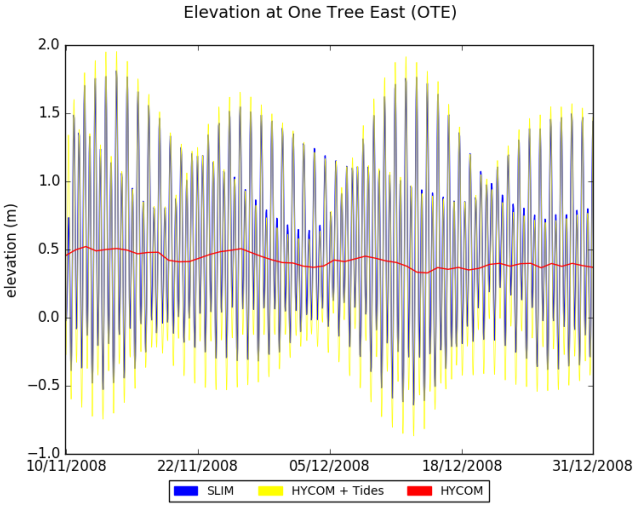

(d) Water elevations

Figure A.9: Current speeds, current amplitudes, current directions and water elevations of validation point 5 (One Tree East) in 2008.

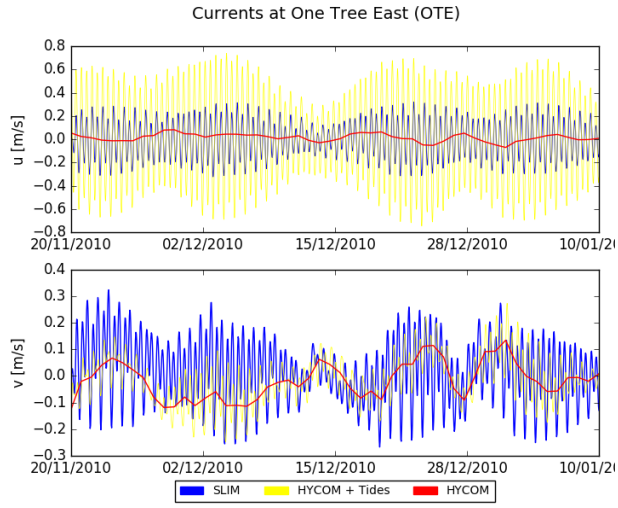

(a) Current speeds

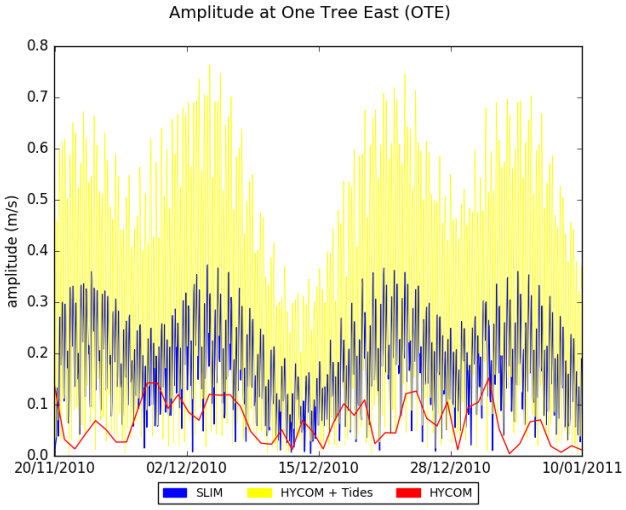

(b) Current amplitudes

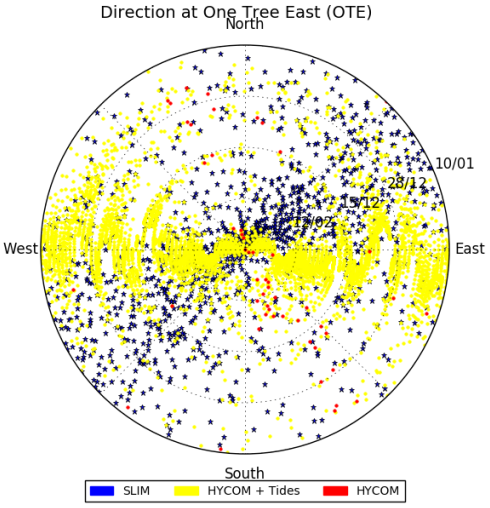

(c) Current directions

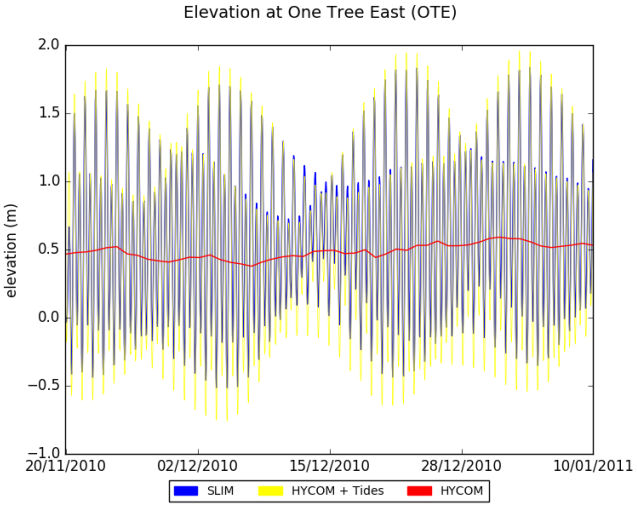

(d) Water elevations

Figure A.10: Current speeds, current amplitudes, current directions and water elevations of validation point 5 (One Tree East) in 2010.

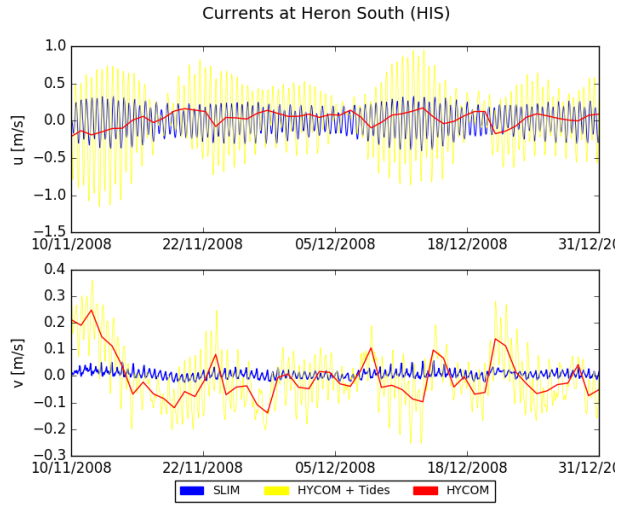

(a) Current speeds

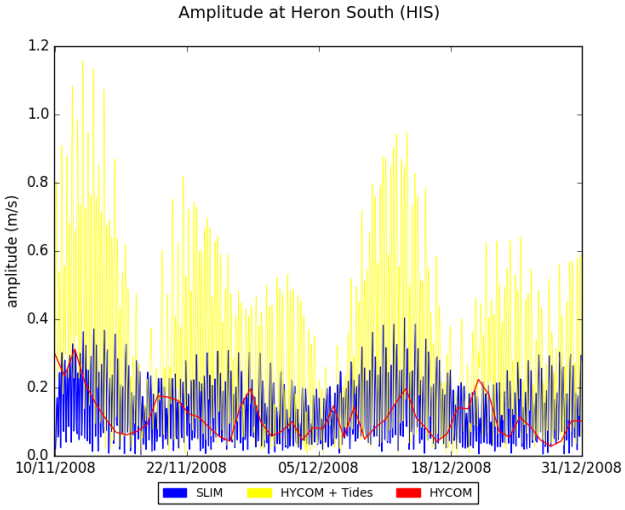

(b) Current amplitudes

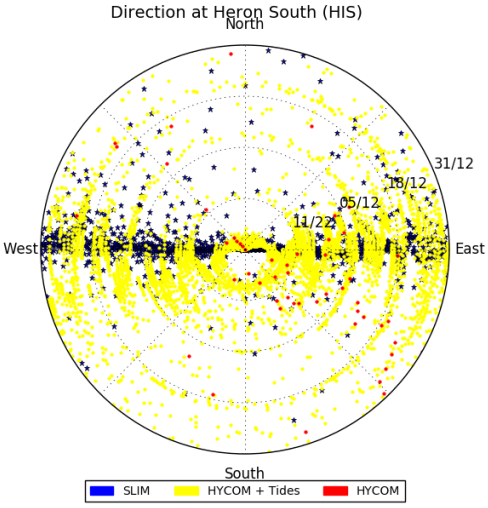

(c) Current directions

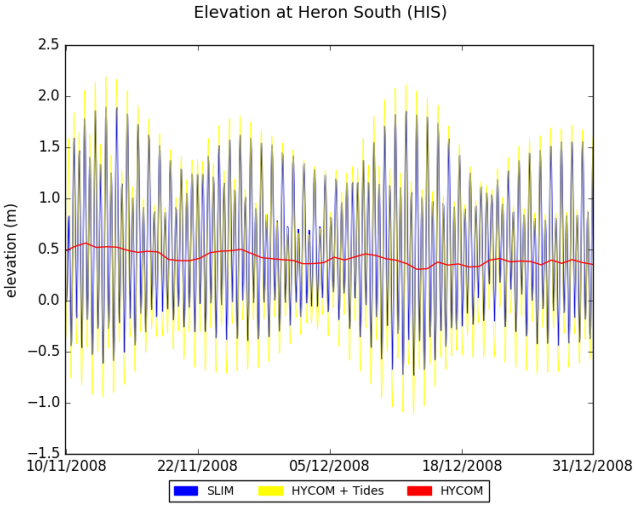

(d) Water elevations

Figure A.11: Current speeds, current amplitudes, current directions and water elevations of validation point 6 (Heron South) in 2008.

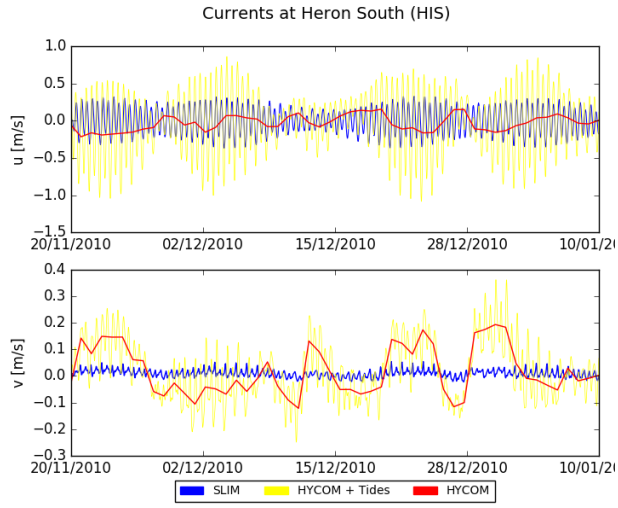

(a) Current speeds

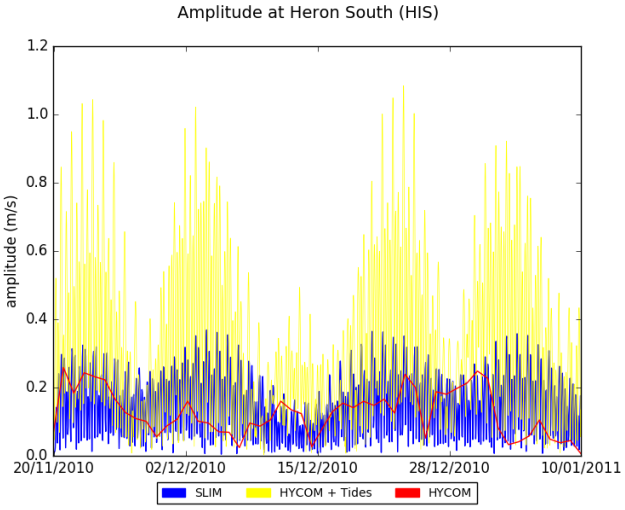

(b) Current amplitudes

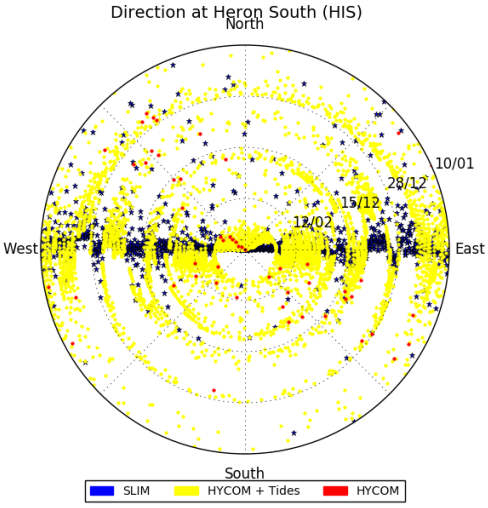

(c) Current directions

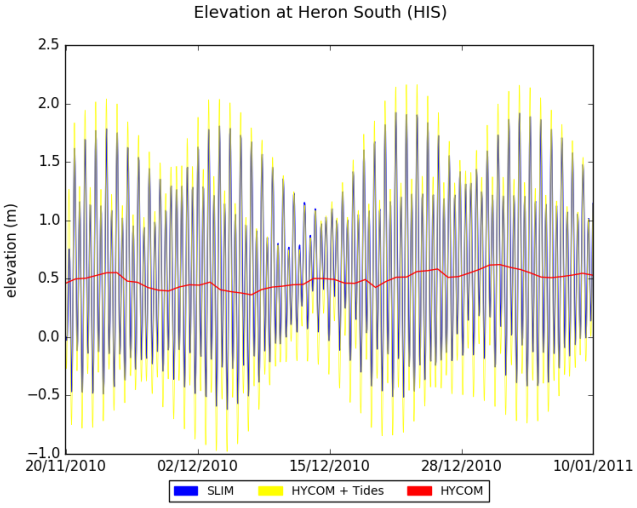

(d) Water elevations

Figure A.12: Current speeds, current amplitudes, current directions and water elevations of validation point 6 (Heron South) in 2010.

A.2 Connectivity measures

This section contains all figures for the connectivity measures in 2008 and 2012.

A.2.1 Local retention

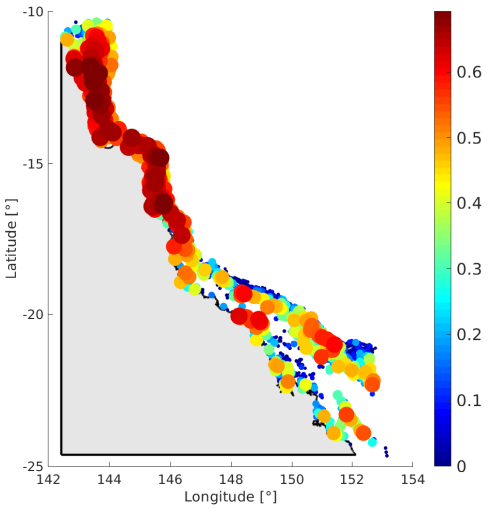

Figure A.13: Local retention in 2008

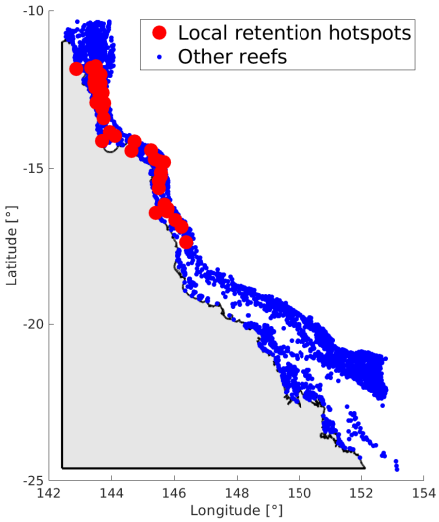

Figure A.14: Local retention hotspots in 2008

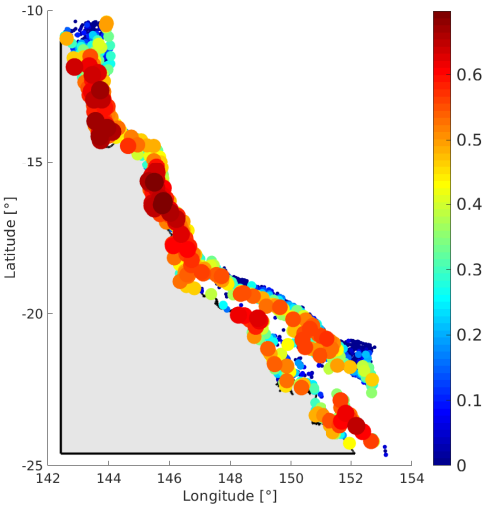

Figure A.15: Local retention in 2012

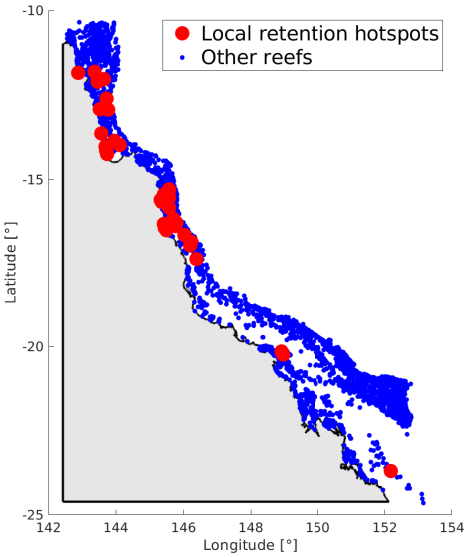

Figure A.16: Local retention hotspots in 2012

A.2.2 Self-recruitment

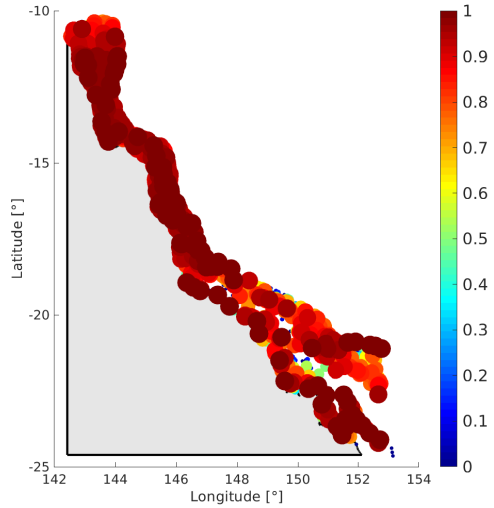

Figure A.17: Self-recruitment in 2008

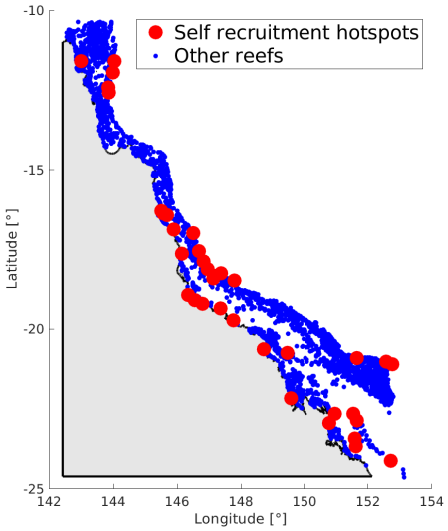

Figure A.18: Self-recruitment hotspots in 2008

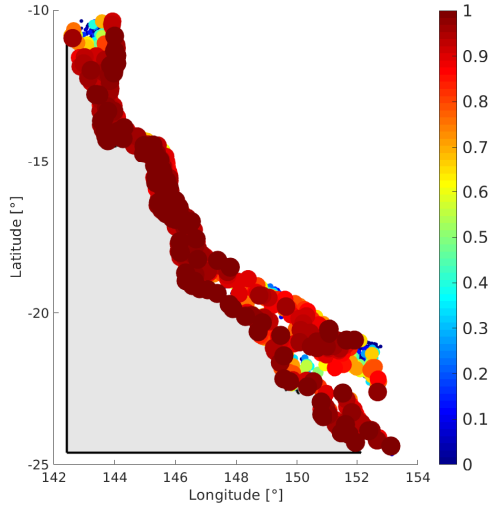

Figure A.19: Self-recruitment in 2012

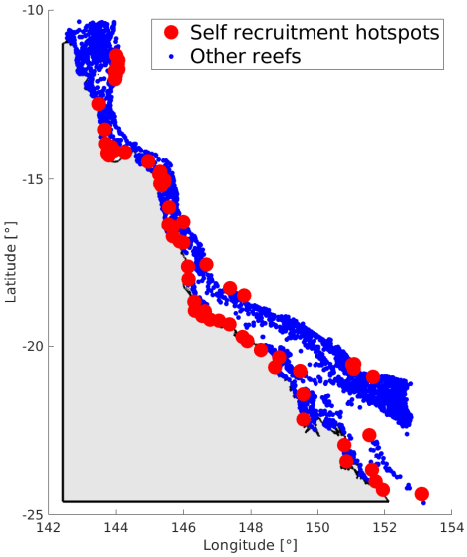

Figure A.20: Self-recruitment hotspots in 2012

A.2.3 Degree centrality

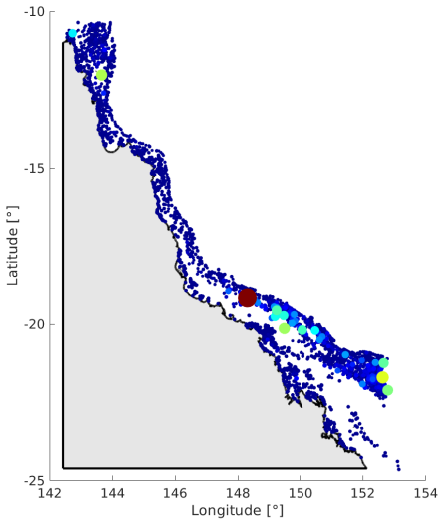

Figure A.21: Incoming degree centrality in 2008

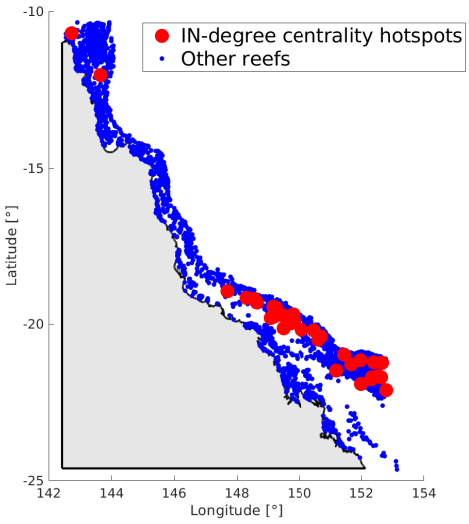

Figure A.22: Incoming degree centrality hotspots in 2008

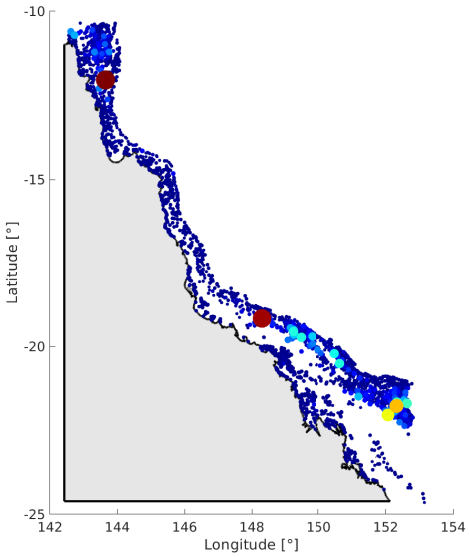

Figure A.23: Incoming degree centrality in 2012

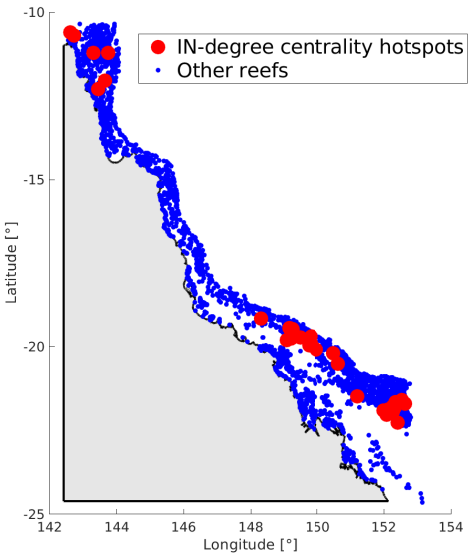

Figure A.24: Incoming degree centrality hotspots in 2012

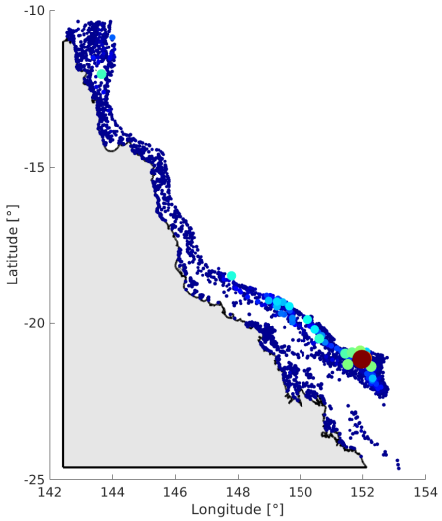

Figure A.25: Outgoing degree centrality in 2008

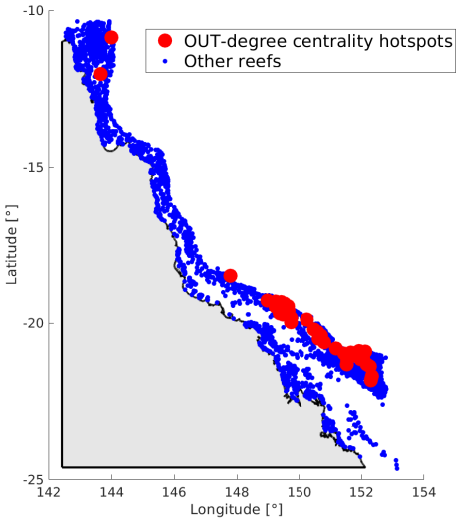

Figure A.26: Outgoing degree centrality hotspots in 2008

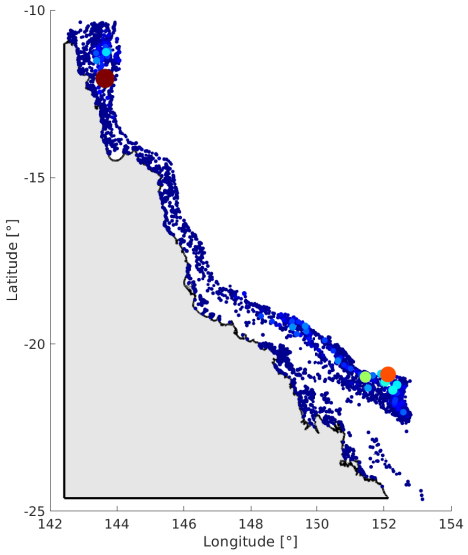

Figure A.27: Outgoing degree centrality in 2012

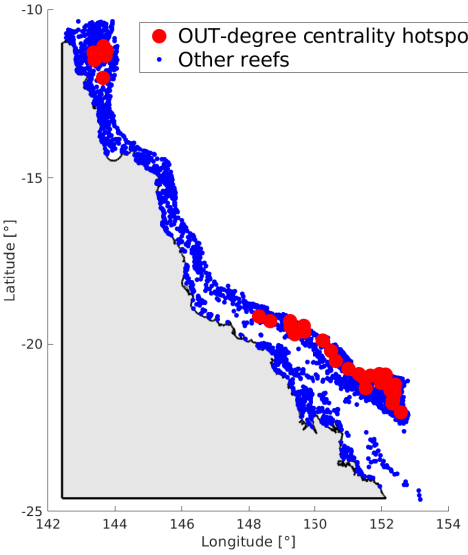

Figure A.28: Outgoing degree centrality hotspots in 2012

A.2.4 PageRank

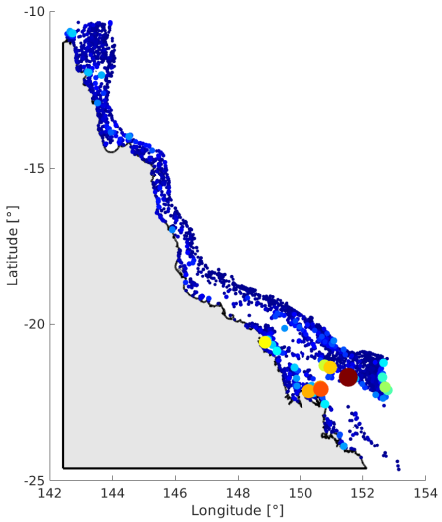

Figure A.29: Incoming PageRank in 2008

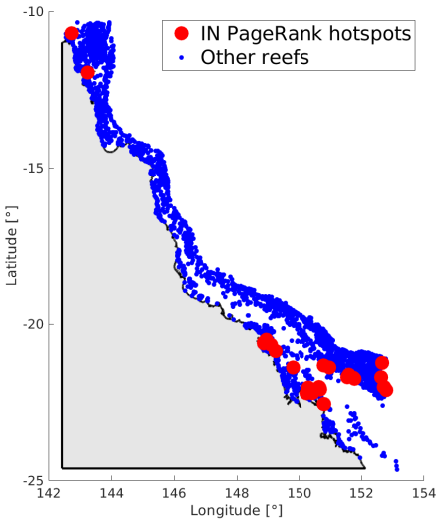

Figure A.30: Incoming PageRank hotspots in 2008

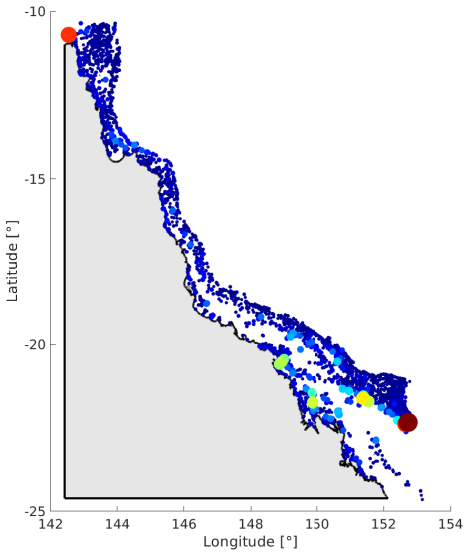

Figure A.31: Incoming PageRank in 2012

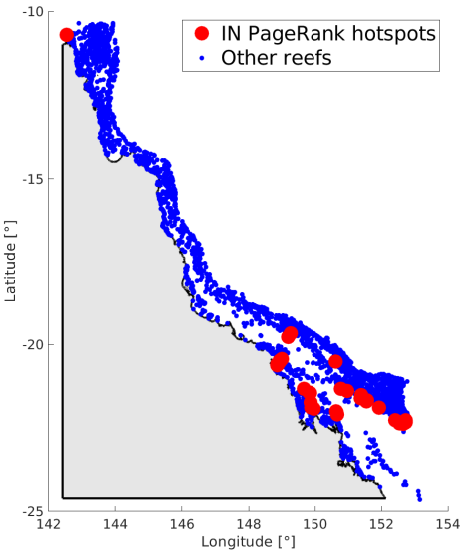

Figure A.32: Incoming PageRank hotspots in 2012

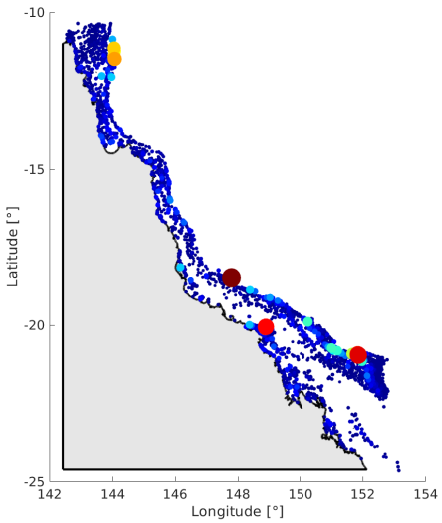

Figure A.33: Outgoing PageRank in 2008

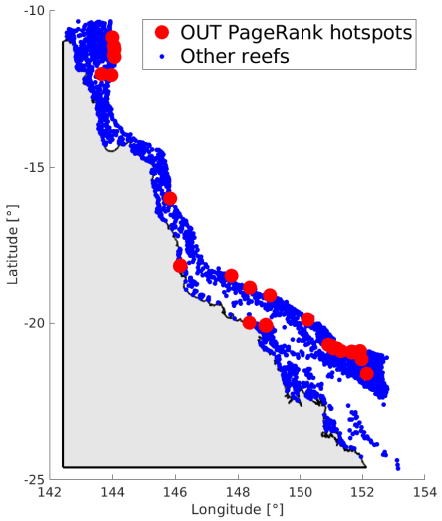

Figure A.34: Outgoing PageRank hotspots in 2008

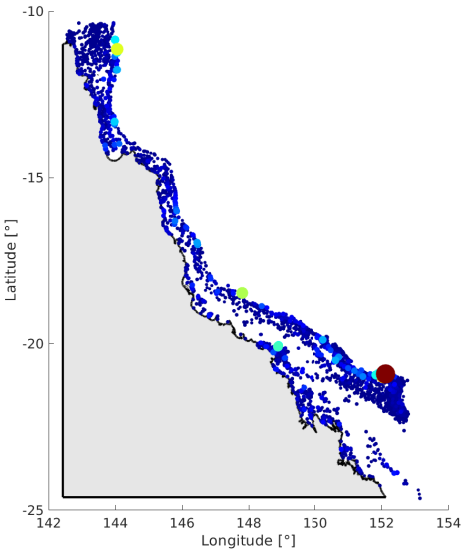

Figure A.35: Outgoing PageRank in 2012

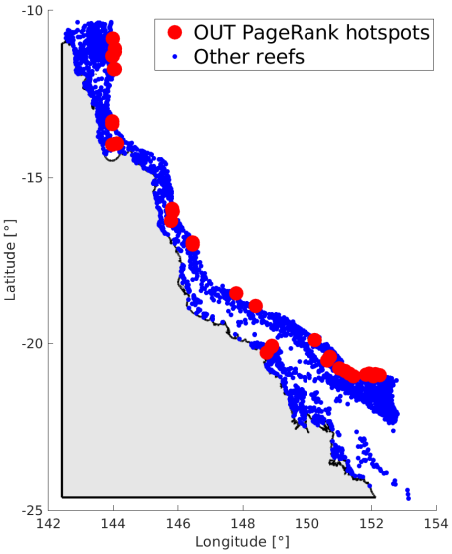

Figure A.36: Outgoing PageRank hotspots in 2012

A.3 Protection and restoration measures

This section contains all figures for the protection and restoration measures in 2008 and 2012.

A.3.1 Protection measures

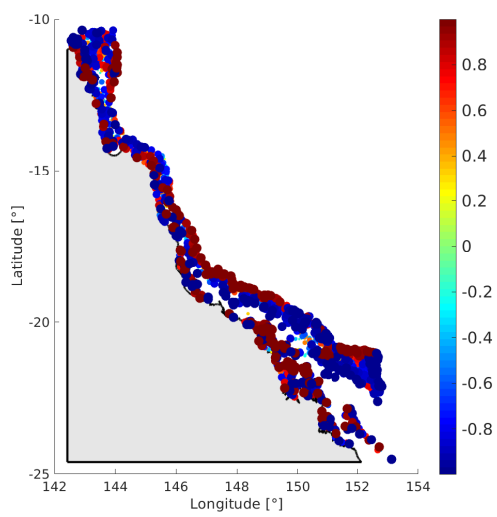

Figure A.37: Degree centrality protection in 2008

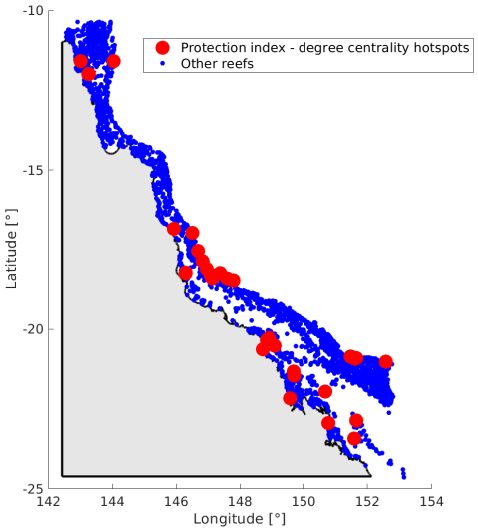

Figure A.38: Deree centrality protection hotspots in 2008

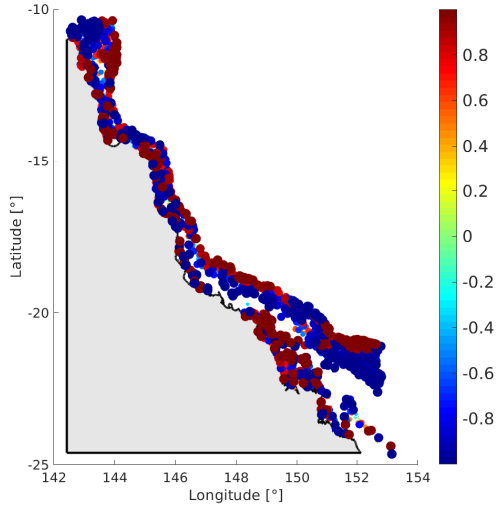

Figure A.39: Degree centrality protection in 2012

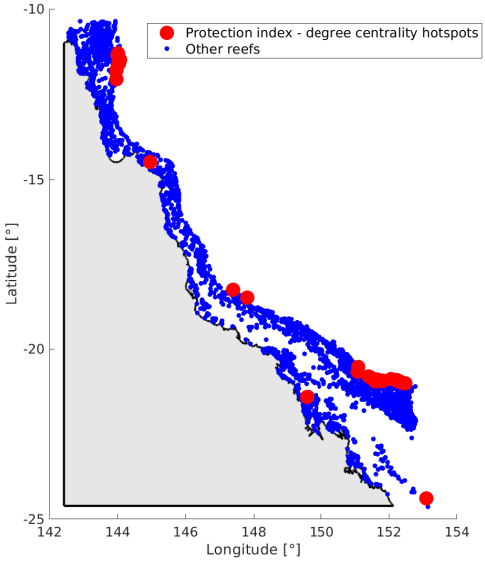

Figure A.40: Deree centrality protection hotspots in 2012

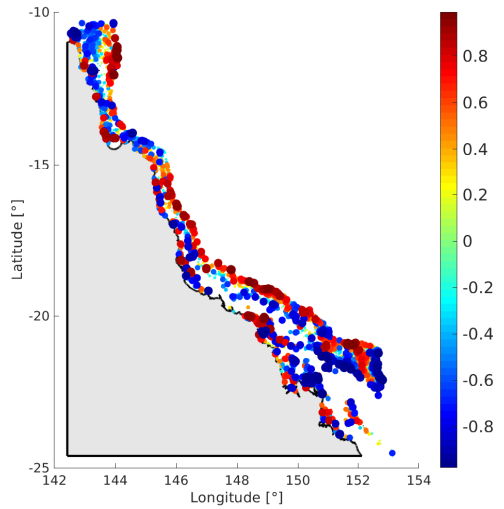

Figure A.41: PageRank protection in 2008

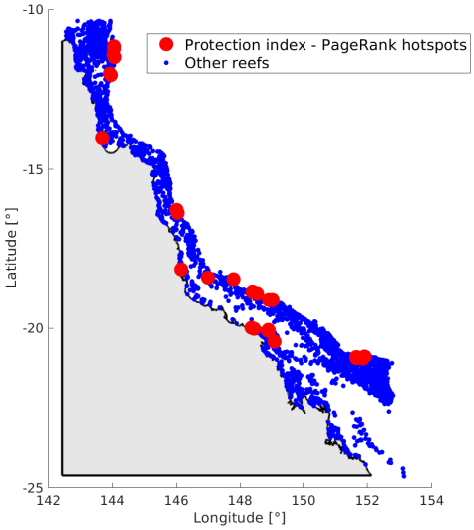

Figure A.42: PageRank protection hotspots in 2008

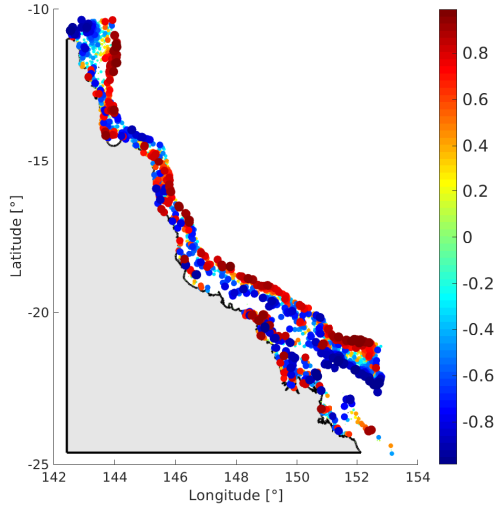

Figure A.43: PageRank protection in 2012

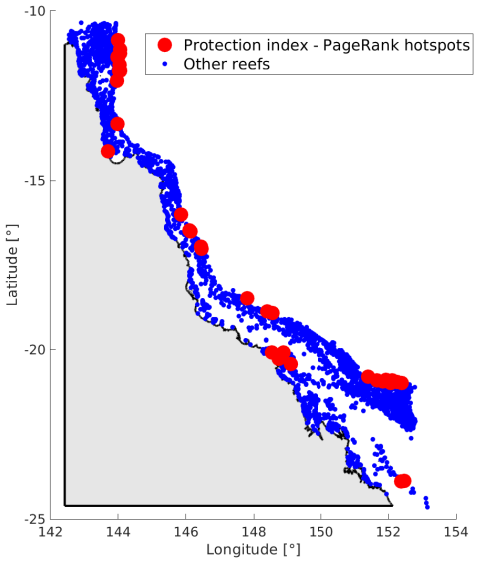

Figure A.44: PageRank protection hotspots in 2012

A.3.2 Restoration measures

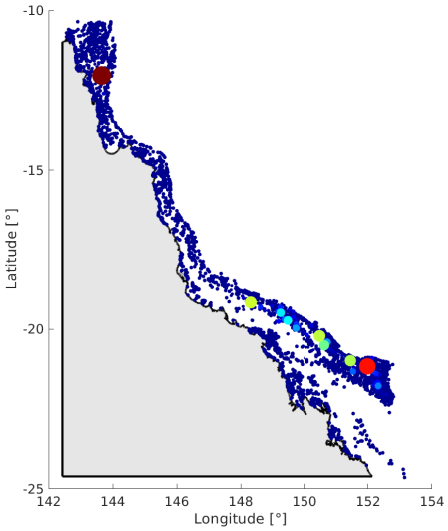

Figure A.45: Degree centrality restoration in 2008

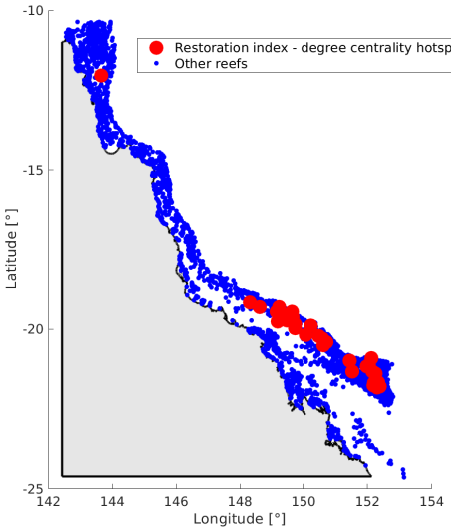

Figure A.46: Degree centrality restoration hotspots in 2008

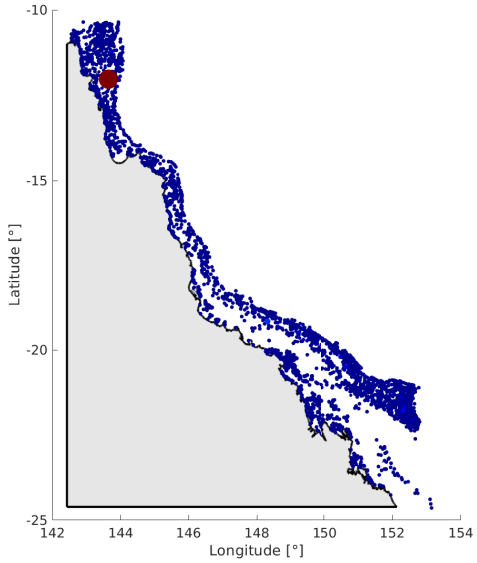

Figure A.47: Degree centrality restoration in 2012

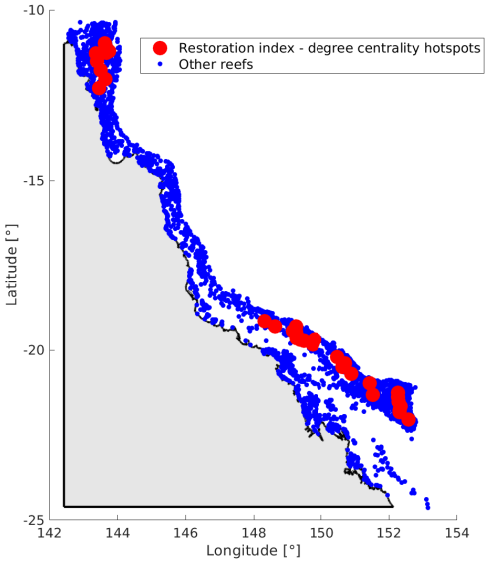

Figure A.48: Degree centrality restoration hotspots in 2012

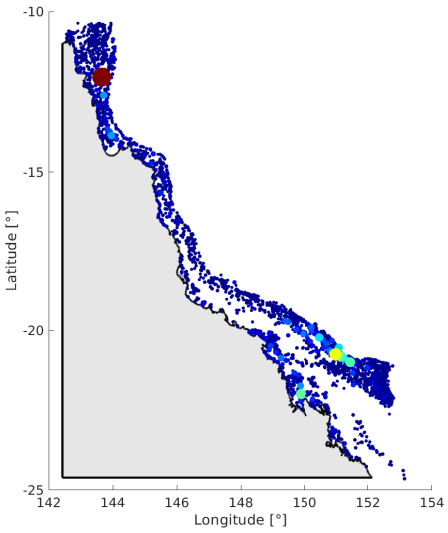

Figure A.49: PageRank restoration in 2008

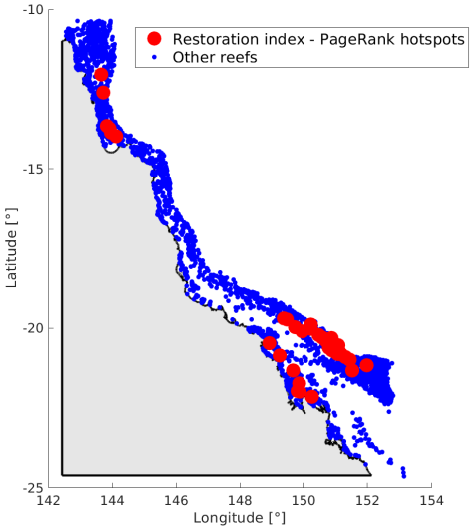

Figure A.50: PageRank restoration hotspots in 2008

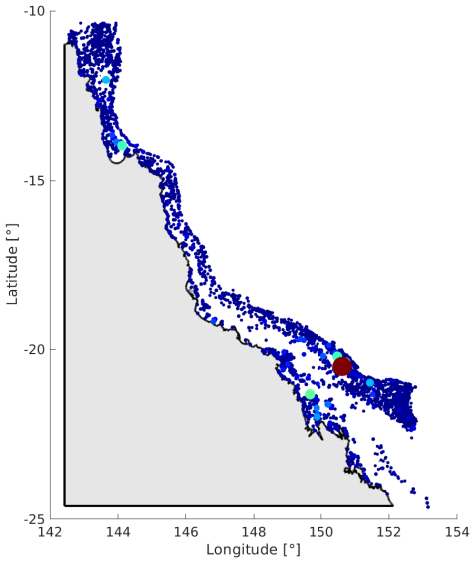

Figure A.51: PageRank restoration in 2012

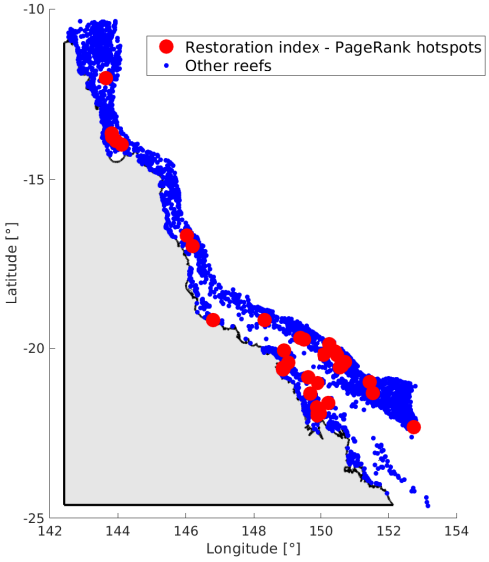

Figure A.52: PageRank restoration hotspots in 2012

A.4 Identification of reef clusters

This section contains all figures for the identification of reef clusters in 2008 and 2012.

A.4.1 Strongly connected components

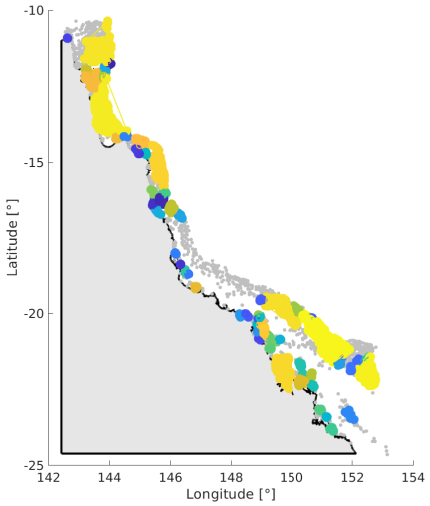

Figure A.53: Number of strongly connected components with more than 5 reefs in 2008: 69

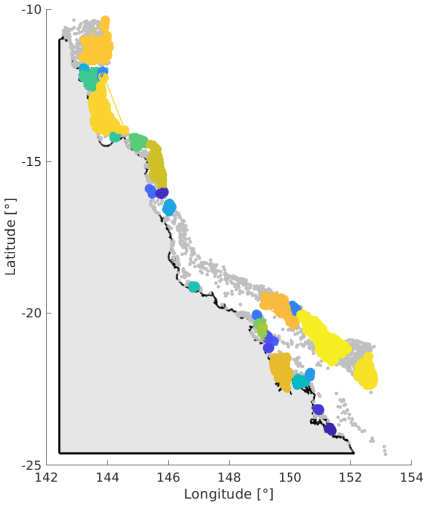

Figure A.54: Number of strongly connected components with more than 10 reefs in 2008: 29

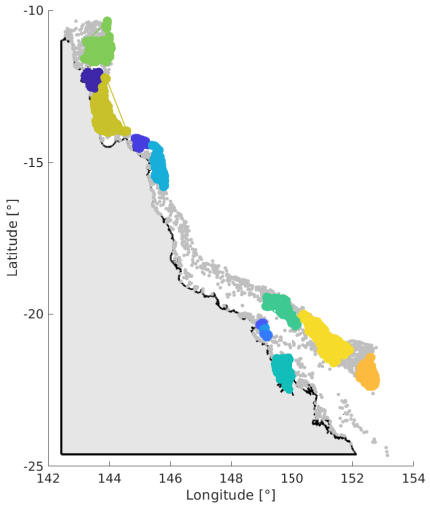

Figure A.55: Number of strongly connected components with more than 20 reefs in 2008: 12

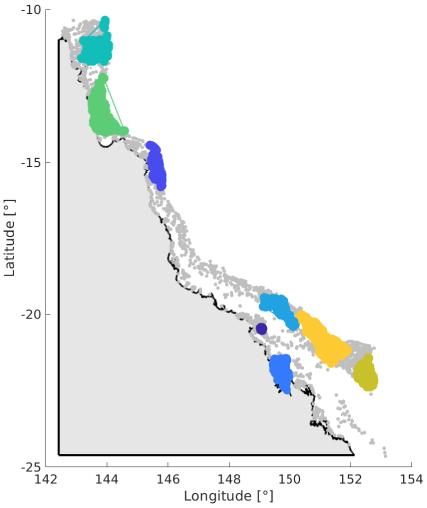

Figure A.56: Number of strongly connected components with more than 35 reefs in 2008: 8

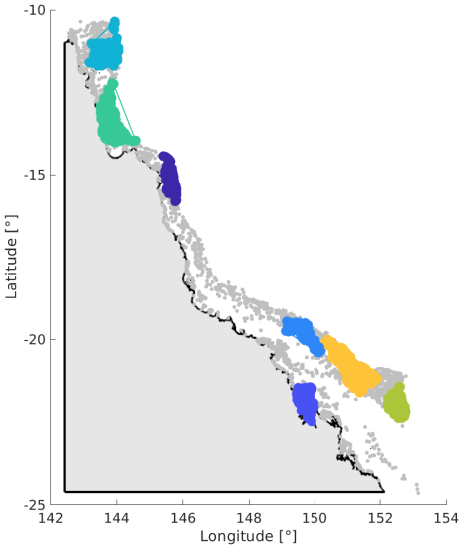

Figure A.57: Number of strongly connected components with more than 50 reefs in 2008: 7

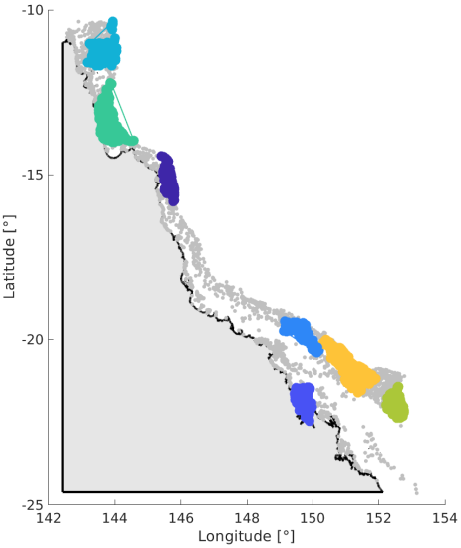

Figure A.58: Number of strongly connected components with more than 75 reefs in 2008: 7

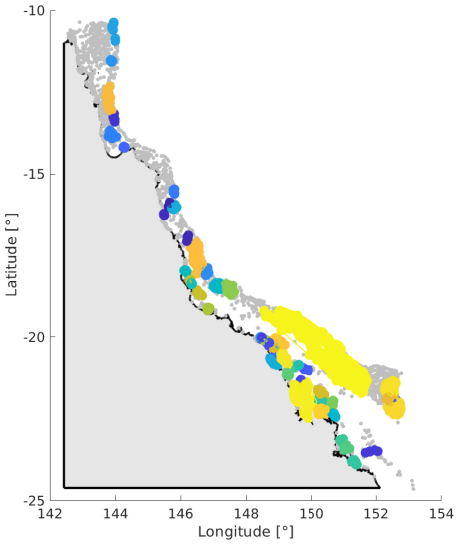

Figure A.59: Number of strongly connected components with more than 5 reefs in 2012: 56

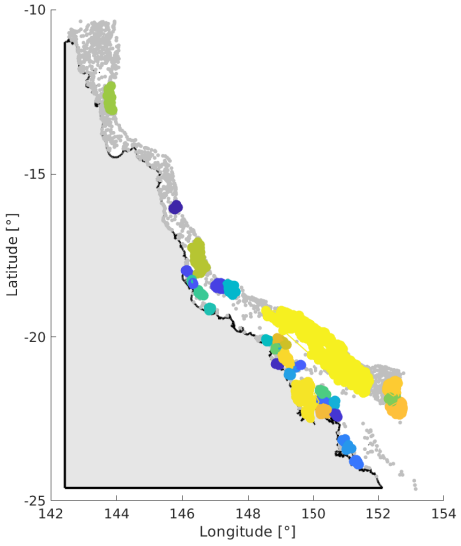

Figure A.60: Number of strongly connected components with more than 10 reefs in 2012: 33

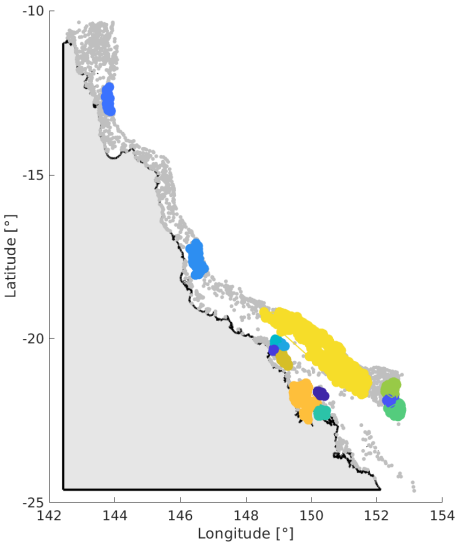

Figure A.61: Number of strongly connected components with more than 20 reefs in 2012: 13

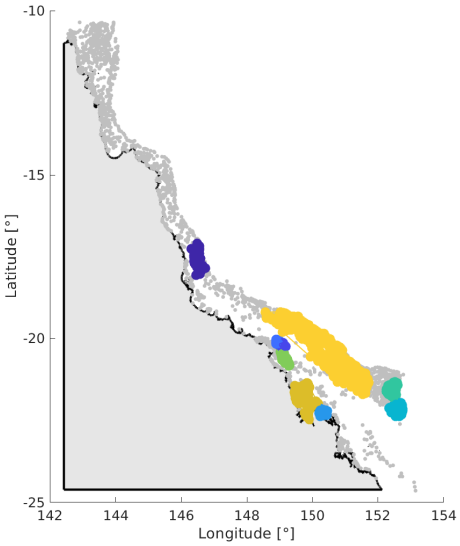

Figure A.62: Number of strongly connected components with more than 35 reefs in 2012: 9

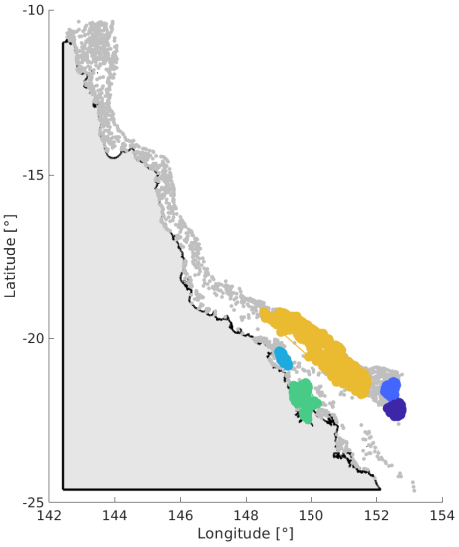

Figure A.63: Number of strongly connected components with more than 50 reefs in 2012: 5

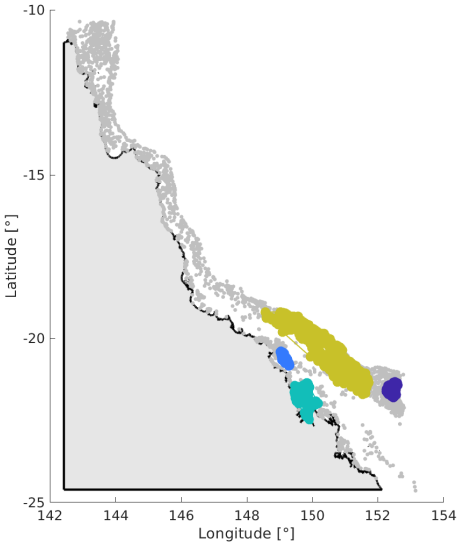

Figure A.64: Number of strongly connected components with more than 75 reefs in 2012: 4

A.4.2 Community detection

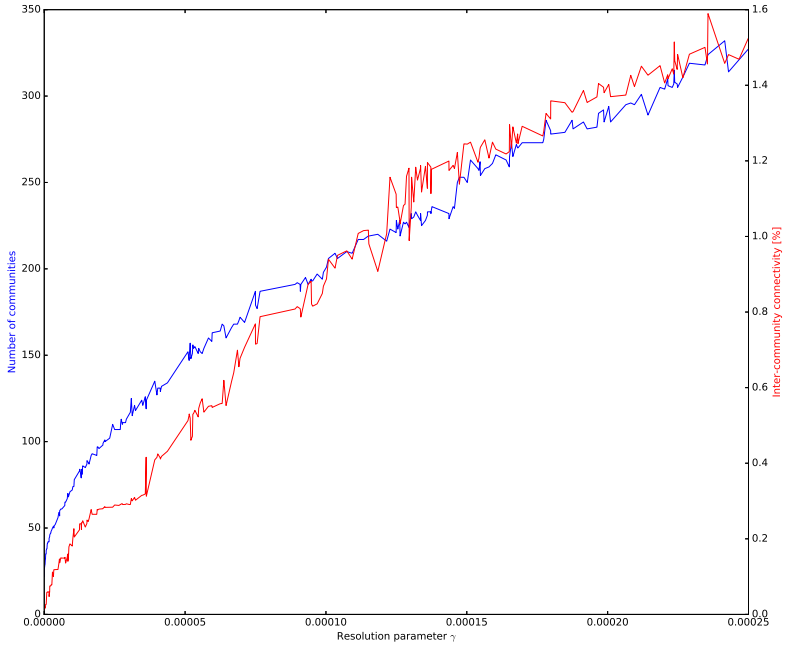

Figure A.65: Number of communities and percentage of inter-community connectivity in 2008 as a function of the resolution parameter γ

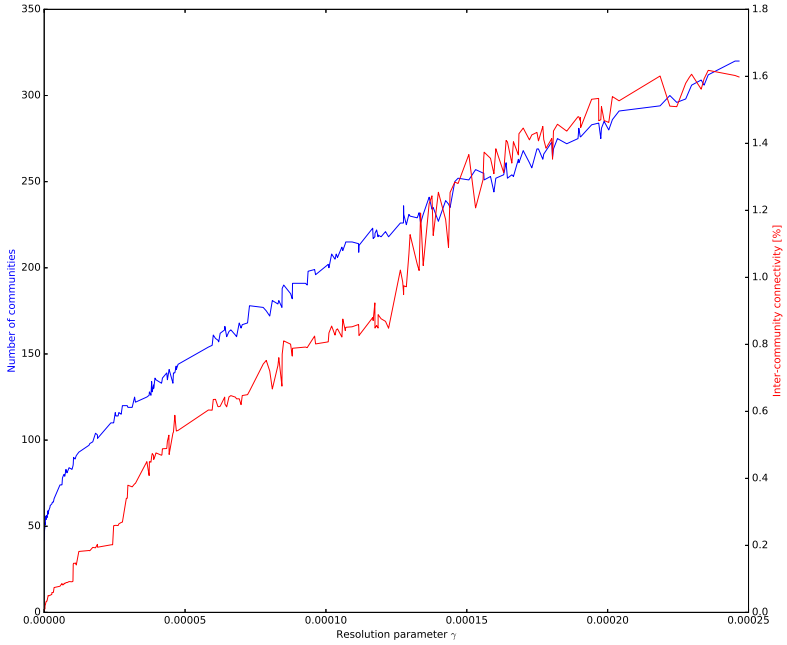

Figure A.66: Number of communities and percentage of inter-community connectivity in 2012 as a function of the resolution parameter γ

A.5 Variability of the connectivity

This section shows the mean value for each indicator.

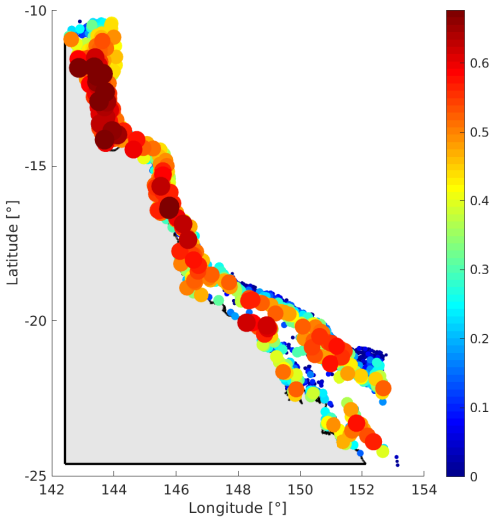

Figure A.67: Local retention in the GBR

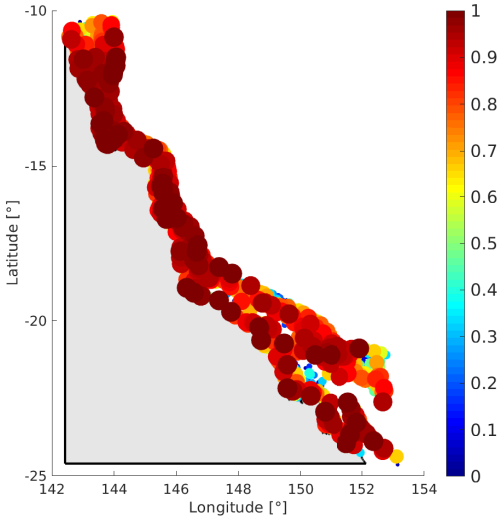

Figure A.68: Self-recruitment in the GBR

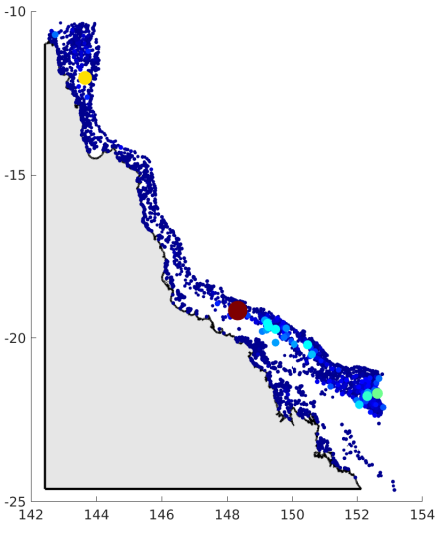

Figure A.69: Incoming degree centrality in the GBR

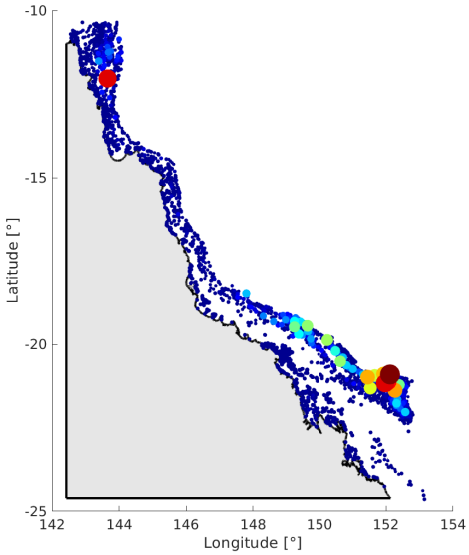

Figure A.70: Outgoing degree centrality in the GBR

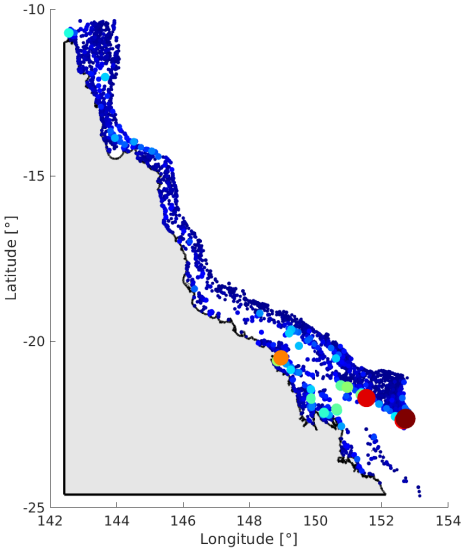

Figure A.71: Incoming PageRank in the GBR

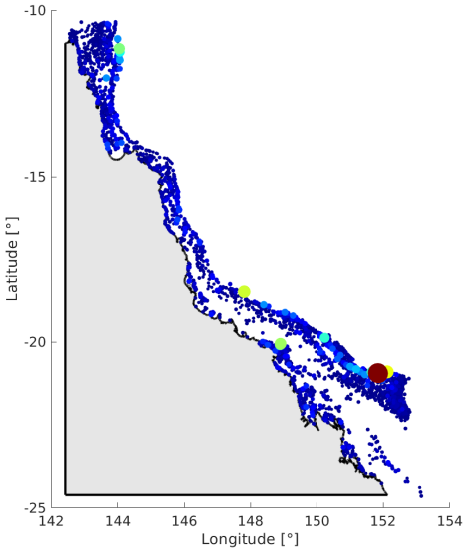

Figure A.72: Outgoing PageRank in the GBR

Rue Archimède, 1 bte L6.11.01, 1348 Louvain-la-Neuve **www.uclouvain.be/epl**